**Republic of Iraq**
**Ministry of Higher Education**
**And Scientific Research**
**University of Babylon**
**College of Science**
**Department of Physics**

# Measurement of Radon Gas Concentration and It's Health Effect on the Employees in Al–Najaf Governorate Refinery/ Iraq

A Thesis

Submitted to the Physics Department, College of Science, University of Babylon in Partial Fulfillment of the Requirements for the Degree of Master of Science in Physics

By

**Mokhalad Abbas Mohammed Aziz**

B.Sc. in Physics (2009)

Supervised by

**Asst. Prof. Dr. Rawaa Mezher Obaid Ashoor**

**2022 A.D.** **1444 A. H.**

بِسۡمِ ٱللَّهِ ٱلرَّحۡمَٰنِ ٱلرَّحِيمِ

﴿قَالُواْ سُبۡحَٰنَكَ لَا عِلۡمَ لَنَآ إِلَّا
مَا عَلَّمۡتَنَآۖ إِنَّكَ أَنتَ ٱلۡعَلِيمُ
ٱلۡحَكِيمُ ٣٢﴾

**صدق الله العلي العظيم**

**سورة البقرة / آية (٣٢)**

## Supervisor Certification

I certify that this thesis is titled (**Measurement of Radon Gas Concentration and It's Health Effect on the Employees in Al–Najaf Governorate Refinery/ Iraq**) was prepared by **(Mokhalad Abbas Mohammed Aziz)** under my supervision at Department of Physics, College of Science, University of Babylon, as a partial fulfillment of the requirements for the degree of master of philosophy science in physics.

**Signature:**

**Supervisor: Dr. Rawaa M. Obaid**

**Title: Asst. Prof.**

**Address: Department of Physics,**

**College of Science, University of Babylon.**

**Date: / / 2022**

**Certification of the Head of the Department**

In view of the available recommendation, I forward this thesis for debate by the examination committee.

**Signature:**

**Name: Asst. Prof. Dr. Samira Adnan Mahdi**

**Title: Asst. Prof.**

**Address: Head of Physics Department,**

**College of Science, University of Babylon.**

**Date: / / 2022**

# Dedication

**To ...**

**My mother and my father..**

**My teachers at the primary learning stage.**

**My teachers at the secondary learning stage.**

**My professors.**

**My colleages.**

**My family.**

**Every one who supported the work..**

***Mokhalad***

# Acknowledgments

First, I would like to express my deep thanks for the Almighty ALLAH, JALA JALALAH, for what I have been, prayer and peace be upon the best of his creation Mohammed and his progeny.

I would like to express my deep gratitude and appreciation to my supervisor **Asst. Prof**. **Dr. Rawaa M. Obaid Ashoor**, for suggesting the topic of the thesis, supporting at all levels, giving advice, and continous tracking the work..., and I also want to thank **Prof. Dr. Abdul R.H. Subber** for his valuable advices and support.

I would like to thank my professor **Prof. Dr. Mohsin K. Muttaleb Al-Janabi** for his valuable advices and support.

I also would like to thank **Dr. Inaam H. Kadhim Hadi** for her cooperation and valuable advices about issues related to our work.

I would like also to express my special thanks and appreciation for the head of the Department of Physics Prof. **Dr. Abdulazeez O. Mousa Al-Ogaili** for his support and advices.

Finally, all thanks and appreciation are to the administrations that facilitates the task of getting the job done:

- **University of Kufa – College of Science – Physics Department.**
- **Al-Najaf refinery administration.**
- **University of Karbala – College of Science – Physics Department.**

***Mokhalad***

## Summary

In the present work, Radon–222 gas concentration was measured for environmental samples (soil and water) collected from selected locations inside AL-Najaf refinery. CR – 39 detector (passive method) was used for soil and water measurements, and also, RAD7 monitor of DURRIDGE company, USA (active method) was used for water measurements. The location of the study was divided into four sectors, each one was divided into squares in order to achieve a comprehensive study of the study area.

Fifty soil samples were collected at a depth of 20 cm from the surface and nine different samples of water were collected from the following locations: RO unit (drinking water), tap water, water from the boiler in the refining units, well water and waste water.

The results reveal that the Radon–222 gas concentration in the soil gas ranges from 7341∓ 857 Bq/$m^3$ for the sample which was near the flare to 39 ∓ 186 Bq/$m^3$ for the sample at the end of the refinery with an average of 1342 ∓ 123 Bq/$m^3$.

The results for water samples measured by RAD7 monitor show that the Radon–222 gas concentration lies between 471 Bq/$m^3$ (0.471 Bq/L) for well water and 0 Bq/$m^3$ for boiler water in the refining units with an average of 108 Bq/$m^3$ (0.108 Bq/L), but for the results of water samples that were measured with CR-93 detector (passive method) reveals that radon–222 gas concentration ranges between 297 ∓ 53 Bq/$m^3$ (0.297 ∓ 0.053 Bq/L) for the sample of well water at RO units and 12 ∓ 48 Bq/$m^3$ (0.012 ∓ 0.048 Bq/L) for boiler water with an average of 148 ∓ 32 Bq/$m^3$ (0.148 ∓ 0.032 Bq/L).

The concentrations of Radon–222 gas in the air of the refinery that resulted from water contribution and soil contribution were estimated according to

Environmental Protection Agency (EPA), USA. The concentrations of Radon–222 gas in the air near the soil that resulted from the contribution of soil were also estimated.

The Annual Effective Doses ($AED_{inhalation}$) due to inhalation Radon–222 gas and it's progeny in indoor and outdoor air were calculated according to United Nations Scientific Committee on the Effects of Atomic Radiation (UNSCEAR) relations. The Annual Effective Doses ($AED_{inhalation}$) resulting from the contribution of the soil samples were all below the accepted limits recommended by WHO which equals to 0.1 mSv/y.

The Annual Effective Doses ($AED_{inhalation}$) resulted from the contribution of water samples were all below the accepted limits recommended by WHO and ICRP, which were equal to 0.1 mSv/y and 1 mSv/y, respectively.

# Contents

# List of Figures

# List of Tables

# List of Symbols

| Symbol | Description |
|---|---|
| $T_{1/2}$ | The Half-Life |
| $\lambda$ | The constant of decay |
| $\tau$ | The Mean Life |
| ${}^{A}_{Z}P$ | The parent nucleus, where A is the mass number and Z is the atomic number. |
| ${}^{A-4}_{Z-4}D$ | The progeny (daughter nucleus) |
| ${}^{4}_{2}He$ | Helium nucleus (alpha particle) |
| $K_T$ | Total kinetic energy |
| $\beta^-$ | Beta particle |
| $\beta^+$ | Positron particle |
| $\upsilon$ | Neutrino |
| $\overline{\upsilon}$ | Anti neutrino |
| $\beta$ | Reduced velocity |
| Z | Atomic number |
| A | Mass number |
| Sv | Sievert |
| Gy | Gray |
| $H_T$ | Equivalent dose |
| $W_R$ | Radiation weighting factor |
| $W_T$ | Tissue weighting factor |
| $C_W$ | The concentration of radon gas in the water inside the pore space. |
| $C_a$ | The concentration of radon gas in the air inside the pore space. |
| T | The transfer coefficient of radon gas from water to air. |
| $\overline{C_a}$ | The estimation of the average of radon gas concentration in indoor air. |

| Symbol | Description |
|---|---|
| $\overline{C_W}$ | The average radon concentration in water. |
| e | Transfer efficiency |
| W | The rate of use of water per person. |
| $C_{Rn}$ | Radon activity concentration in $Bq/m^3$. |
| $P_{PAEC}$ | Cumulative radon activity concentration |
| WL | Working Level |
| EEDC | Equilibrium-Equivalent Decay-Product |
| F | Equilibrium factor |
| $C_{eq}$ | Equilibrium Equivalent Concentration |
| I | The mean of time spent at outdoor air for a person per year (1760 $hy^{-1}$). |
| O | The average occupancy time per person at indoor air which equals 7000 h/y. |
| $C_{radon\ near\ the\ soil}$ | Radon gas concentration near the soil |
| $E_P$ | Exposure to radon progenies in WLM/y |
| n | The fraction of time spent indoors |
| PAEC | Potential Alpha Energy Concentration |
| WLM | Working Level Month |
| C | Radon gas concentration in the sample |
| $\lambda_{Rn}$ | Radon decay constant |
| h | The distance between the detector and the surface of the sample in (cm). |
| $T_e$ | The effective exposure time |
| $E_A$ | The area exhalation rate in $Bq.m^{-2}.h^{-1}$ |
| $E_M$ | The mass exhalation rate in $Bq.kg^{-1}.h^{-1}$ |
| $C_U$ | Uranium concentration in mg/kg. |
| $C_{Ra}$ | Radium content |
| $\rho_t$ | Track density in track $/cm^2$ |
| $A_P$ | The activity of the parent nuclide. |

| Symbol | Description |
|---|---|
| $A_D$ | The activity of the daughter nuclide. |
| V | The volume of building per person |
| $W_s$ | Sample weight |
| $W_{mol}$ , M | Molar weight |
| $V_{cup}$ | The volume of the cup |
| $N_{av}$ | Avogadro's number |
| $\theta_C$ | Critical angle |
| $V_G$ | The velocity of along the normal surface |
| $V_T$ | The velocity of etching along the particle's track |
| $M_s$ | Sample mass |
| D | The constant of the exhalation diffusion |
| D | Eddy diffusion coefficient |
| K | Calibration factor |
| $N_D$ | The number of the nuclei for the daughter |
| $N_P$ | The number of the nuclei for the parent |
| $A_s$ | The surface area of the sample |

# List of Abbreviations

| Abbreviation | Description |
|---|---|
| **LET** | **Linear Energy Transfer** |
| **NORM** | **Naturally Occurring Radioactive Materials** |
| **TENORM** | **Technologically Enhanced Naturally Occuring Radioactive Materials** |
| **SSNTDs** | **Solid State Nuclear Track Detectors** |
| **Rem** | **Roentgen equivalent man** |
| **EPA** | **Environmental Protection Agency** |
| **DOE** | **Department of Energy** |
| **ICRP** | **International Commission on Radiological Protection.** |
| **IAEA** | **International Atomic Energy Agency** |
| **CEC** | **Commission of the European Communities** |
| **UNSCEAR** | **United Nations Scientific Committee on the Effects of Atomic Radiation** |
| **BEIR** | **Committee on the Biological Effects of Ionizing Radiation** |
| **NIOSH** | **National Institute for Occupational Safety and Health.** |
| **NRC** | **National Research Council.** |
| **A.E.R.** | **Air Exchange Rate** |
| **$AED_{inhalation}$** | **Annual Effective Dose for inhalation** |
| **DCF** | **Dose Conversion Factor for Radon Exposur.** |
| **$AED_{outdoor\ inhalation}$** | **Annual Effective Dose for inhalation at out door air.** |
| **$AED_{indoor\ inhalation}$** | **Annual Effective Dose for inhalation at indoor air.** |
| **LCR** | **Lung Cancer Risk in (case/year.million)** |
| **TASL** | **Track Analysis System Limited system** |
| **GIS** | **Geographic Information System** |

| Abbreviation | Description |
|---|---|
| **SRD** | **Smart Radon Duo** |
| **SRM** | **Scintillation Radon Monitor** |
| **Fps** | **Frame per second** |
| **ICRU** | **International Commission on Radiation Units and Measurements.** |
| **NCRP** | **The National Council on Radiation Protection and Measurement.** |

# Chapter One

# General Introduction

## 1.1: Introduction

Radiation, in general, can be classified into two types: charged particulate radiation and uncharged radiation, the first one, includes fast electrons and heavy charged particles, and the second one, includes electromagnetic radiation and neutrons. They differ in mass, energy, and their ability to penetrate bodies. What we are interested in is the radiation which is come from nuclei (alpha particles, beta particles, and gamma photons), which is called nuclear radiation [1].

Our world is naturally radioactive, this radioactivity comes from the development of our universe $1.5 \times 10^{10}$ years ago, where, there are two types of radiation due to their effect on the atoms of the matter: ionizing radiation and non-ionizing radiation [2,3].

There is about 3000 radionuclide on the chart of nuclides but only a few hundreds of them have been detected on the earth where 90% of them decayed away and vanished from the earth as their half-lives were short [3].

The geology of the earth depends on the decay of the radionuclides, where very slow decay of Uranium, Thorium, and even an isotope of potassium provide the heat to the core of the earth and keep it molten as a result, the earth stays geologically active and the continents of the earth keep drifting [4].

Naturally Occurring Radionuclides come from Uranium-238 and Thorium-232 decay, where the majority of radionuclides in these materials are Radium and Radon, and there are other materials arise due to human activities (technological operations) which leads to an increase of radionuclides [2].

Radiation affects the biological tissues of the organisms and can cause biological damage to them if the exposure is acute or chronic. The symptoms resulting from radiation exposure depend on the dose, dose rate, type of radiation, distribution of dose, and response to radiation [5].

## 1.2: Natural Radioactive Decay Chains

There are three naturally occurring decay chains, Uranium-238 decay chain with a notation 4n+2, Uranium-235 decay chain (Actinium decay chain) with a notation 4n+3 and Thorium-232 decay chain with a notation 4n, where the notation referred to the mass number of the members of the chain, and n ranges between 50 and 60, as shown in Figures (1 – 1), (1 – 2) and (1 – 3) [6].

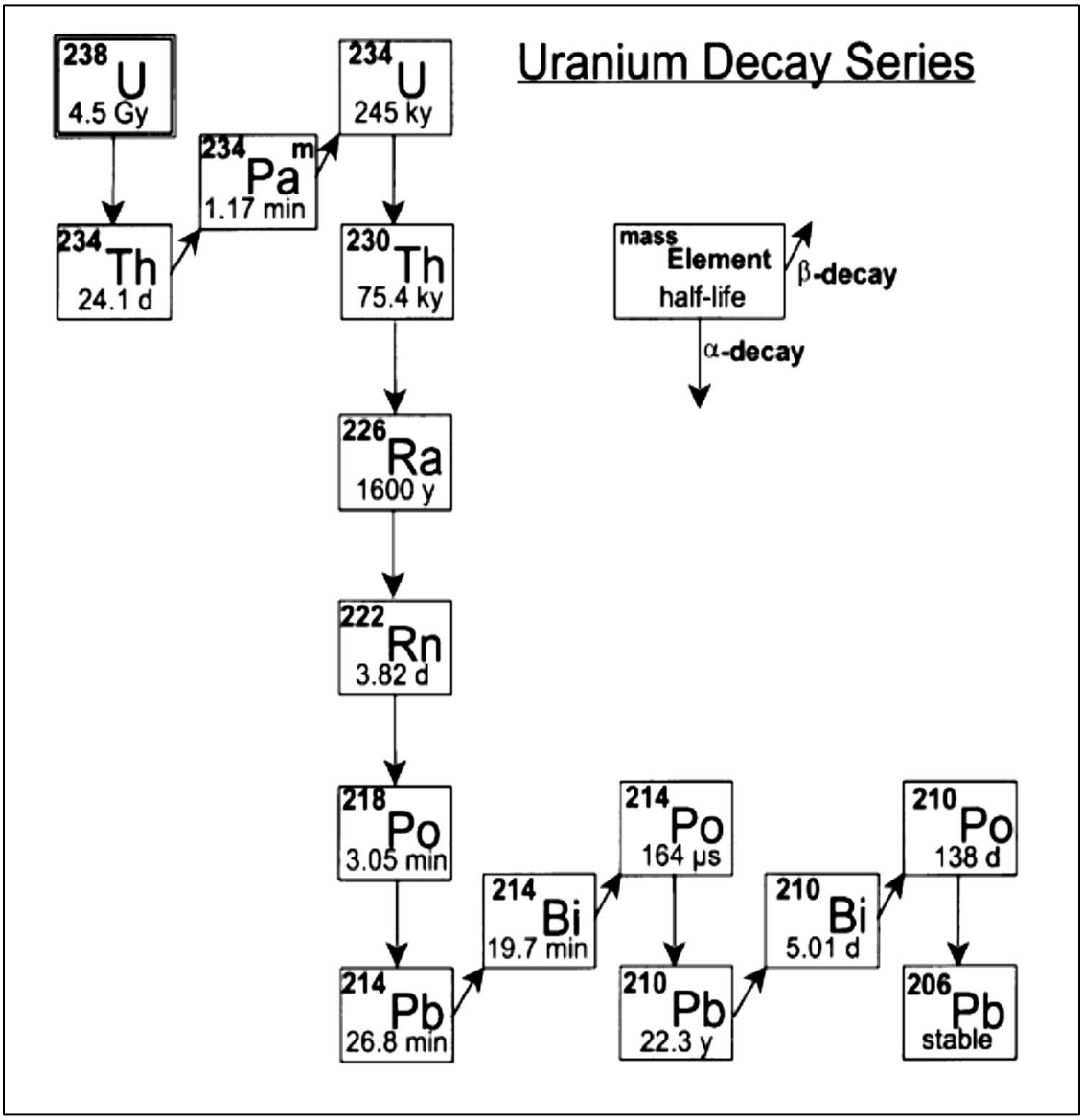


**Figure (1 – 1): Uranium – 238 decay chain series** [7].

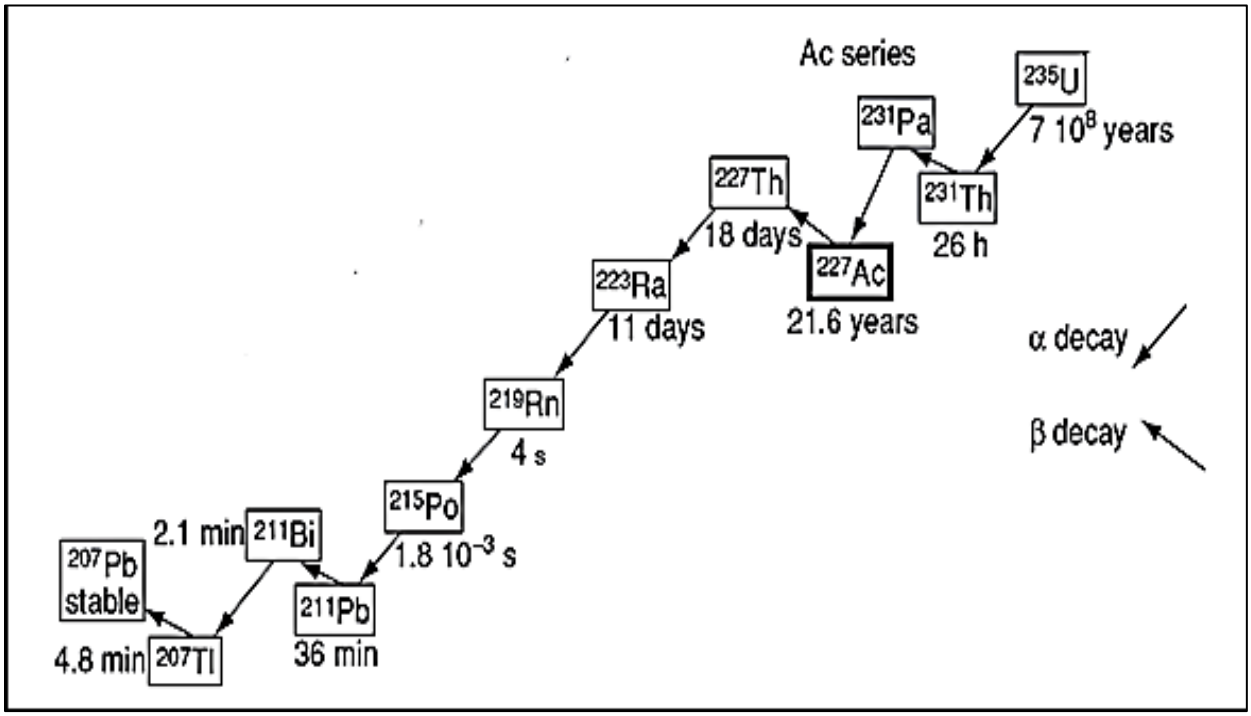


**Figure (1 – 2): Uranium – 235 decay series** [2 , 8]**.**

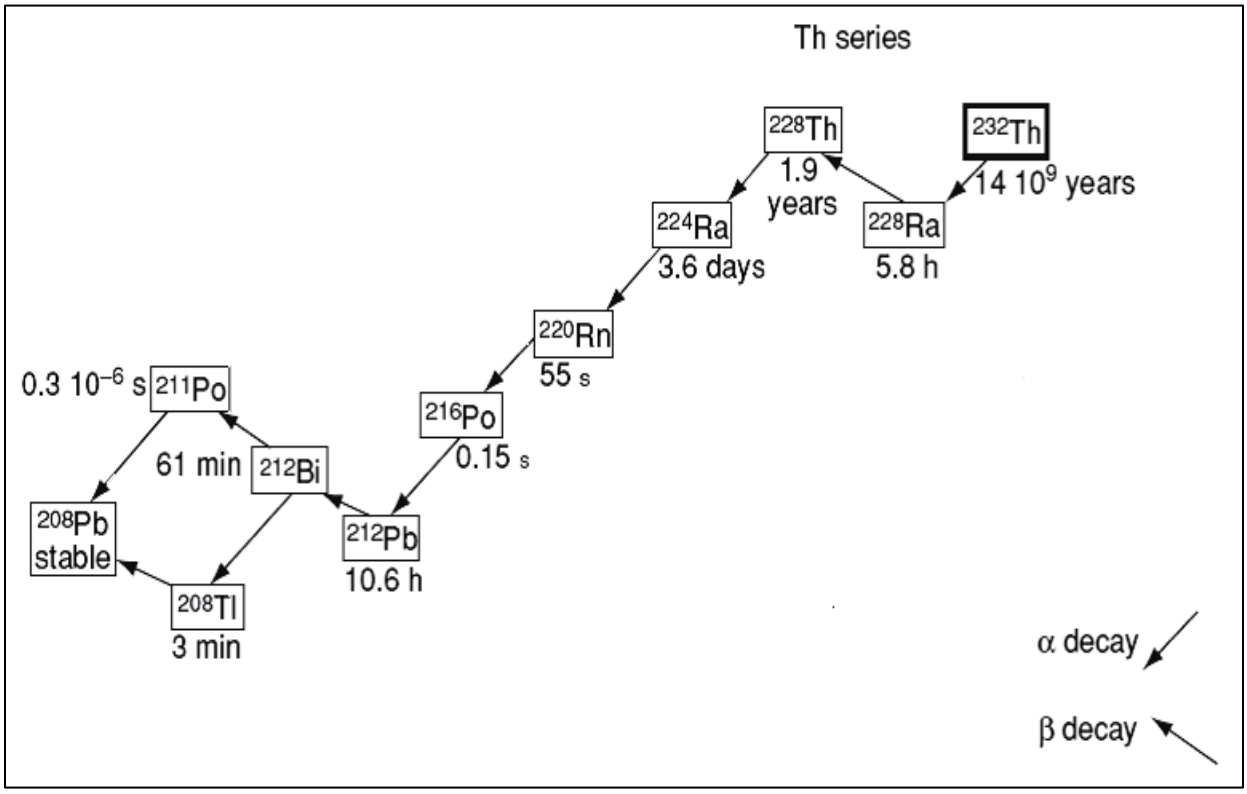


**Figure (1 – 3): Thorium – 232 decay series** [2]**.**

## 1.3: Radiation and Cancer

Radiation carcinogenic effects started with skin cancer and leukemia in 1911. Radiations with high energy such as X-ray, ultraviolet, beta radiation, gamma rays, and alpha particles can lead to carcinogenic effects on the cells of the body via DNA damage [9]. However, it is difficult to recognize between the cancer caused by radiation and the cancer which is naturally developed, or from exposure to chemicals. Cancer development in the cells of the body depends on the time of exposure, radiation type, the part of the body affected by the radiation, and the distance between the source and the body [10].

The damage of DNA may happen directly by passing ionizating radiation, or may happen indirectly by a chemical reaction following the passage of an ionizing radiation, as shown in Figure (1 – 4). An indirect effect of ionizing radiation occurs when the radiation reacts with a water content of the body resulting hydroxyl radical, as the body of human consists of 70% of water [11].

Radiation with Linear Energy Transfer (LET) can indirectly affect the cells of the body, as shown in Figure (1 – 4), and the effect of ionization radiation depends on the energy transfered to the cells of the body, and the length of the particle path [12].

The damage in DNA can be repaired by the cell if it is a simple damage, however, if there are many damages occurring in the cell, then , the damage is called a complex damage, and it can not be repaired, and it may lead to cell death or genetic mutations (cancer) [13].

The radiations can be released from nuclear accidents, natural sources, or medical equipement such as X-ray scanning. The probability of developing cancer from medical equipements is very low in comparison with other exposures [14].

The main source of Ultraviolet (UV) radiation is the sun, and it can not penetrate the skin, as a result, the effectiveness of this type is only on the skin. The sources of alpha particles are many, but the main source comes from Radon – 222 gas progenies, alpha particle has a relatively big mass this enable it to ionize the atoms, Radon – 222 progenies can get stick to the aerosoles, as a result, it affects the respiratory systems, and cause lung cancer [15].

Beta particles can cause burns to the skin, and penetrate the skin, but it can not pass through the clothes. Gamma ray and X – ray are of a great danger for the whole body [11].

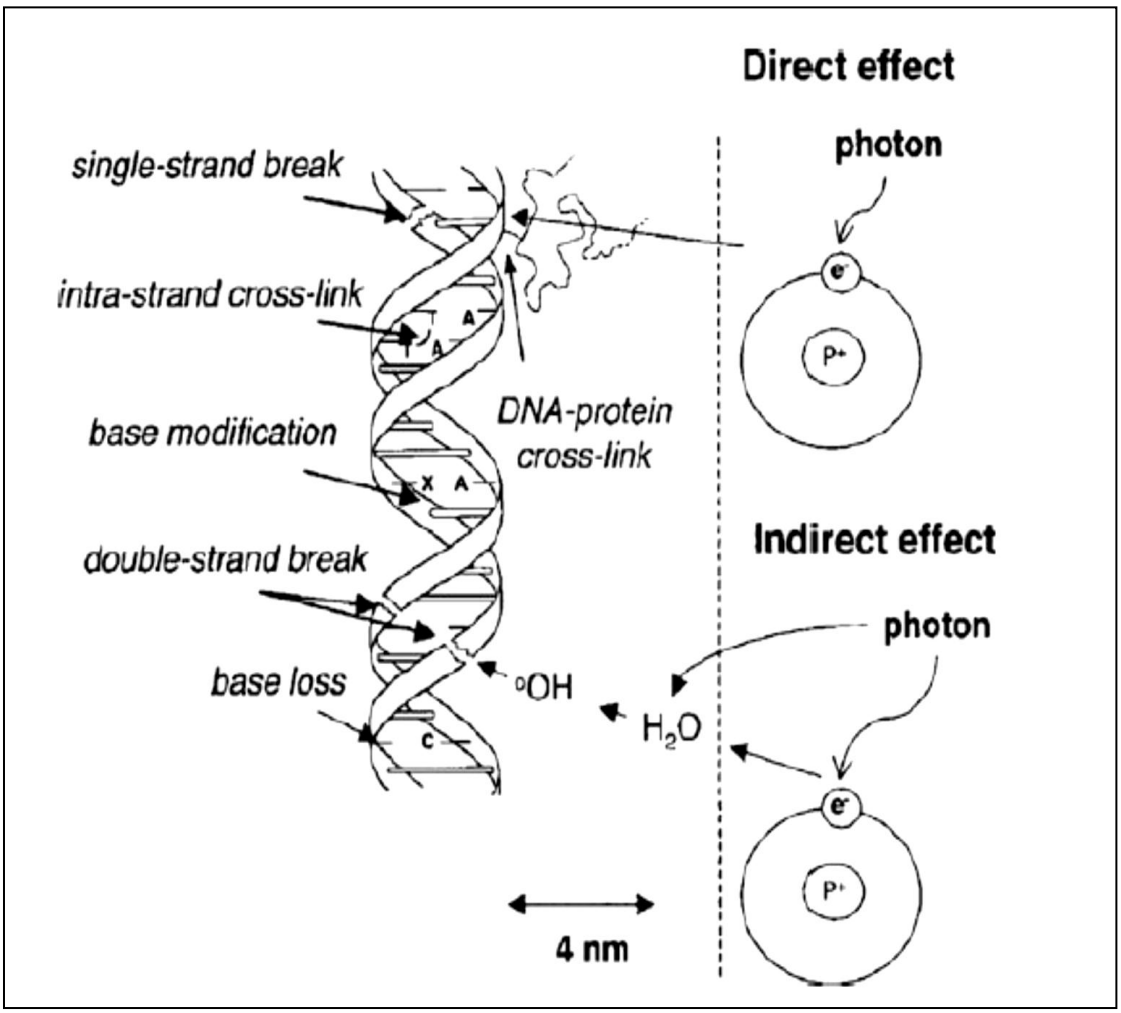


**Figure (1 – 4): DNA damage induced by ionizing radiation** [16]**.**

## 1.4: Naturally Occurring Radioactive Materials and Technologically Enhanced Naturally Occurring Radioactive Materials

Materials named Naturally Occurring Radioactive Materials (NORM) are natural materials existing in the earth that come from Uranium and Thorium decay, where the most of the radionuclides in these materials are Radium – 226 and Radon – 222, there are other materials named Technologically Enhanced Naturally Occurring Radioactive Materials (TENORM), these materials arise due to human activities (technological operations) which leads to an increase of radionuclides in NORM [3,18]. TENORM produces by industrial operations, such as mining, ore beneficiation, phosphate fertiliser production, water treatment, oil and gas production, scrap metal treating, and waste burning. Radiological exposure which comes from TENORM is more dangerous than NORM, as it contains high concentrations of radioactive elements [3,19].

Human health is affected by TENORMs as they emit Radon – 222 gas at high rates and contain a high content of Radium – 226, as a result, these materials are isolated and put in an industrial landfill to protect the public. TENORM is produced durring various industrial processes as a by – product or a waste, and the concentration of the radionuclides and their type depends on the raw materials that are used in the industrial process and the steps of the process, where some radionuclides become volatile durring the industrial process. The landfills that are used for TENORM are made of special materials to protect the geological structure of the earth, and they put above the aquifer to prevent the radioactive materials to be leaked into the groundwater [19].

Radon – 222 gas emissions from TENORM or NORM which are present in solid environmental samples such as building materials and soil are used to get knowledge about the distribution of the other radionuclides such as Potassium –

40, Rubidium – 87. Radon – 222 gas emissions can be evaluated using many techniques such gamma – ray spectrometry and alpha or beta particles counting method. The effect of these materials on the health of human is long – term, therefore, the study of environmental samples which are considered TENORM or NORM is important for the the public health. The health risks resulting from these materials is also related to the activity of human such as the existence of human at a high elevation above the earth surface [20].

## 1.5: Types of Radiation

### 1.5.1: Alpha Particles

These particles are emitted from alpha decay. This decay occurs for a radioactive nucleus that has an atomic number greater than 83. Alpha decay can be described in general by the following scheme [6]:

$$^{A}_{Z}P \longrightarrow {}^{A-4}_{Z-2}D + {}^{4}_{2}He + K_T$$

where:

$^{A}_{Z}P$: the parent nucleus, where A is the mass number and Z is the atomic number.

$^{A-4}_{Z-2}D$: the progeny (daughter nucleus) .

$^{4}_{2}He$: Helium nucleus (alpha particle).

$K_T$: total kinetic energy.

Alpha particle interacts with the atoms of matter, whether it was a gas, a liquid, or a solid, in two ways: A Coulombic interaction and a direct collision. interaction is probable with the Coulombic barrier of the nuclei of mater but it is very low (0.001%), and this interaction is going to be by scattering or deflection.

The ejection of atomic electrons of the matter happens with each interaction, and this creates an ion pair, each one consisting of ejected electrons and a positive ion.

Thousand of ion pairs are created as an alpha particle traverses the matter before dissipating its energy. The big difference in mass between alpha particles and atomic electrons of the matter facilitates the ionization process, and creates ion pairs. The energy required to produce an ion pair differs from one material to another whereby one can calculate the number of ion pairs, as the following:

The energy of alpha particle / the energy required for one ion pair = number of ion pairs.

Here are some values of energy required for one ion pair formation: 35 eV for air, 25 eV for argon gas, and 2-3 eV for semiconductors. The value is low for semiconductors so it is used as detectors [6].

### 1.5.2: Beta Particles

These particles emit by a nuclear processes as shown in the following schemes [6]:

$$ {}^{A}_{Z}P \longrightarrow {}_{Z+1}{}^{A}D + \beta^{-} + \bar{\nu} + K_T \qquad (\beta^{-} \text{ emission}) $$

$$ {}^{A}_{Z}P \longrightarrow {}_{Z-1}{}^{A}D + \beta^{+} + \nu + K_T \qquad (\beta^{+} \text{ emission}) $$

$$ {}^{A}_{Z}P + e \longrightarrow {}_{Z-1}{}^{A}D + \nu + K_T \qquad \text{electron capture (EC)} $$

where: $K_T$: the total kinetic energy, $\upsilon$: the neutrino, $\bar{\upsilon}$: the antineutrino, $\beta^{+}$: the positron, $\beta^{-}$: beta particle, ${}^{A}_{Z}P$: parent nucleus with an atomic number z and a mass number A, e: an electron.

### 1.5.3: Gamma Ray

Electromagnetic radiation (photons) emit in discrete energies from the product nuclides as they are left in an excited state (isomers), called (isomeric transitions), it has a high ability to penetrate objects and soft tissues as a result, it causes health risks to human [6].

There are two types of isomeric transitions, short – lived transitions and long – lived transitions, short – lived isomeric transitions occur immediately after a decay process as in beta decay of Rubidium – 86 to Strontium – 86. Long – lived isomeric transitions take a long period of time as in gamma decay of Tin – 119m to Tin – 119. The annihilation of the electron and the positron is accompanied by emitting two photons of gamma each one has an energy equals to 0.51 MeV [21].

## 1.6: Solid State Nuclear Track Detectors (SSNTDs)

In 1961, Fleischer, Price, and Walker, American scientists discovered the idea of SSNTDs. In the beginning, the substances of SSNTDs were natural substances such as minerals, and then, many of them were artificially made [22].

These detectors depend on the damage that occurred by the incident charged particle on dielectric materials such as crystals, inorganic glasses, and plastics, the damage in the material is referred to as a track. The track formation depends on the energy of the incident particle, the tracks are not formed unless the rate of energy dissipation exceeds a critical value and the store of tracks in the material for some time depending on the electrical resistivity of the material [23].

In general, materials with electrical resistivity are larger than 2000 ohm. cm can keep tracks, as a result, tracks are not formed in metals and semiconductors. Tracks can be defined as damage regions composed mainly of displaced atoms rather than electronic defects so that they are unchanged over time. The diameter of the track's opening ranges between (1 – 10) nm and the length of the track represents the range of the charged particle in the material [23].

The detection threshold for SSNTDs represents the ratio between the atomic number (Z) and the reduced velocity β, where $\beta = \frac{V}{C}$, and it represents the minimum detection limit of a detector. The values of this ratio (Z/β) for CR-39

detector, Cellulose Nitrate (CN), Cellulose Acetate (CA), and Lexan are 6, 30, 40, and 60 respectively. Also, the detection thresholds can be described in terms of the energy loss rate, where for inorganic SSNTDs is 15 Mev/mg.cm$^2$ and for organic SSNTDs such as Lexan, CN – 85, CR-39 and SR-86 are 4, 1, and less than 0.05 MeV/mg.cm$^2$ respectively [23].

The key properties of SSNTDs make them widely used in the field of nuclear physics. Where they are inexpensive and convenient to use. They can be obtained in any size. The register of tracks stays permanent for the phenomenon under study. SSNTDs do not get affected by the variations of the atmospheric conditions such as temperature, pressure, humidity .... etc. They do not show any sensitivity to light, beta radiation, gamma-ray, and X-ray, and the etching process for SSNTDs is simple. Many rapid techniques are used with SSNTDs to count the number of tracks occurring [23].

## 1.7: Some Concepts Related to Radiological Protection

### 1.7.1: Absorbed Dose (D)

It is the energy dose imparted to the material per unit mass and it was used with all types of radiation. It is measured in gray (Gy), rad, erg/g and J/Kg, where $1\ Gy = 1\frac{J}{kg} = 100\ rad = 10000\ erg/g$ [24]:.

### 1.7.2: Equivalent Dose ($H_T$)

The effect of different types of radiation on a biological material can be represented with a quantity called equivalent dose, it represents the sum of the multiplication of the radiation weighting factor ($W_R$) with the absorbed dose by a certain tissue [24]. The units of $H_T$ are Sievert (Sv) in SI and roentgen equivalent man (rem), where 1 Sv= J/Kg = 100 rem [24].

**Table (1 – 1): Values of $W_R$ for different types of radiation according to ICRP 60** [12,26].

| Particulate radiation | $W_R$ |
|---|---|
| Photons, electrons with all energies | 1 |
| Protons | 2 |
| Alpha particle, fission fragment, and heavy nucleus | 20 |
| Neutrons with energy does not exceed 10 keV | 5 |
| Neutrons with energy in the range (10 – 100) keV | 10 |
| Neutrons with the range of energy (100 – 2) MeV | 20 |
| Neutrons with the range of energy (2 – 20) MeV | 10 |
| Neutrons with energy that exceeds 20 MeV | 5 |
| Protons with energy that exceeds 2 MeV | 5 |

## 1.7.3: Effective Dose (E)

It represents the effect of different types of radiations on different types of tissues of the body, where each tissue has its weighting factor ($W_T$) as shown in Table (1 – 2). The unit of effective dose is Sv, and it can be calculated for different types of radiations [24]:

**Table (1 – 2): Values of $W_T$ for different types of tissues** [12,26].

| Type of Tissue | $W_T$ |
|---|---|
| Lung, colon, bone marrow (red), and stomach | 0.12 |
| Bladder, breast, esophagus, liver, and thyroid | 0.05 |
| Skin and bone surface | 0.01 |
| Gonads | 0.20 |
| Others | 0.05 |

## 1.7.4: Linear Energy Transfer (LET)

LET represents the deposited energy by an incident charged particle per unit path length in the material [11]. The radiations with (LET) such as alpha particles

and fission fragments can cause biological damage to the cells more than those with low LET such as gamma, Xrays, and beta particles [5]. The density of energy deposition in the cell for a photon and an ion is shown in the following figure:

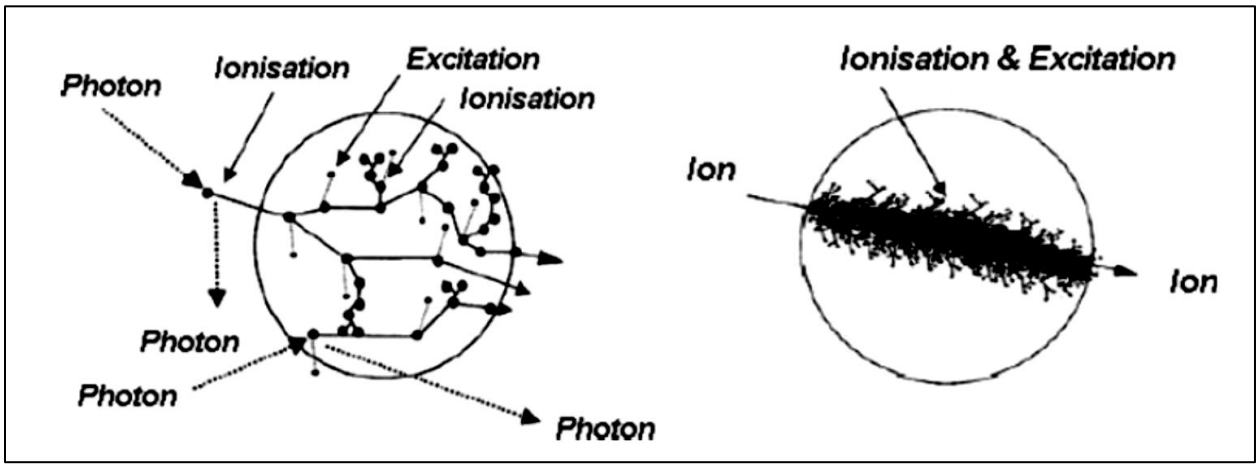


**Figure (1 – 5): A density of energy deposition in the cell for a photon and an ion** [12,27]**.**

LET is also referred to as "stopping power", LET stands on the charge and the velocity of the charged particle and the material in which the particle lose its energy through the interaction with the electrons of the atoms and with the nucleus. LET can be calculated in MeV/cm or keV/μm [27].

## 1.8: Previous Studies

The health risks related to Radon gas in many countries propelled many researchers worldwide to focus on this issue in their country, here we have some studies that were conducted by some researchers in Iraq from 2011 to 2022 about Radon gas monitoring:

**In (2011), Ali K. Hasan et al.,** measured Radon gas concentration in soil gas for fifteen locations in Al-Najaf city, Al-Najaf governorate, Iraq by using a RAD7 monitor, the results were for four depths (5cm, 25cm, 35cm, and 60cm), the

maximum value was 9290∓400 Bq/$m^3$ at depth 60cm, and the minimum value was 9∓17 Bq/$m^3$ at depth of 5cm [28].

**In (2012), Israa Kamil Ahmed,** measured Radon gas concentration for fifty-four soil samples collected from three sectors of AL-Ansar region, Al-Najaf governorate, at the first sector, the results varied from 56.2 – 758 Bq/$m^3$, and at the second sector, the results ranged between 66.7 – 660 Bq/$m^3$, and at the third sector were between 758.6 – 106.6 Bq/$m^3$, some of the results were above the accepted limits, that is why, there were cancer cases in this region [29].

**In (2013), Zakariya A. Hussein *et al.*,** measured the concentration of Radon gas for different types of building materials used in Iraqi markets by using the can technique, the maximum value was in sand 480.71 Bq/$m^3$ and the minimum value was in ceramic tiles 154.3 Bq/$m^3$ [30].

**In (2013), Ali Abid Abojassim and Ahmed Rahim Shitake,** used RAD7 monitor to measure Radon gas concentrations in some samples of drinking water collected from Al-Najaf city, the results ranged between 2.4 Bq/$m^3$ and 225 Bq/$m^3$, all the results were within the accepted limits of WHO [31].

**In (2014), Ali Abdulwahab Ridha *et al.*,** determined the concentration of Radon gas for samples of soil and channel water collected from different regions in Salahaddin province by using CR-39 detectors, the results for soil samples varied from 100.75±11.25 Bq/$m^3$ to 45.25±15.75 Bq/$m^3$, and the results for water samples ranged between 0.46±0.11 Bq/L and 0.24±0.10 Bq/L, all the results were within the accepted limits recommended by (ICRP) agency [32]**.**

**In (2015), Ali Abid Abojassim *et al.*,**. measured the concentration of Radon gas for twenty-four samples of ground water taken from Al-Haidariya region/ Al-Najaf

governorate by using a RAD7 monitor, for different times, the results were between 1270 Bq/$m^3$ and 66 Bq/$m^3$, the results expressed that the concentration of radon gas decreased as time increased and there is a good agreement between experimental and theoretical results, all the results were under the safe limit recommended by EPA [33].

**In (2016), Khalid Hussain Hatif *et al.*,** measured the concentration of Radon gas dissolved in drinking water for sixteen schools of AL-Kifel region/ Babylon governorate by using a RAD7 monitor, the maximum value was 1150 Bq/$m^3$ (1.15 Bq/L) and the minimum value was 0.0362 Bq/L (360.2 Bq/$m^3$), the results did not show any radiological risks for the people living in the study area [34].

**In (2017), Ali Abid Abojassim *et al.***, measured the Radon gas concentration of 10 samples of soil collected from different locations in Al-Najaf Governorate, Iraq, by using CR-39 detectors and CN-85 detectors ( sealed can technique), the results ranged between 506 Bq/$m^3$ and 1194 Bq/$m^3$ with a mean value equals 894 Bq/$m^3$, an exhalation rates, annual absorbed dose, effective dose equivalent, and Annual Effective Dose were also calculated in this study [35].

**In (2018), I. T. Al-Alawy and A. A. Hasan,** measured the Radon gas concentrations for some well water samples collected from various locations in Karbala province, Iraq by using CR-39 detectors ( sealed can technique), the maximum value was 4112 Bq/$m^3$ in Al-Hurr region and the lowest value was 2156 Bq/$m^3$ in Hay Ramadan region, and the average value was 2840 Bq/$m^3$, all the results were within the accepted limits where the recommended limit equals 11000 Bq/$m^3$ (11 Bq/L), and this study also involved calculating the annual effective dose resulting from these samples and it was under the safe limit [36].

**In (2019), Ahmed A. Sharrad and Abdulameer K. Farhood,** measured Radon gas concentration for thirty locations located around Sawa lake, Samawa city, south of Iraq, by using RAD7 monitor, the results lied between 86 $Bq/m^3$ and 6448 $Bq/m^3$, the doses due to inhalation was within the accepted limits according to WHO and ICRP [37].

**In (2019), Abdalsattar Kareem Hashim and Sara Salih Nayif,** assessed Radon – 222 gas concentrations in the air of some schools in Karbala city using SSNTDs (LR-115 TypeII and CN-85), the results showed that the concentrations ranged between 13 $Bq/m^3$ to 38 $Bq/m^3$ with an average of 25 $Bq/m^3$ using LR-115 TYPEII, and the results for CN-85 were between (13 – 36 ) $Bq/m^3$ with an average of 34 $Bq/m^3$ [38].

**In (2020), Ali Abid Abojassim,** made a comparative study between a passive technique (CR-39 detectors) and an active technique (RAD7 monitor) by measuring some samples collected from the ground water at Al-Najaf city, the correlation coefficient between the techniques was 0.8, and the results of passive technique varied between 179 $Bq/m^3$ and 557 $Bq/m^3$, while the results of active technique ranged from 174 $Bq/m^3$ to 2000 $Bq/m^3$ [39].

**In (2020), Abdalsattar K. Hashim *et al.*,** measured Radon gas concentration in the air of twenty five buildings located around Imam Hussain holy shrine, Karbala province, Iraq, by using CR-39 detectors, the results were between 39.3 $Bq/m^3$ and 23.9 $Bq/m^3$, and it did not pose any risk to the inhabitants inside these building according to the international limits [40].

**In (2021), Abdalsattar Kareem Hashim *et al.*,** measured Radon gas concentrations in air and soil of some buildings in the city of Karbala, Iraq, by using CR-93 detectors (sealed can technique), the results of soils varied from

28.44∓0.58 Bq/$m^3$ to 479.76 Bq/$m^3$ with an average of 220.33 Bq/$m^3$ and for air, ranged from 1.95 Bq/$m^3$ to 46.82 Bq/$m^3$, the average value of this study was 21.52 Bq/$m^3$ [41].

**In (2022), Awsam Abdulsattar Marzaali *et al.***, measured Radon gas concentration for twenty samples of ground water in Dhi-Qar governorate, Iraq, by using a RAD7 monitor, the results ranged between 320 Bq/$m^3$ to 7800 Bq/$m^3$, with an average of 5200 Bq/$m^3$, some results were above the permissible limit recommended by WHO for drinking water, but all the results were within the permissible limit recommended by EPA [42].

## 1.9: The Aim of the Study

1 – This study aims to carry out a preliminary survey of Radon gas concentrations in the soil of Al-Najaf refinery.

2 – Monitor the concentrations of Radon gas dissolved in different types of water inside Al-Najaf refinery.

3 – Identifying the health risks and the environmental problems that may result from the concentrations of Radon gas in the soil and water inside Al-Najaf refinery.

# Chapter Two

# Theoretical Part

## 2.1: Introduction

Radon – 222 (Rn) element is one of the noble gases, and it is the heaviest one. There are thiree isotopes for Radon, all of them are radioactive, and they are present naturally, they are Radon – 222 (Radon), Radon – 219 (Actinon) and Radon – 220 (Thoron), they are constantly produced from Uranium – 238 series, Uranium-235 series and Thorium-232 series, respectively [43].

Radon element was discovered by a German scientist Friedrich Ernest Dorn after the discovery of Uranium – 238, Thorium, Radium – 226, and Polonium by others. The concern about radon gas emission began in 1900 when Dorn published his first paper [43]. The environment that people live in contains natural radiation (background radiation), and all people receive a daily dose resulting from this natural radiation [24].

The largest fraction of the dose that people receive due to natural radiation comes from Radon-222 gas as shown in Figure (2 – 1) [24].

Many organizations focus on the issue of radiation protection, and develop recommendations about public protection such as “Environmental Protection Agency” (EPA), “The Nuclear Regulatory Commission”, “The Department of Energy” (DOE), “The International Commission on Radiological Protection” (ICRP), The Health Physics Society, World Health Organization (WHO), The International Atomic Energy Agency (IAEA) and “The Commission of the European Communities” (CEC) [44].

EPA (2003), “United Nations Scientific Committee on the Effects of Atomic Radiation (UNSCEAR) 2000” and “Committee on the Biological Effects of Ionizing Radiation (BEIR) 1999” consider radon gas and it’s progenies inhalation is a main source of exposure coming from natural radiation [45].

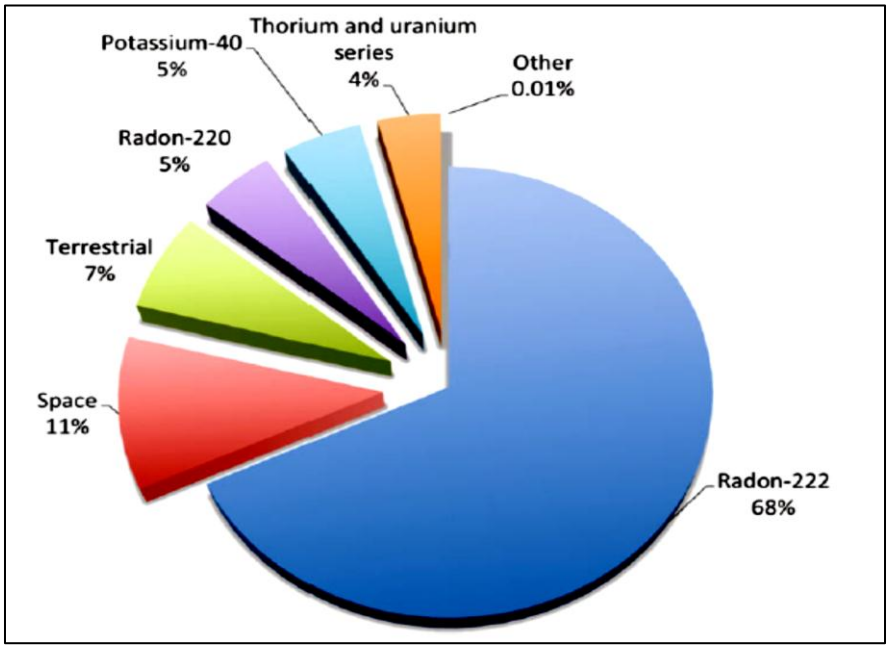


**Figure (2-1): Background dose distribution in USA** [46]**.**

## 2.2: Radon-222 Gas Properties

Radon element with an atomic number of 86 has characteristics that lie between metals and non–metals, therefore, it is a metalloid element like Silicon, Boron, Germanium, Arsenic, Tellurium, Polonium, and Astatine. The heat of vaporization is defined as the energy needed to overcome interatomic attractive forces, radon–222 gas has the highest value of it, as it increases with the increase of the atomic number [1].

The mean atomic velocity of Radon gas is slower than other noble gases which equal 165 m/s (at a "mean global temperature of 14 °C"), radon gas like other noble gases is a chemically inert gas. Table (2 – 1) shows the physical, atomic, and chemical, properties of Radon – 222 gas, and Table (2 – 2) shows the nuclear and physical properties of Radon – 222 gas, thoron, and actinon, it shows that the half–life of Radon – 222 gas is less than Radon – 220 gas (Thoron), as a result, the abundance of Radon–222 is higher than thoron [1].

The solubility of Radon gas is very high as this property increases with the increase of atomic number (Z), and Radon–222 gas is more soluble in organic liquids in comparison with water [1].

**Table (2 – 1): Physical, atomic, and chemical properties of radon–222 gas** [43].

| Property | Values |
|---|---|
| Standard atomic weight | 222 |
| Outer shell electron configuration | $6s^2 6p^6$ |
| Density | 9.73 kg/$m^3$ at (0 °C, a pressure of $1.013\times10^5$ Pa) |
| Melting point | -71 °C |
| Normal boiling point | -64 °C |
| Heat of fusion | 3.247 kJ/mol |
| Heat of vaporization | 18 kJ/mol |
| The enthalpy of the first ionization | 1037 kJ/mol |
| Oxidation number | 0, 2, and 6 |
| Electronegativity | 2.2 (Pauling scale) |
| Covalent radius | 0.150 nm |
| Van der Waals radius | 0.220 nm |

**Table (2 – 2): A comparison among Radon–222, Radon–220 and Radon–219** [43].

| Parameter | Radon-222 | Radon-220 | Radon-219 |
|---|---|---|---|
| Half-life | 3.823 day | 55.83 s | 3.983 s |
| Decay constant | $2.098\times10^{-6}$ $s^{-1}$ | $1.242\times10^{-2}$ $s^{-1}$ | 0.174 $s^{-1}$ |
| Average recoil energy on formation | 86 keV | 103 keV | 104 keV |
| Diffusion coefficient in air | $1\times10^{-5}$ $m^2/s$ | - | - |
| Diffusion coefficient in water | $1\times10^{-9}$ $m^2/s$ | - | - |

## 2.3: Radon Gas Health Risks

Radon gas is a carcinogenic gas, which is considered the second factor which leads to lung cancer after tobacco smoking according to the National Institute for Occupational Safety and Health (NIOSH) in 1971 and the World Health Organization (WHO) in (1987 and 2009), The National Research Council (NRC) in 1999, and the studies conducted on miners showed that there is a link between exposure to Radon-222 gas and lung cancer, according to ICRP(2012), adults aged 30 – 35 year need 5 years to develop lung cancer and this period changing according to work and person's habit (smoker or non-smoker) [4,47]. Henshaw and others claimed that radon gas is also related to other cancers such as melanoma, cancer of the kidney, and prostate [5]. Radon gas progenies can easily get stuck to aerosols in the air, skin, and any other surfaces [6].

Living cell exposure to alpha particles that comes from radon gas and its progenies decay leads to cytogenetic effects, such as mutations, chromosome aberration, cell cycle modification and an increase in protein production [6].

The dose delivered to the cell in the airways of the lung depends on the size of the deposited aerosols. The dose that comes from Radon gas is lower than the dose that comes from radon gas progenies because of the location of the Radon gas atom in the airway relative to the target cell. The dose that comes from Radon gas dissolved in the tissue is also smaller than the dose which comes from Radon gas decay products [7].

In addition to lung cancer risk, dissolved radon gas in the water can directly affect the sensitive cells of the gastrointestinal tracks but this effect depends on Radon atoms, where alpha particles are not able to pass through the mucus layer lining the epithelium, and therefore, the stem cells of the stomach wall are not affected. But, Radon–222 gas dissolved in blood has a risk to the other organs [48].

## 2.4: Radon Gas Sources

Radon gas comes from Radium element decay, where Radium element is one of the Uranium-238 series members as shown in Figure (2 – 2), and it can be found in rocks, soils, and building materials, with different concentrations [8].

This means Radon gas can be emitted from many products containing an amount of Uranium-238 or one of its progenies such as cigarettes [9].

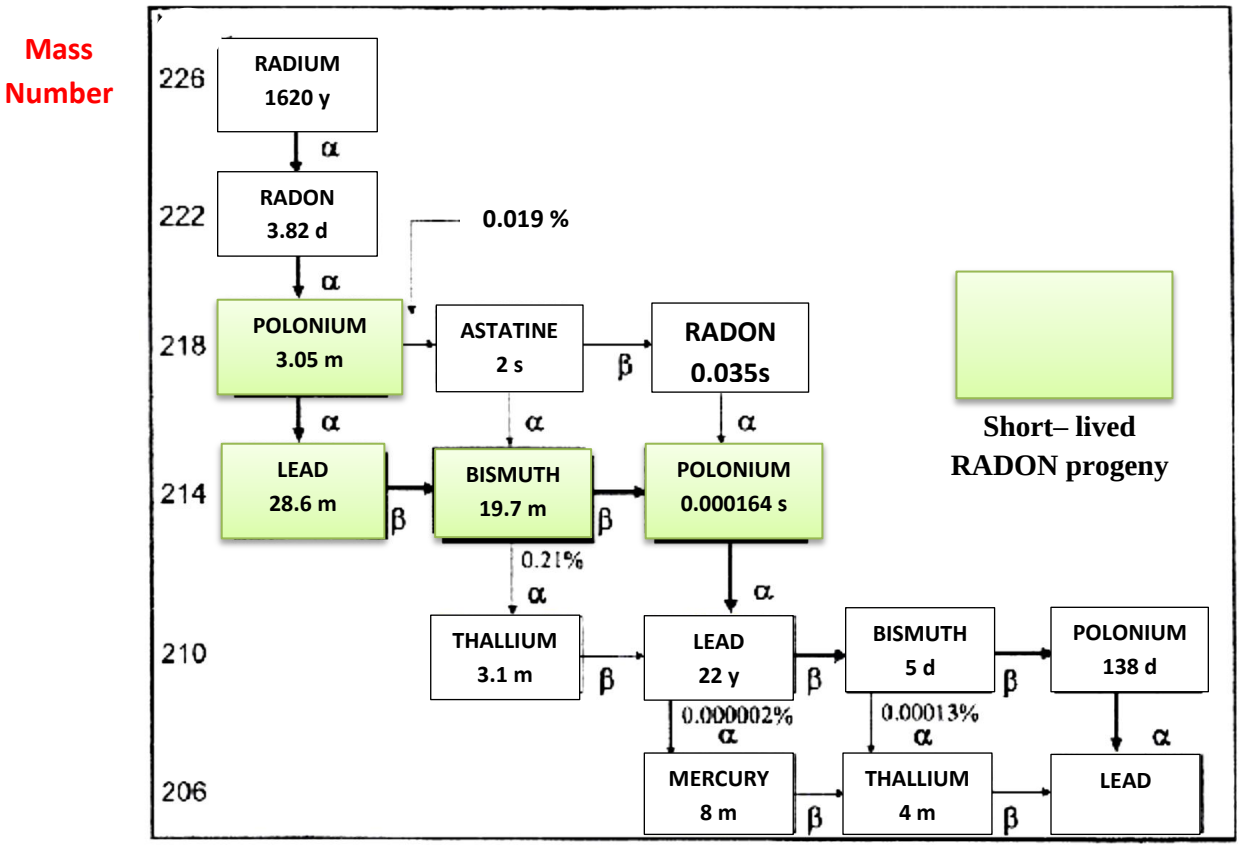


**Figure (2 – 2): Radon decay chain** [49].

## 2.4.1: The Radon in Soil and Rocks

The soil is derived from rocks, and the mineralogy of the soil depends on two factors, the first one is the natural conditions by which the soil is formed and the second one is the minerals in rocks from which the soil is derived, where rocks are merely combinations of minerals, and minerals have specific chemical

compositions. Rocks in general can be classified into three main types: igneous rocks, sedimentary rocks, and metamorphic rocks.

The soil has three phases: solid phase, gas phase, and liquid phase. The solid phase consists of minerals and a small amount of humus (organic particles), the proportion of this phase in the soil is nearly half of the soil's volume. The other phases' proportions occupy the other half of the soil's volume and vary according to the soil's moisture, as shown in Figure (2 – 3 (a)). The minerals of soil consist of particles of various sizes, and they are classified into three types: sand, silt, and clay, as shown the Figure (2 – 3 (b)).

Quartz is usually the dominant mineral in sand because it is the most resistant to weathering of the common minerals in rocks; thus, its breakdown is extremely slow. Many other minerals are found in sand, depending on the rocks from which the sand derived. The pores of soil may be filled with water or air, the air inside the pores has the same composition of the atmospheric air if the surface of soil has free exchange [50].

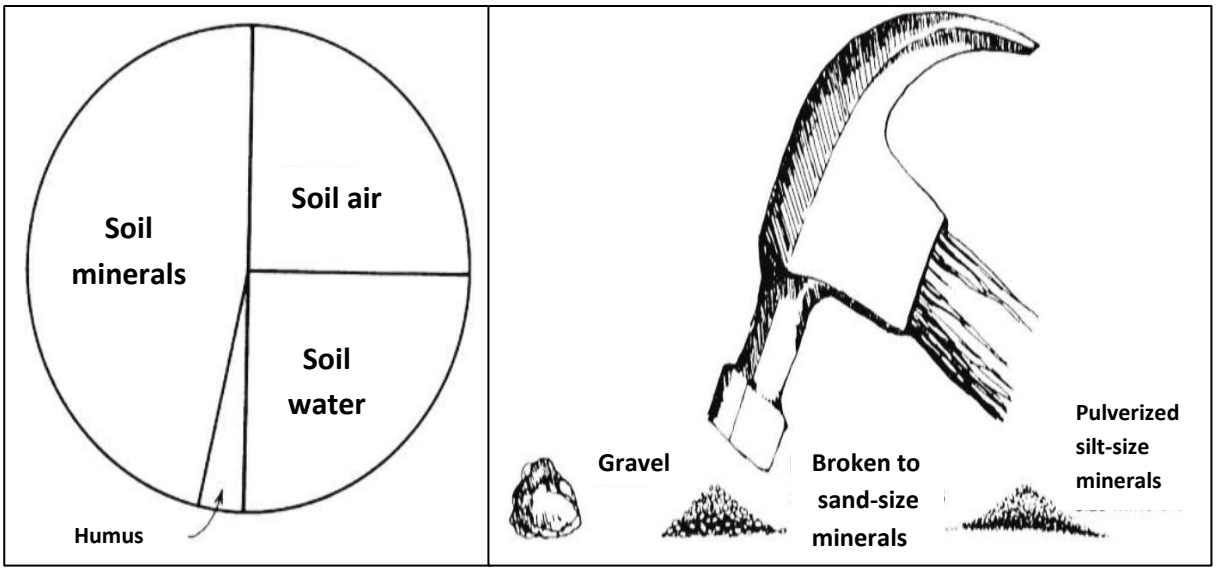


(a) (b)

**Figure (2 – 3): (a) Soil phases proportions at the surface of a moist soil.**
**(b) The surface area of the soil increases when it is pulverized** [50]**.**

The concentration of Radium is not constant, it varies from material to another as shown in Table (2 – 3). Radium content determines how many Radon atoms are emitted from the material or emanated from the pores of the soil. There are other factors influence Radon-222 emanation from the soil such as the size of the grain, permeability of the soil, temperature and pressure [51].

Radon–222 emission is highly dependent on the concentration of Uranium, and the concentration of Uranium depends on the location of the soil [52,53].

**Table (2 – 3): Radium content for different materials from previous studies in Iraq.**

| Material | Region, country and year | Radium content (Radium-226) | Refrence |
|---|---|---|---|
| Storm dust | AL-Najaf, Iraq, 2013 | (52.99 – 13.04) Bq/kg | [54] |
| Soil | Al-Najaf, Iraq, 2014 | 22.455 Bq/kg | [55] |
| Soil | Al-Najaf, Iraq, 2017 | (77.19 – 181.95) Bq/kg | [35] |
| Building materials | Kurdistan, Iraq, 2013 | (3.35 – 9.72) Bq/kg | [30] |
| Building materials | Local markets, Iraq, 2015 | (0.037 – 4.986) $Bq/m^3$ | [57] |
| Oily wastes | Oil fields, Basrah, 2013 | (96452∓160 – 38∓4) Bq/kg | [58] |

Soil moisture prevents the emanation of Radon – 222 gas from the soil surface and the diffusion in the soil pores where soil moisture becomes a thin film of water surrounding soil grains and capture radon recoils from the solid matrix, as a result, Radon – 222 atoms remain in the pore space instead of crossing the pores [56,59]. When Radium – 226 decays in the grain, Radon-222 is released from the solid by recoil to the pore space, this decay must occur within the range of the recoil distance, where the recoil distance in common minerals is from 20 nm to 70 nm, 100 nm in water and 63 μm in the air [59].

Radon gas inside soil pores can be transported to outer space through advection or diffusion and this transportation is called emanation. The fraction of gas atoms that are released inside the soil pores is called the coefficient of the emanation, or the emanation power or, the emanation factor, the value of the emanation power ranges between 0.05 and 0.7 [59].

Molecular diffusion of Radon gas is the process by which molecules migrate toward regions with lower concentrations. Advection flow is the process by which the air flows from regions with high pressure to regions with low pressure. the temperature inside buildings is lower than the temperature inside the pore space, this leads to an air flow from soil to indoor air [7].

Radon atoms inside the pore space are partitioned between water and air, this partitioning is described by the Oswald coefficient as given by [7]:

$$\text{Oswald coefficient} = \frac{C_W}{C_a} \qquad (2.1)$$

where $C_W$ is the concentration of Radon gas in the water inside the pore space and $C_a$ is the concentration of Radon gas in the air inside the pore space.

The Oswald coefficient varies inversely with temperature, it equals to 0.3 at 10 °C and it becomes 0.5 at 0 °C. this means that $C_W$ increases with an increase in temperature [7].

## 2.4.2: Radon in Water

Radon – 222 gas is soluble in water, where its solubility increases with the increase of temperature, pressure, acidity, and Carbon dioxide saturation [60]. It transfers to the indoor or outdoor air via agitation caused by many activities related to water usage.

Transfer coefficient represents the contribution of the initial average radon concentration in water to the indoor Radon concentration in air, and it is given by the following relation [7].

$$\overline{C_a} = T \times \overline{C_w} \quad (2.2)$$

where:

T: Radon gas transfer coefficient from water to air.

$\overline{C_a}$ : is the estimation of the average Radon gas concentration in indoor air.

$\overline{C_w}$ : is the average Radon concentration in water.

Water transfers a small amount of Radon gas to the air and the coefficient of transfer lying between $0.8\times10^{-4}$ and $1.2\times10^{-4}$, but the value of transfer coefficient which was adopted by EPA is $1 \times 10^{-4}$ [7].

Transfer factor value can be experimentally determined or by using mathematical models, one of these models estimate the contribution of Radon gas in water to air by measuring the rate of use of water per person (W), the volume of building per person (V), the volume V can be calculated by dividing the internal total volume of the building over the number of persons living inside it, transfer efficiency (e), Air Exchange Rate (A.E.R.), and the average of radon–222 gas concentration in water ($\overline{C_W}$), as shown in the following equation [7].

$$T = \frac{\overline{C_W} \times W \times e}{V \times (A.E.R.)} \quad (2.3)$$

Transfer efficiency (e) is the fraction of Radon–222 gas in water that is released to the air during domestic activities related to water use such as dishwashing, cloth washing, showering, cleaning and other uses.

Transfer efficiency (e) depends on the amount of water used per day and the concentration of Radon gas in the water and it can be experimentally determined by knowing the amount of Radon–222 gas concentration transferred to the air during a certain activity [61].

In general, Radon gas concentration for the surface water is less than 4000 $Bq/m^3$, while ground water contains high levels of Radon gas that may reach up to $10^7$ $Bq/m^3$ [48].

### 2.4.3: Radon in Oily Wastes and Oily Products

The wastes resulting from the oil industry, such as sludge and scale contain an amount of Radium, the Radium content in sludge is not constant because the sludge has a complex chemical composition, but in the scale, the variation of Radium content is relatively less than the sludge content [62].

Oily products such as diesel, jet fuel, gasoline, crude oil, sour kerosene, sweet naphtha and asphalt contain amounts of Uranium – 238, Thorium – 232, Radium – 226, Potassium – 40 and Uranium – 235, so, these products emit Radon – 222 gas with different concentrations [63].

### 2.4.4: Radon in Building Materials

Building materials such as sand, block, soft gypsum, bricks, white cement, stone, dye powder, limestone, ceramics, marble, granite, gravel, porcelain and thermostone contain an amount of Radium, as a result they emit Radon gas, Radon exhalation rate from these materials should not exceed the average of the world exhalation rate which equils $57.6 \times 10^{-3}$ $Bq.m^{-2}.h^{-1}$ ($16\times10^{-3}$ $Bq.m^{-2}.s^{-1}$) [57].

### 2.4.5: Radon in Other Sources

A cigarette is a source of Radon – 222 gas as tobacco leaves contains an amount of Uranium – 238 which comes from soil and phosphate fertilizers, the concentration of Radon – 222 gas in tobacco differs from product to another [64]. Decorations that are used in the walls of homes such as mirrors, rocks, white cement, Alabaster and cement can emit Radon – 222 gas and the emission depends on the materials from which the products are made [65].

## 2.5: Quantities, Definitions and Units Related to Radon Gas

1- **Radon Activity Concentration ($C_{Rn}$)**: Radon activity per unit air volume. The unit of $C_{Rn}$ is $Bq/m^3$ [48].

2- **Cumulative Radon Activity Concentration ($P_{PAEC}$)**: The Radon activity concentration over exposure time, and the unit of $P_{PAEC}$ is ($Bq/m^3$)h [66].

$P_{PAEC}= C_{Rn}\times$ exposure time (2.4)

3- **Radon Exposure**: a general term for cumulative Radon activity concentration $C_{Rn}$ and cumulative potential alpha energy concentration [66].

4- **Working Level (WL)**: a combination of the short-lived progenies in 1 liter of air which gives a maximum release of energy $1.3 \times 10^5$ meV, and this energy comes from alpha particles. From the definition, one can concludes that WL=$1.3\times10^5$ meV/L= $2.08\times10^{-5}$ $J/m^3$ [67].

5- **Equilibrium-Equivalent Decay-Product (EEDC)**: defined as the collective activity of Radon – 222, Polonium-218, Lead-214 and Bismoth-214 [67].

$$EEDC = 0.106A_{Polonium-218} + 0.213A_{Lead-214} + 0.381A_{Bismoth-214} \quad (2.5)$$

6- **Equilibrium Factor:** it is referred to as the ratio of the equilibrium equivalent concentration ($C_{eq}$) to the Radon activity concentration ($C_{Rn}$) [66].

$$F = \frac{C_{eq}}{C_{Rn}} \quad (2.6)$$

where $C_{eq}$ is Equilibrium Equivalent Concentration (EEC) and is given by the following relation:

$C_{eq}= 0.105\ A_{Polonium-218}+ 0.516\ A_{Lead-214}+ 0.379\ A_{Bismoth-214}$ (2.7)

7- **Action Level:** the level of the concentration of the activity, above which, remedical procedures or protective actions should be taken in the case of chronic exposure or an emergency exposure situation, the purpose behind the action levels is to protect the public and workers in the workplace, but this concept is superseded by a concept called a reference level [68].

8- **The Annual Effective Dose for Inhalation (AED $_{inhalation}$)**: the Annual Effective Dose can be calculated according to Equations [69,70]:

$$AED_{indoor\ inhalation}(\mu Svy^{-1}) = \overline{C_W} \times T \times F \times O \times DCF \quad (2.8)$$

Where: $\overline{C_W}$: is the average of Radon gas in water samples in kBq/m$^3$, T: is the transfer factor ($10^{-4}$ according to EPA), F: is the equilibrium factor between Radon gas and it's products which equals 0.4, O: is the average occupancy time per person at indoor air which equals 7000 h/y, and DCF: is the Dose Conversion Factor for Radon exposur which equals 9 nSvy$^{-1}$ (Bq/m$^3$)$^{-1}$ [69]. The Annual Effective Dose ($AED_{outdoor\ inhalation}$) in (mSv/y) due to radon gas inhalation in the outdoor air can be calculated due to the following equation [37,71]:

$$AED_{outdoor\ inhalation} = C_{\text{Radon near the soil}} \times F \times I \times DCF \quad (2.9)$$

where: F: is the equilibrium factor between Radon gas and it's progenies (0.6), I: is the mean of time spent at outdoor air for a person per year (1760 hy$^{-1}$), and DCF: the Dose Conversion Factor (9000000 mSv.m$^3$/h for Radon exposure) [37].

9- **the Lung Cancer Risk (LCR) in (case/year.million):** the exposure to Radon progenies($E_P$) and Potential Alpha Energy Concentration (PAEC) can be calculated according to the following equations [72]:

$$LCR = AED_{inhalation}(\frac{mSv}{y}) \times (18 \times 10^{-6})(\frac{y}{mSv}) \quad (2.10)$$

$$E_P(\frac{WLM}{y}) = \frac{8760 \times n \times F \times \overline{C_a}}{170 \times 3700} \quad (2.11)$$

$$PAEC\ (WL) = \frac{F \times \overline{C_a}}{3700} \quad (2.12)$$

Where: (n=0.8) is the fraction of time spent indoors, 8760 is the number of hours per year, and 170 is the number of working hours per month. The concentration of radon gas in Equations (2.11 and 2.12) is in Bq/m$^3$.

**10- Radon Entry Rate:** the Radon activity entering a building per unit time, Bq/s is the unit of Radon entry rate [48].

**11- Working Level Month (WLM)**: the unit of potential alpha energy exposure, it represents the cumulative exposure resulting from breathing of air with a concentration of 1 WL during 170 h (working hours per month) [48].

$$WLM=WL\times170 \quad (2.13)$$

**12- Potential Alpha Energy (PAE)**: the sum of alpha energies resulted from Radon – 222 and its short-lived progenies in radiological equilibrium. The unit of PAE is J (Joule)= $6.242\times10^{12}$ MeV [66].

## 2.6: Passive Method Calculations

In cup technique (passive method), the concentration of Radon – 222 gas in the air of the space inside the cup ($C_{Rn}$) is given by th following equation [73,74]**:**

$$C_{Rn} = \frac{\rho_t}{KT} \quad (2.14)$$

where: $\rho_t$: is the track density in (Track/cm$^2$), k: calibration factor in (track. m$^3$/ Bq. cm$^2$. day) and T: exposure time in (day)**.**

The concentration of Radon gas in sample (C) can be calculated according to Equation (2.15), where the thickness of the sample inside the cup was taken into the consideration [73,75]:

$$C = \frac{\lambda_{Rn}\times C_{Rn}\times h\times T}{thickness\ of\ the\ sample\ inside\ the\ cup} \quad (2.15)$$

Radium concentration in the soil ($C_{Ra}$) in (Bq/kg) can be calculated using the following equation [35]:

$$C_{Ra} = \frac{\rho_t h A_S}{M_S K T_e} \quad (2.16)$$

where h is the distance between the detector and the surface of the sample in (cm), $A_S$: is the sample surface area ($cm^2$), $M_S$: sample mass in (kg), $T_e$: is the effective exposure time in (day) as shown in the following equation [35]**:**

$$T_e = T - \frac{1}{\lambda_{Rn}(e^{-\lambda_{Rn}T}-1)} \quad (2.17)$$

where $\lambda_{Rn}$: is the Radon decay constant in ($day^{-1}$), the area exhalation rate ($E_A$) in ($Bq.m^{-2}.h^{-1}$), mass exhalation rate ($E_M$) in ($Bq.kg^{-1}.h^{-1}$), $A_{Rn}$ is the Radon – 222 activity in (Bq) are given by the following equations [35]**:**

$$E_A = \frac{C \times V_{cup} \times \lambda_{Rn}}{A_S[T+\lambda_{Rn}{}^{-1}(e^{-\lambda_{Rn}T}-1)]} \quad (2.18)$$

$$E_M = \frac{C \times V_{cup} \times \lambda_{Rn}}{M_S[T+\lambda_{Rn}{}^{-1}(e^{-\lambda_{Rn}T}-1)]} \quad (2.19)$$

$$A_{Rn} = C_{Rn} \times V_{cup} \quad (2.20)$$

Also, $A_{Rn} = \lambda_{Rn} N_{Rn}$ (2.21)

$\lambda_U N_U = \lambda_{Rn} N_{Rn}$ (secular equilibrium) (2.22)

The weight of Uranium ($W_U$) and the Uranium concentration ($C_U$) in (g/kg) (or can be calculated in (mg/kg) and (part per million (ppm)) are given in the following equations [35]:

$$W_U = \frac{N_U \times W_{mol}}{N_{Av}} \quad (2.23)$$

$$C_U = \frac{W_U}{W_S} \quad (2.24)$$

where $V_{cup}$: The internal volume of the cup in ($m^3$) $\lambda_U$: Uranium-238 decay constant ($4.98\times10^{-18}$ $S^{-1}$), $N_U$: number of Uranium-238 nuclei, $W_U$: Uranium weight in (g), and $W_S$: sample weight in (g) [35]. Radon concentration near the soil ($C_{Radon\ near\ the\ soil}$) can be calculated as in the following equation [37]:

$$C_{\text{Radon near the soil}} = C\sqrt{d/D} \quad (2.25)$$

Where: d: the constant of the exhalation diffusion (0.05 $cm^2/s$), and D: eddy diffusion coefficient (50000 $cm^2.s^{-1}$) [37].

## 2.7: Radiological Equilibrium

Radiological equilibrium can be defined as the case in which the formation rate of the daughter from the parent nuclide equals it's decay rate. Radiological equilibrium depends on the values of half-lives for the parent and it's daughters, as a result, there are three cases of radiological equilibrium [76]:

## 1- Secular Equalibrium

It is also called long-term or permanent equilibrium, it occurs when the half-life of the parent ($t_{\frac{1}{2}P}$) is very long in comparison with the half–life of the daughter ($t_{\frac{1}{2}D}$). The activity of the daughter (the progeny) ($A_D$) at any time before reaching the equilibrium state can be written in terms of the activity of the parent nuclide ($A_P$) as shown in the following equations (2.26 and 2.27) [76]:

$$A_D = A_P(1 - e^{-\lambda_D t}) \quad (2.26)$$

$$N_D\lambda_D = N_P\lambda_P(1 - e^{-\lambda_D t}) \quad (2.27)$$

Where $N_D$, $N_P$, nuclei number of daughter and parent. The parent activity can be considered constant during the time of observation due to it's long half-life. The parent and the daughter reach to the secular equilibrium after seven daughters half-lives as shown in Figure (2 – 4), where the parent activity equals to the daughter activity, and the equations (2.26 and 2.27) become as the following [76]:

$$A_D = A_P \quad (2.28)$$

$$\frac{N_D}{N_P} = \frac{\lambda_P}{\lambda_D} = \frac{t_{\frac{1}{2}D}}{t_{\frac{1}{2}P}} \quad (2.29)$$

$$N_D = \frac{m_D \times N_A}{M} \quad (2.30)$$

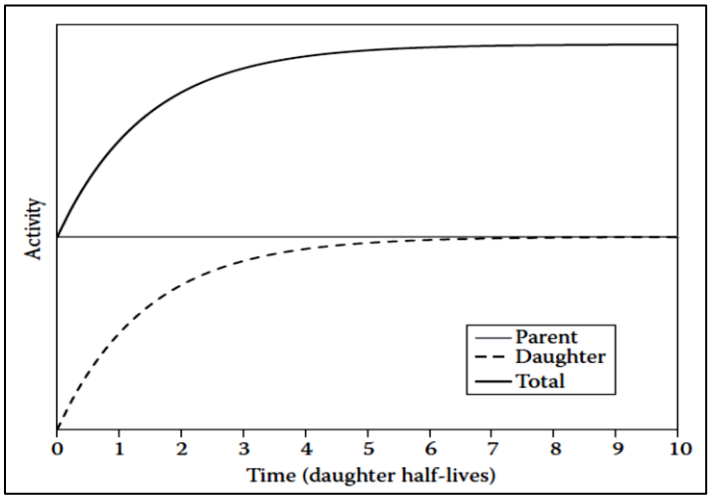


**Figure (2 – 4): Secular equilibrium** [76].

The mass and $t_{\frac{1}{2}P}$ can be determined by using Equations (2.26, 2.27 and 2.28) if the mass ratio and the half-life of the daughter are known.

## 2- Transient Equilibrium

In this case, the half-life for the parent is greater than the half-life for the daughter, but the values of the half-lives for the parent and the daughter are closer together. The time required for reaching the transient equilibrium is from 7 to 10 daughter half-lives as shown in Figure (2 – 5) and a lot of the parent nuclei decay during this period. The activity of the parent decreases with time and this decrease can be observed during the time of observation.

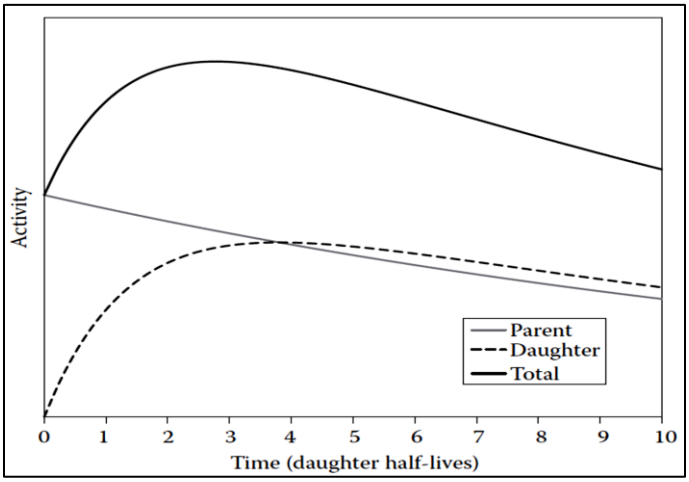


**Figure (2 – 5): Transient equilibrium** [76].

When the transient equilibrium is achieved, the following equations can be applied to calculate $A_P$ or $A_D$ [76].

$$\frac{A_P}{A_D} = 1 - \frac{t_{\frac{1}{2}D}}{t_{\frac{1}{2}P}} \quad (2.31)$$

$$N_D = \frac{m_D \times N_A}{M} \quad (2.32)$$

$$A_P = \lambda_D \times N_D \quad (2.33)$$

**3- No Equilibrium**

In this case, the half-life of the parent is shorter than the half-life of the daughter, and the mother is depleted before it's daughter as shown in Figure (2– 6), so that the mother has not reached to an equilibrium state with it's daughter.

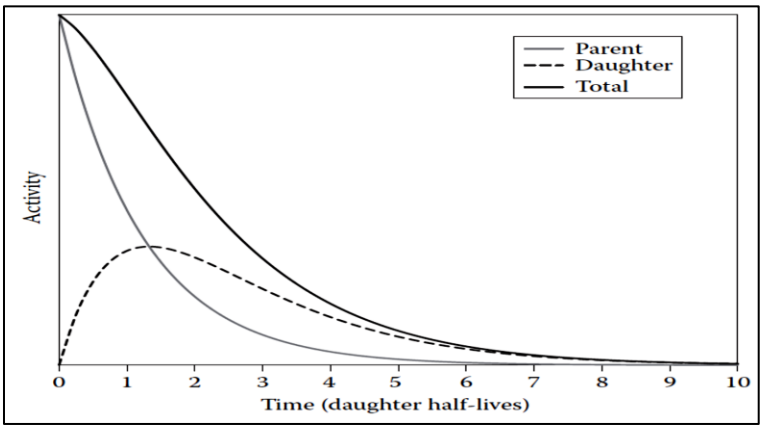


**Figure (2 – 6): No equilibrium between the parent and it's daughter** [76]**.**

## 2.8: The Safe Limits for Radon Gas Concentration

According to UNSCEAR (2000) report, the average value of Radon gas concentration in the soil gas over the world equals 4000 Bq/m$^3$ and the action level of radon gas concentration in the soil gas lies between (400 – 4000) Bq/m$^3$ [37].

EPA (Environmental Protection Agency) considered that the maximum contamination level of Radon gas in water to be equal 11 Bq/L (11000 Bq/m$^3$) [7].

According to WHO (2008), the safe limit of Radon gas concentration in water equals to 400 Bq/m$^3$ [42]. But, the department of public health in

Connecticut state in the USA recommended that the concentration of Radon gas in water should not exceed 5000 pCi/L (135 Bq/L or 135000 Bq/$m^3$), and it poses a health risk if the level of radon gas in water is above this value [77].

The safe limit of radon gas concentration in water ranges from 4 Bq/L to 40 Bq/L according to UNSCEAR, 2008 [69].

The safe limit for the Annual Effective Dose due to Radon gas inhalation (AED) recommended by WHO (2004) and European Council (1998) equils 0.1 mSv/y but ICRP recommended that AED to be equal to 1 mSv/y [37].

## 2.9: The Benefits of Radon Gas and It's Uses

1- Radon gas uses to treat rheumatic diseases, spondylitis, enclosing in this issue, there are three therapeutic systems: thermal bath, thermal gallery (old silver or gold mine) and vapor bath (vapor chamber) [78].

2- Radon gas emanations are used as tracer for predicting the occurring of the earth quakes [67]. Radon is also used as a tracer for helium exploration [79].

3- In geothermal areas, Radon gas measurements for the soil gas are used as a tool to determine the permeable zones [80].

4- Radon gas gives information about the masses, aerosols and contaminators (such as "dimethyl sulfide") in the air [67].

5- Determination of the coefficients of the vertical eddy diffusion in the ocean and other aqueous bodies [67].

6- Radon gas is used for the dating of ground water and as a tracer for monitoring no aqueous phase liquids [67].

7- Radon gas is used to identify the subsurface hydrocarbon deposits [67].

8- Study the exchange of gases between the sea and the air in the ocean, estuaries and lakes [67].

9- Calculation the amount of the ground water discharge [67].

## 2.10: Radon Gas Detection Techniques

Radon gas measurement techniques depend on whether the technique measures Radon gas (direct measurements) or its progenies (indirect measurements), time resolution and the type of radiation detected by the detector (alpha particles, beta emission, or gamma ray) [67].

Most of the techniques depend on alpha detection where alpha particles resulting from Polonium–218 decay are used to measure Radon–222 gas concentration and some methods depends on gamma radiation emitted from the decay of the radon progenies (Bismuth–214, Lead–214). There are three main techniques due to time resolution: grab-sampling technique, continuous technique and integrating technique [67]**.**

Grab sampling technique includes measurements of Radon–222 gas concentration in discrete (selective) samples of water or air collected during a very short period of time in comparison with the mean life of Radon–222 gas. RAD7 monitor (active method) works according to this technique when it is used for measuring Radon gas in some samples of water for a short period of time [67].

The continuous technique involves continuous monitoring of Radon – 222 gas concentration in the soil gas and water by using special instruments such as Smart Radon Duo (SRD) and Scintillation Radon Monitor (SRM), this technique is used for predicting earthquakes [67].

The integrating technique provides an average concentration of Radon gas during a certain period of time (annually or monthly), SSNTDs such as CR-39 detectors (passive method) work according to this technique, the results of this technique are considered long–term results for a building or a certain location [67].

## 2.10.1: CR-39 Detector

The CR-39 detector is a thermoset polymer with an atomic composition ($C_{12}H_{18}O_7$) that can detect alpha particles with an energy range lies between (0.1–100) Mev, as a result, it can be used to measure Radon concentrations [1], the range of alpha particles energies of CR-39 detector is wide in comparison with other plastic detectors, such as, Lexan, Makrofol E polycarbonates, Cellulose nitrate (CA80-15, CN85, LR115 and Daicel), where each detector has it's own energy range. The chemical structure of CR-39 is shown in Figure (2 – 7) [81].

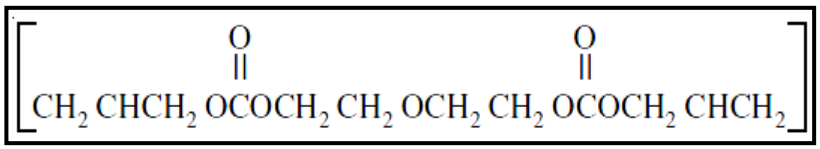

**Figure (2 – 7):Chemical Structure of the Monomer $C_{12}H_{18}O_7$ of CR-39** [81].

Chemical etching of CR-39 detectors requires NaOH solution or KOH solution with molarity ranging between 1-12 M and a temperature ranges between 40 °C and 70 °C, the purpose behind the etching process is to enlarge the latent tracks and make them visible. The chemical reaction between NaOH solution and CR-39 detector is shown in Figure (2 – 8) [81]. The amount of NaOH can be calculated in grams (W) due to the following relation [82]:

$$W(g) = \frac{N \times V \times M_w}{1000} \qquad (2.34)$$

where: N: normality, V: water volume (mL), $M_W$ is the molecular weight.

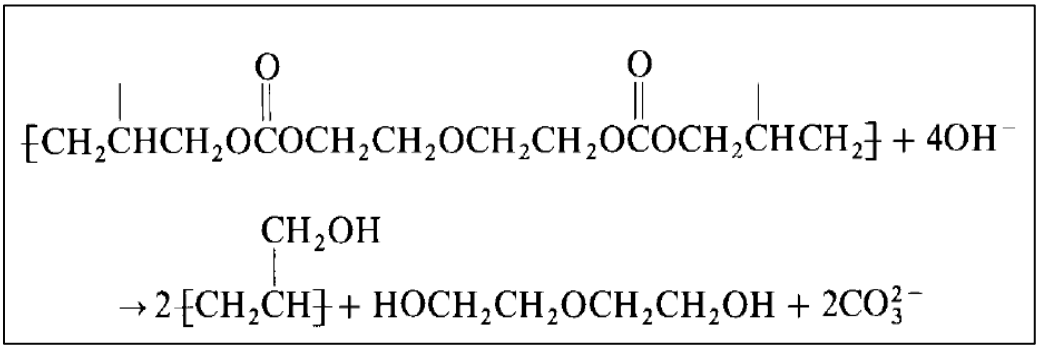


**Figure (2 – 8): The chemical reaction between the etchant and CR-39 detector** [81]**.**

During the etching period, the velocity of etching along the particle track ($V_T$) is ten times faster than the velocity of etching for the normal surface ($V_G$), as shown in Figure (2 – 9 – a) as a result pits appear on the surface of the detector.

If the incident angle ($\phi$) is less than the critical angle of CR–39 detector, the pits will not appear on the surface of the detector after the etching process as shown in Figure (2 – 9 – (b , c)) [1].

$$\theta_C = \sin^{-1}\frac{V_G}{V_T} \qquad (2.35)$$

When alpha particles pass through the detector, they transfer an amount of energy to electrons of the detector making a trail of damaged molecules along the particle track, to make the track visible, the detector is etched with a strong acid or base solution, and after the etching process, pits appear on the surface of the detector and can be seen by using a microscope or using Track Analysis System Limited (TASL) system [1].

The range of alpha energies in which the tracks results on CR-39 lies between 0.1Mev and more than 20Mev, this range is wide in comparison with other plastic detectors, such as, Lexan, Makrofol E polycarbonates, Cellulose nitrate (CA80-15, CN85, LR115 and Daicel), the upper and lower limits of alpha

energies depends on etching conditions (etch time) and detector type, where each detector has it's own range [81].

CR-39 detectors are widely used in many fields such as cosmic studies, neutrons studies, dosimetry, X-ray studies and UV and plasma detection, but they are insensitive to low LET gamma rays and electrons, and they can not be used in the case of the track density is high and the etching time is long because of the tracks' overlapping [83].

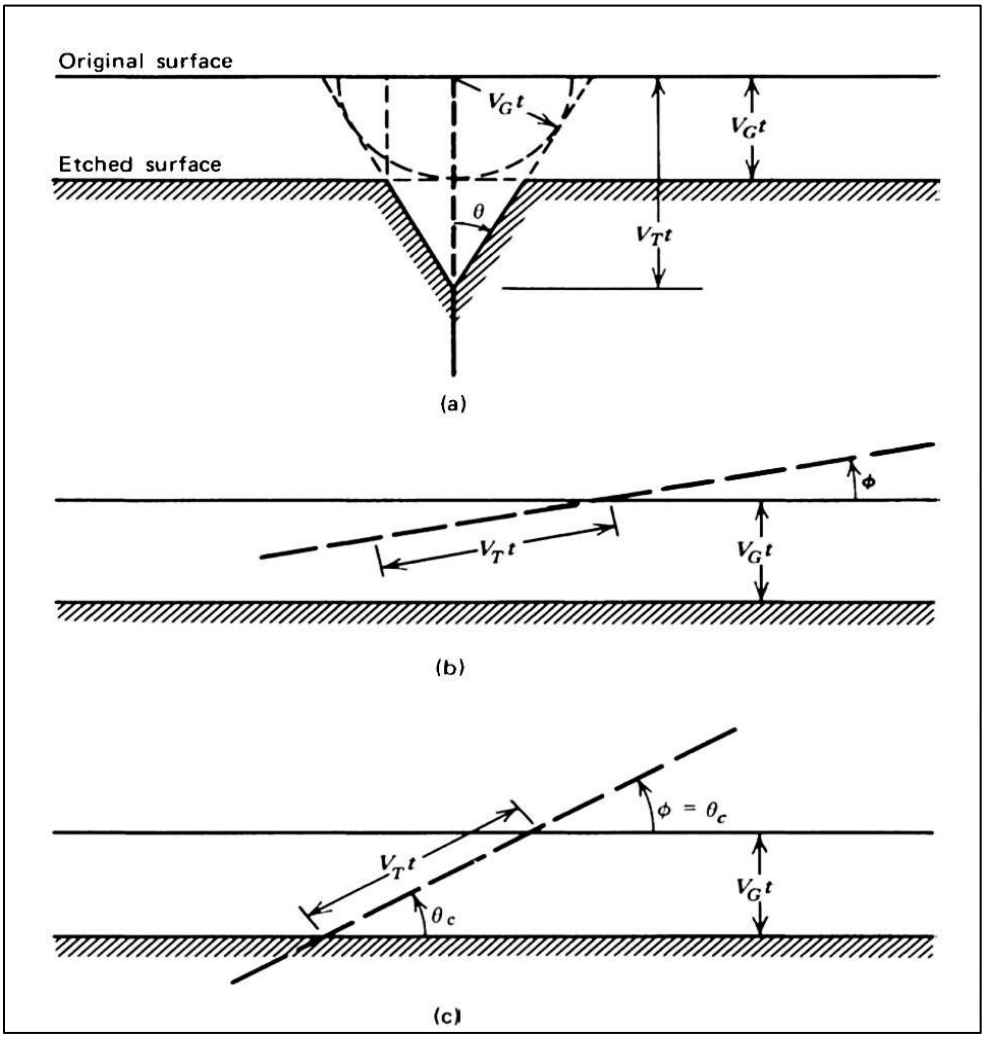


**Figure (2 – 9): (a) The shape of the track when the particle incident normally.**
**(b) Pits will not appear when $\phi < \theta_C$.**
**(c) Particle incident at an angle equals to $\theta_C$** [1].

## 2.10.2: RAD7 Monitor

It is electronic equipment, which is designed to detect only alpha particles among all types of radiations. The RAD7 monitor contains 0.7 L cell, a hemisphere in shape, which is coated with an electrical conductor. At the center of it, a Silicon detector is placed. The hemisphere is charged with a high potential difference which equals 2000 V to 2500 V [84].

The potential difference create an electric field throughout the volume of the cell, and it propels positively charged particles into the detector. Polonium–218 is derived towards the detector after the decay of radon, and the alpha particle resulting from the decay of Polonium – 218 enters the detector and produces an electrical signal proportional in strength to the energy of an alpha particle, where the response of the detector varying due to the energy of the particle [84].

After signals producing, the RAD7 monitor amplify, filter, and sort the signals according to their strength. Signals created from Polonium – 218 are used to determine the concentration of radon, and that come from Polonium-216 are used to determine the concentration of Thoron. The other progenies effect will be neglected by the RAD7 monitor [84].

## 2.10.3: RADH2O

It is a set of items (vial 250mL or vial 40 mL, drying tube, desiccant, glass filter, aerator and tubes) that are used with RAD7 monitor to calculate the concentration of radon gas in water. The range of concentrations that can be measured by this system ranges between 10 pCi/L and 400000 pCi/L, and the units of measurement can be changed according to the user demand into $Bq/m^3$ throughout the RAD7 monitor [85].

There are two types of drying tubes that come with RAD7 monitor, a big tube and a small tube , the small one is used with RADH2O to prevent the dilution of Radon gas resulting from a small sample of water, and also it important to know that the ambient air affect the purging process and it should be a Radon-free air or and an inert gas. The sample with high concentration of Radon can be diluted before measuring, and then the result is multiplied by the ratio of dilution [86].

The concentration of Radon in water using this technique is calculated by multiplying the concentration of Radon in the air of the loop by a fixed conversion coefficient (25 for 40mL vial and 4 for 250mL vial), where this coefficient is derived from the volume of the sample, the volume of air of the loop, the temperature of the room, and the partitioning coefficient between air and water at equilibrium [85].

## 2.11: Track Analysis System Limited (TASL) System

Track Analysis System Limited (TASL) is produced by the W. Physics Laboratory Tyndall Avenue, Bristol (UK). The number of tracks at the surface of CR-39 detectors can be counted by TASL via scanning. The surface of the detector is divided into frames by TASL, and the system scans the surface of the detector frame by frame, and then images are sent to a computer for analysis. TASLimage program analyze the images and count the tracks per unit area, the system also can give information about track size parameters [87,88].

One of TASL tools is a tray which contains 49 openings, the time required to scan every detector (plaques) in the tray ranges between 30 s to 80 s, this depends on the etching process, the other tool in TASL system is a Nikon optical microscope, controlled by motors in three dimensions, the image is viewed by a monochrome 24fps CCD imaging system, the plaques in the tray of TASL are squares of area 2.5 cm × 2.5 cm, the area of view in the plaque equals to 221 $mm^2$

(13 mm × 17 mm). TASL can identify the code the serial number of each detector before starting the scaning process, and the system shows the information of each detector and it's order on the screen of computer [89].

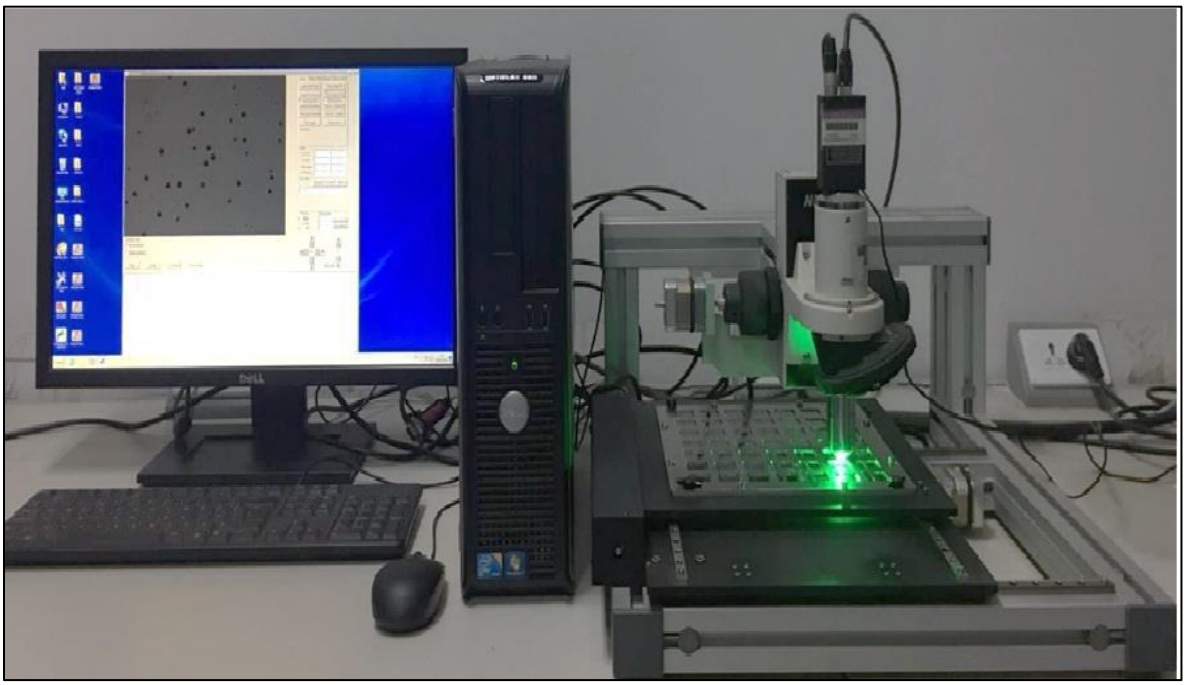

Figure (2 – 10): An image for TASL system [90].

## 2.12: Archgis Program

Geographic Information System (GIS) is one of the common names for Geographic Information Management Technology. GIS history dates back 1960, where computers based on GIS were used.

There are many definitions for GIS: "A system is designed to capture, store, check, manipulate, analyze and display the data which are spatially referenced to the Earth", "A set of procedures based computer or done manually are used to store and manipulate geographically referenced data" [91].

ArcGIS is a program for maps creation and dealing with geographic data, this program was created by organization "Environmental Systems Research Institute (ESRI)", California, USA in 1969 [92, 93].

## 2.13: Radon – 222 Removal Techniques

There are two techniques to get control Radon gas inside buildings according to NCRP(1989): passive technique and active technique, Passive technique involves [94]:

1 – **Source removal**: this action is done durring building instruction, or after building instruction, where the sources of Radon – 222 gas concentrations coming from uranium waste rocks, Uranium refinery wastes, and building materials are removed from the components of the building. This action is expensive and difficult as it is done by hand and machinery, and it requires to restore the area to it's original appearance [94].

2 – **Closure of entry routes**: the basements and foundations of a building contains openings in the flour and walls through which Radon – 222 bearing soil gas can pass from the soil to the indoor air of the building [94].

Closing the openning can reduce the concentrations of Radon – 222 at indoor air, but the closure is not possible for some openings in the building such as sumps [94].

The style of the building and the materials used in the building can decrease the number of the openings. In some cases, this action is expensive and impratical as the building includes suspended floors with bare earth beneath and walls built with rocks [94].

Active technique involves [94]:

1 – **Soil ventilation**: this action is done when the sealing of the openning in the buildings is uneconomical or impractical. Radon entry rate can be reduced by reducing the concentration of Radon – 222 gas in the soil gas, or by diverting the

soil gas from the building to another place, or by reducing the pressure difference between the soil gas and the building atmosphere. These procedures can be done using ventilation systems [95].

The ventilation systems contain a network of pipes that are put under the floor or using special grains beneath the floor. Fans are used in the ventilation systems to increase the pressure between the soil gas and the air inside the pipes [94]. Radon – 222 gas produced from these systems is transferred to a collection system. Natural forces can be used instead of the fans in ventilation systems such as wind and thermal effects [94,96].

2 – **Structure ventilation**: this action is simply a ventilating process to the building using fans but it requires a ventilation rate of 75 liter/s to 150 liter/s while the normal ventilation rate in the buildings ranges between 25 liter/s to 50 liter/s [97]. There are many drawbacks in this action related to the cooling and heating systems of the building, electrical consumption, dust and pollutants in the air, and noise [96].

3 – **Air treatment**: this action is done by special systems such as high efficiency filters, electrostatic precipitation, ceiling fans, and ion generation systems [97].

These systems depend on capturing Radon – 222 gas progenies, and they do not deal with Radon – 222 gas. This technique is the best of all, as it can be available in all places, the cost of the systems is lower than the previous ones, and it does not require a knowledge of the location. The disadvantage of this procedure is the maintenance and the probability of system failure, Figure (2 – 11) shows the components of system that are used for Radon removal from homes, the system takes Radon gas from the pores of soil under the building anf transfer it to outer space above the building [94].

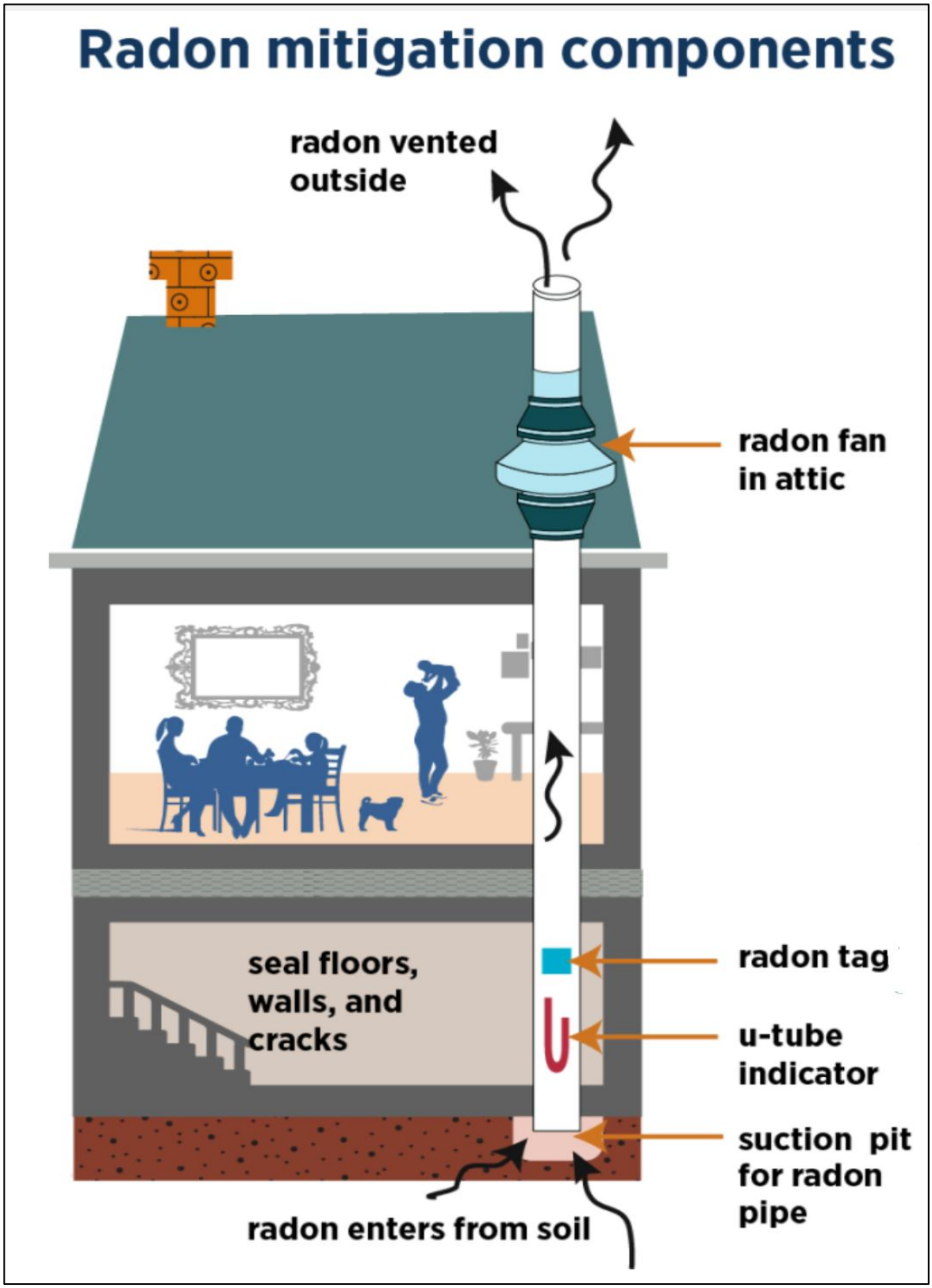


**Figure (2 – 11): One of the systems used for Radon removal** [98].

# Chapter Three

# Practical Part

## 3.1: Introduction

In the present work, two types of methods were conducted to measure Radon gas concentration in soil gas and water for samples collected from the area of study (Al-Najaf refinery – Al-Najaf governorate – Iraq).

The passive method were used for measuring Radon–222 gas concentrations in the samples of the soil, and in the samples of different types of water, where CR-39 detectors were used in this technique. It took three months to be achieved, one month for radiological equilibrium, and two months for exposure, but for the samples of water, active method took only two months (exposure period).

The active method were only used to measure Radon–222 gas concentration in the samples of different types of water collected from the study area (Al-Najaf refinery), and it took only 30 minutes for water samples, where RADH2O, and RAD7 were used to measure the average of Radon gas concentration in the water samples for four cycles of measuring, in this technique, the settings of RAD7 monitor were previously determined before starting the test, and the components of both were assembled and settled.

The coordinates of the position for each sample of soil and water were determined by using the google earth application before collecting it, and then the coordinates of the samples were put on the map of the refinery as shown in the maps that are drawn in this chapter.

The materials used in this work are also mentioned in this chapter besides it’s origin, model, pictures, and specifications, the steps of the passive method and active method are discussed in detail in this chapter, and they are mentioned in the following figure:

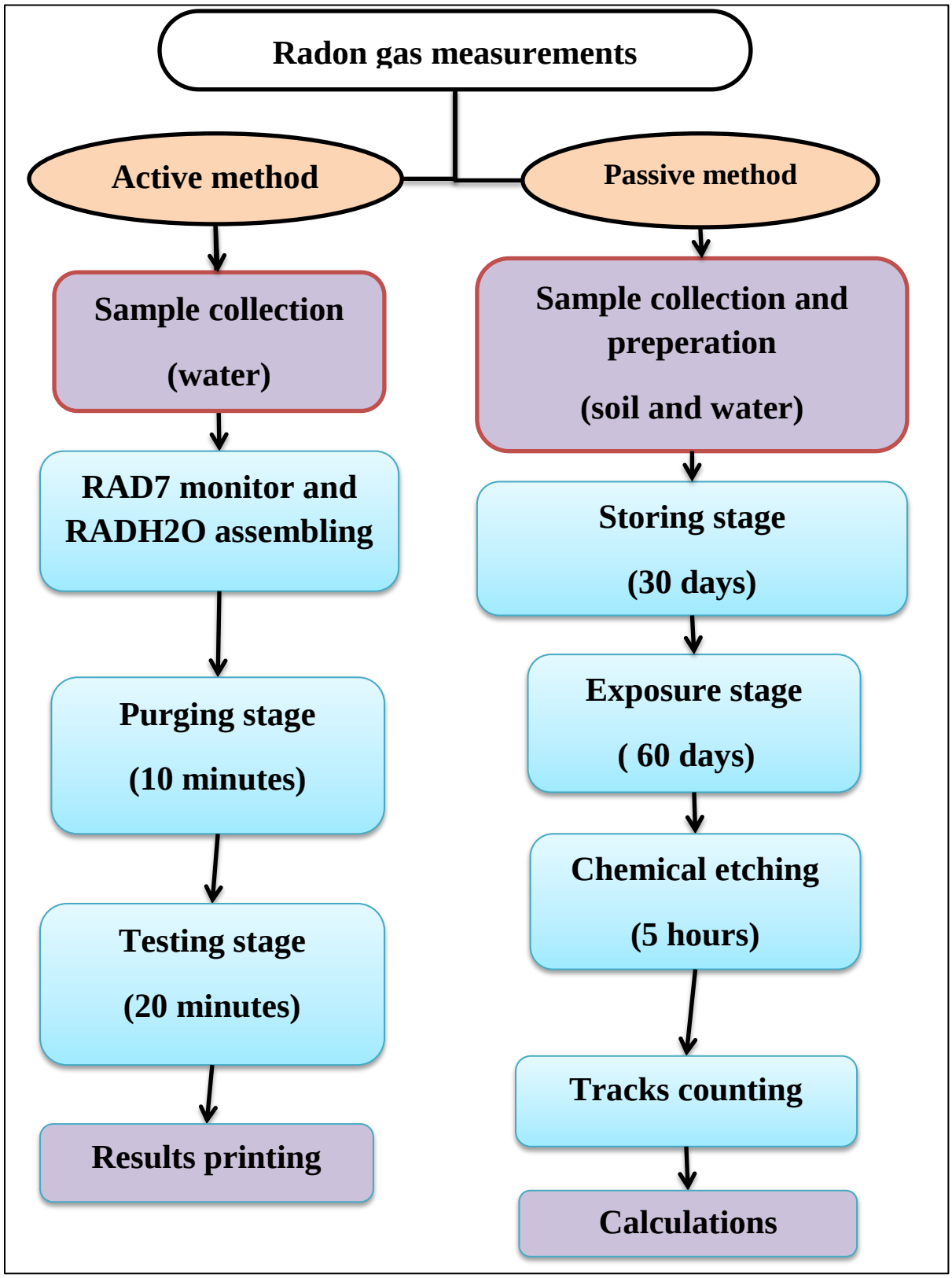


**Figure (3 – 1): A flow chart shows the methods of Radon gas measurement.**

## 3.2: Area of Study

The map of the study area (AL – Najaf refinery) was divided into four sectors to achieve a comprehensive study for the area of the study as shown in Figure (3 – 2). The samples of soil and water were collected from different positions of each sector, and the coordinates of each sample were taken by using the google earth application as shown in Figures (3 – 3 and 3 – 4).

Al – Najaf refinery with an area of 887293 $m^2$, it has three refining units, RO unit for treating the water and producing a drinking water, tanks for storing oily products and water, and wells a long with a source of river water. A mixed water from well water and river water is used for many purposes as it is used in the process of refining and as a drnking water.

The area of study (Al-Najaf refinery) is located in AL-Najaf province, in the western part of the Republic of Iraq at a latitude (32°13' N) and a longitude (44°15'). Al-Najaf refinery was built in October 2006, one hundred mile (160km) from Baghdad the capital, the soil of the refinery is sandy soil with some impurities resulting from the operations conducted inside the refinery, and also from the construction of the refinery.

Al–Najaf governorate is located in the central part of Iraq with an area of 28824 $km^2$ and an elevation above sea level 70 m. The surface of it gradually descends from the southwest to the notheast at a rate of decline equils to 1m per 2 km, the population of Al – Najaf governorate equils 1500522 according to 2017 census [99].

The soil of Al–Najaf governorate consists of layers, the layers are silty sand, clayey sand, gypsum, and sand, the order of these layers due to the depth differs from one location to another inside Al–Najaf governorate, where they are randomly distributed according to the depth [100,101].

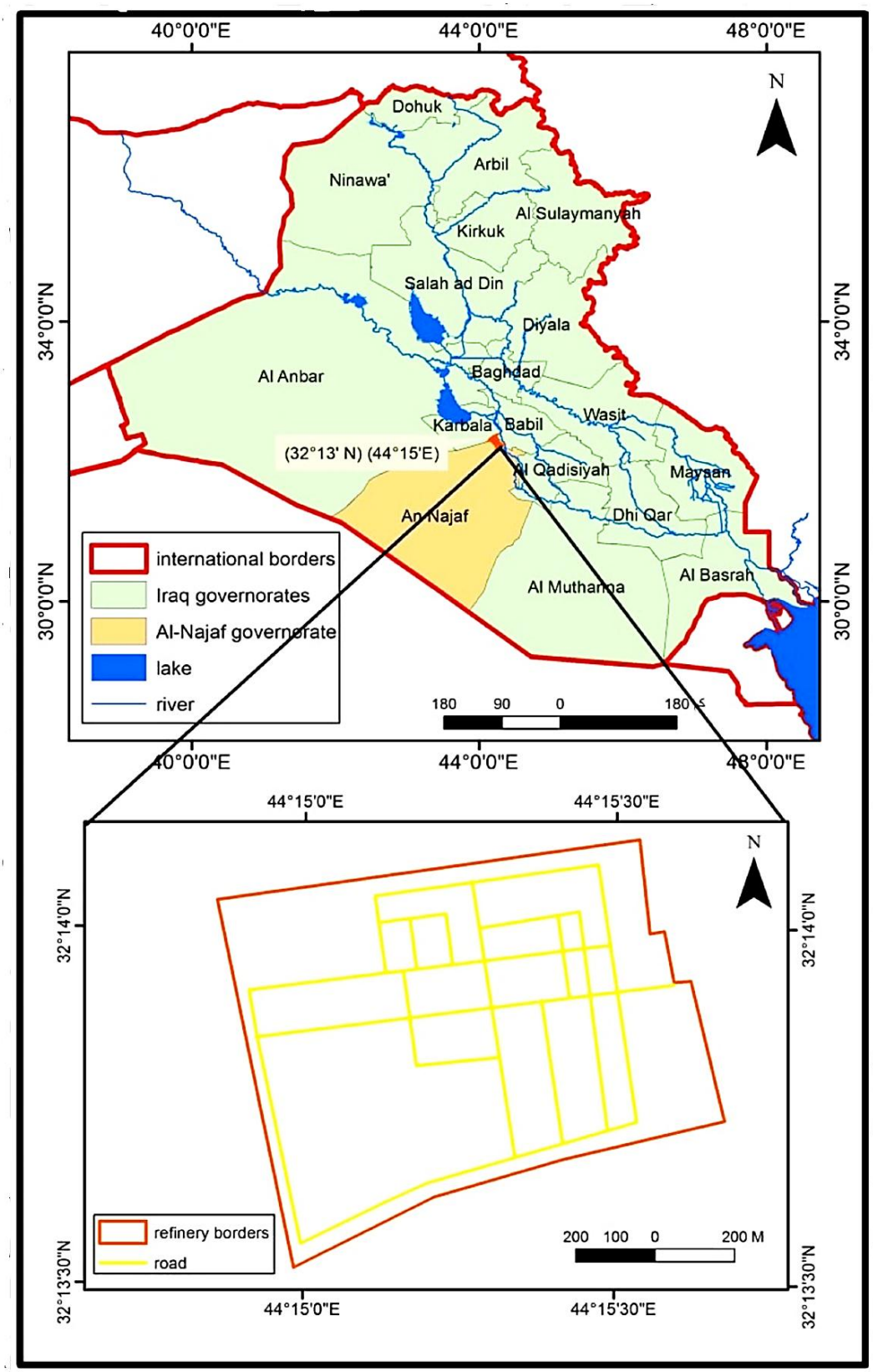


**Figure (3 – 2): The location of study area created by using Archgis program.**

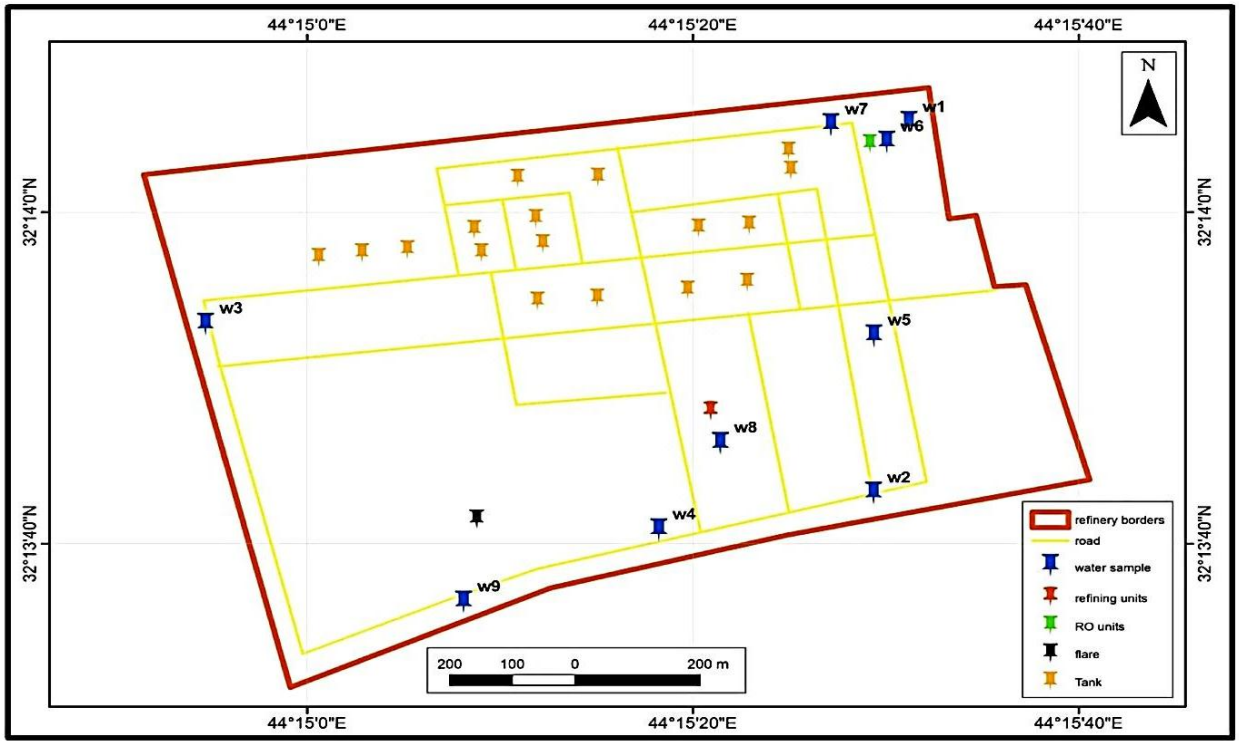


**Figure (3 – 3): The positions of water samples.**

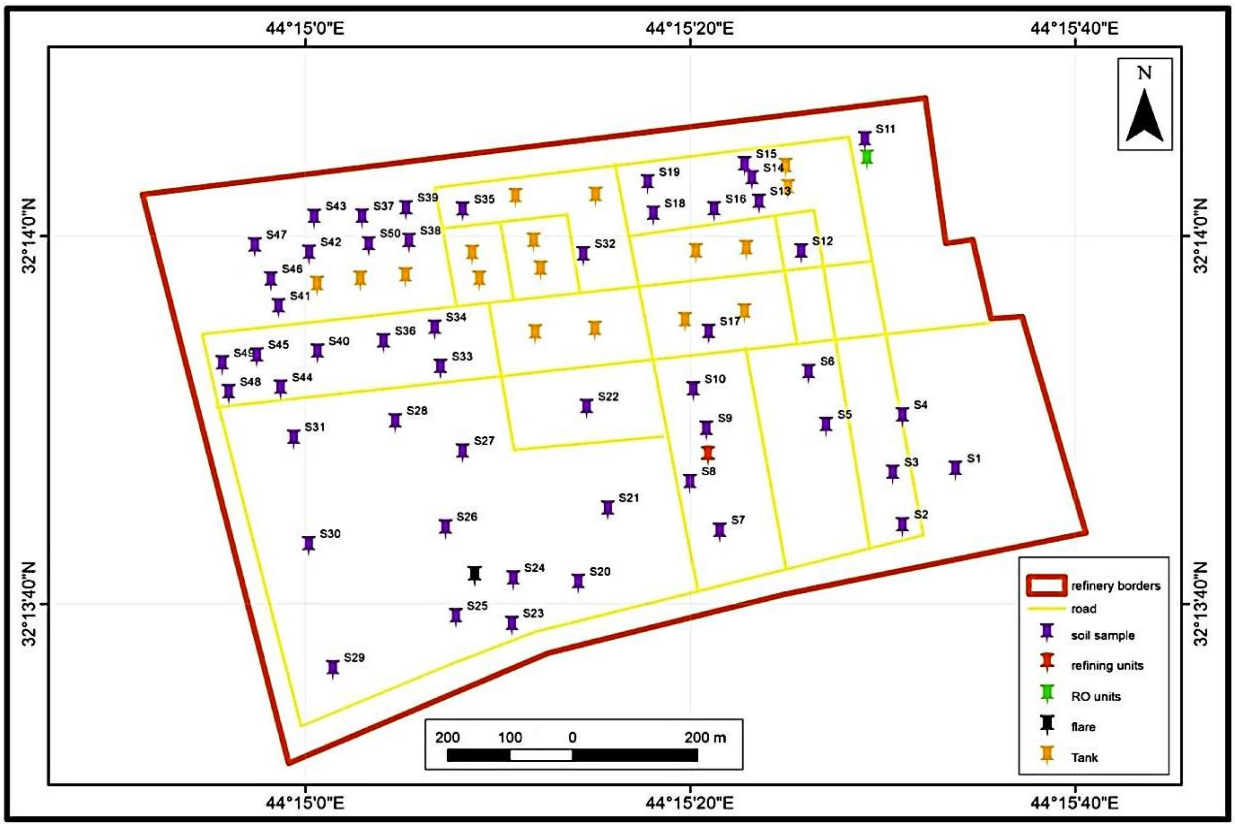


**Figure (3 – 4): The positions of soil samples.**

## 3.3: Passive Method Materials

1 – CR-39 detectors with dimensions of (2.5 × 2.5) cm and a thickness of 2 mm manufactured by SCS company (www.StaticControl.com) , America.

2 – Plastic cups, as shown in Figures (3 – 5 and 3 – 6), with an internal volume 140 mL, 260 mL for the soil cup and water cup, respectively. Plastic bags, gloves, protective glasses, protective mask, sieve with 3 mm mesh aluminum foil with a thickness of 15 mm produced by falconpack company – UAE.

3 – Adhesive tape manufactured by AKKOSTAR – China – Model: AK52824, an ordinary tape and an electrical oven with a temperature range (0 – 240) °C manufactured by KUMTEL – Turkey – Model: kf3100, as shown in Figure (3 – 7)

4 – Sensitive scale with a capacity range (1-10000) g, manufactured by Electronics, China, Model: SF-400, working on a power of batteries 1.5 V × 2 AA, as shown in Figure (3 – 8 – a) and permanent marker produced by PENMAX.

5 – A grinder with the following specification: (capacity of 100 g, an angular velocity 25000 round/minute and a power of 850 W) manufactured by SILVER COOK, German, Model: KSM127, as shown in Figure (3 – 8 – b).

6 – A mobile phone with a google earth application and an internet access manufactured by (Apple – California – USA, mobile type: iPhone S pluse) as shown in (3 – 9 – b).

7 – Water bath, distilled water, NaOH tablets produced by (Central Drug House (P) Ltd – India), beaker 500mL, beaker 100 mL, grid and wires, as shown in Figures (3 – 10 and 3 – 11).

8 – Digging tools (shovel, pick axe, trowel and crowbar), measuring tape.

9 – TASL system manufactured by tasl company – the UK and a computer with a TASLIMAGE software, as shown in Figure (3 – 12).

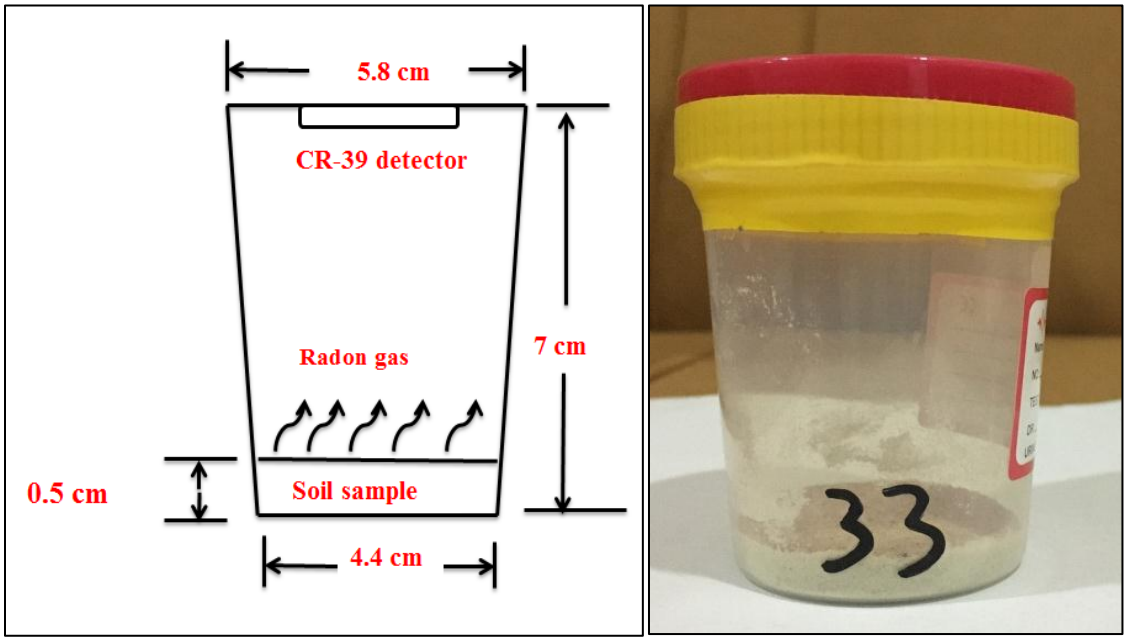


**Figure (3 – 5): Soil cup.**

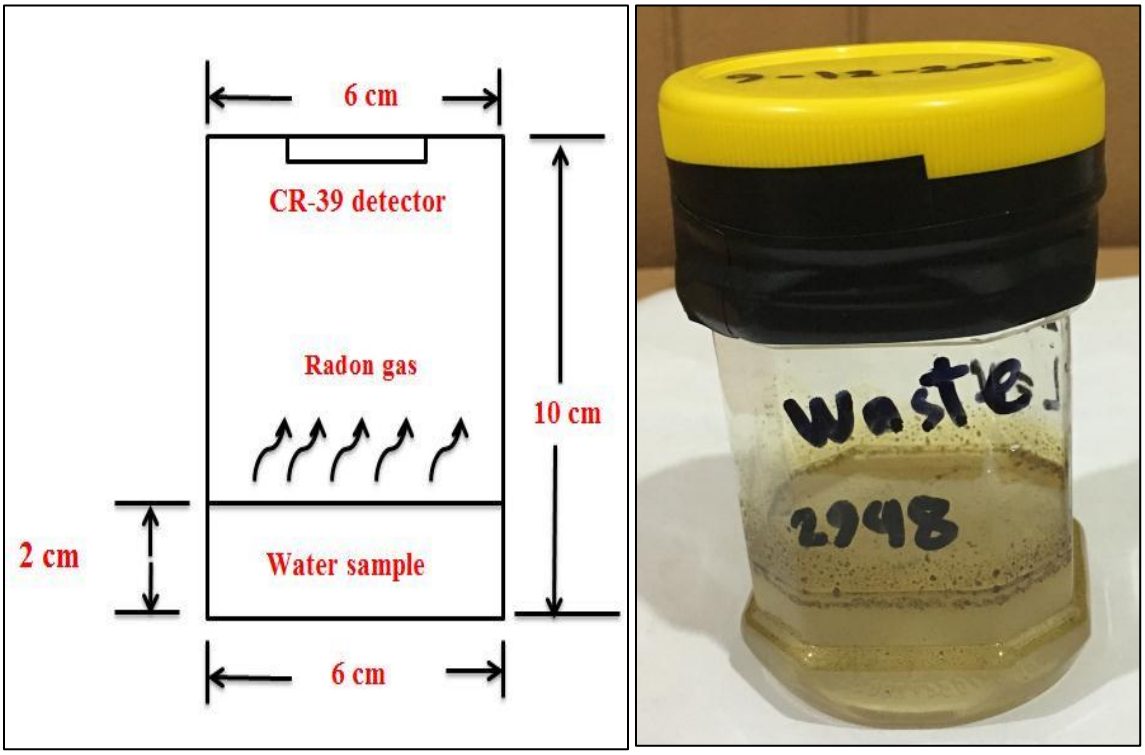


**Figure (3 – 6): Water cup.**


**Figure (3 – 7): (a) Electrical oven. (b) Adhesive tape.**


**Figure (3 – 8): (a) Sensetive balance. (b) Electrical grinder.**

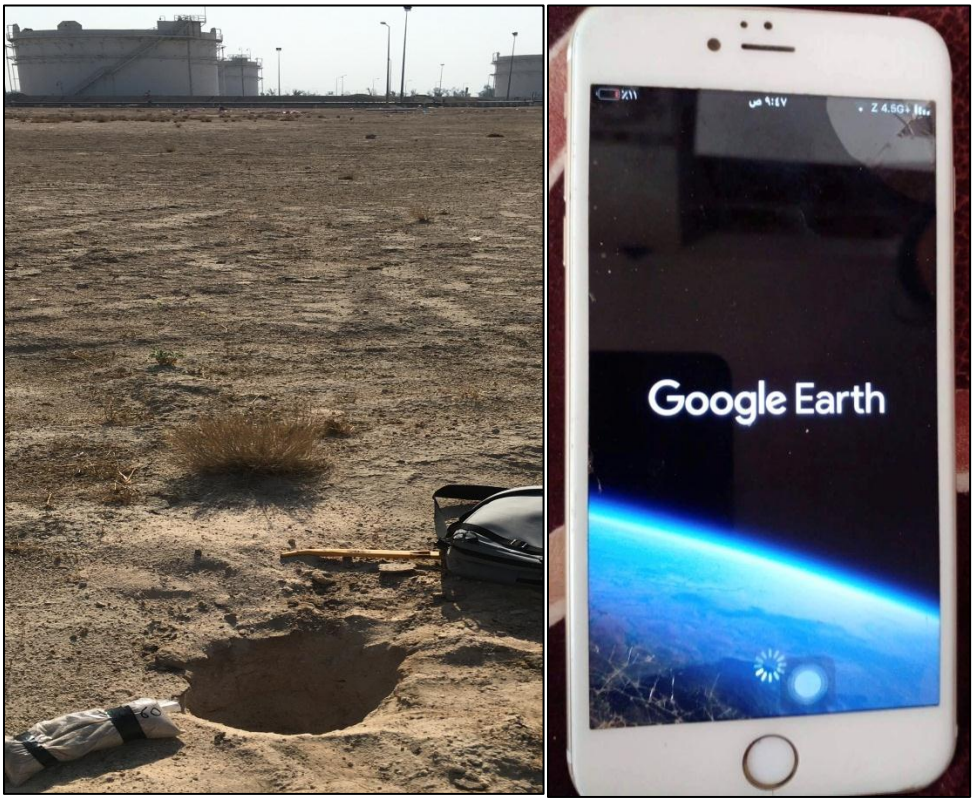


**Figure (3 – 9): (a) Sample collection. (b) Google earth application.**

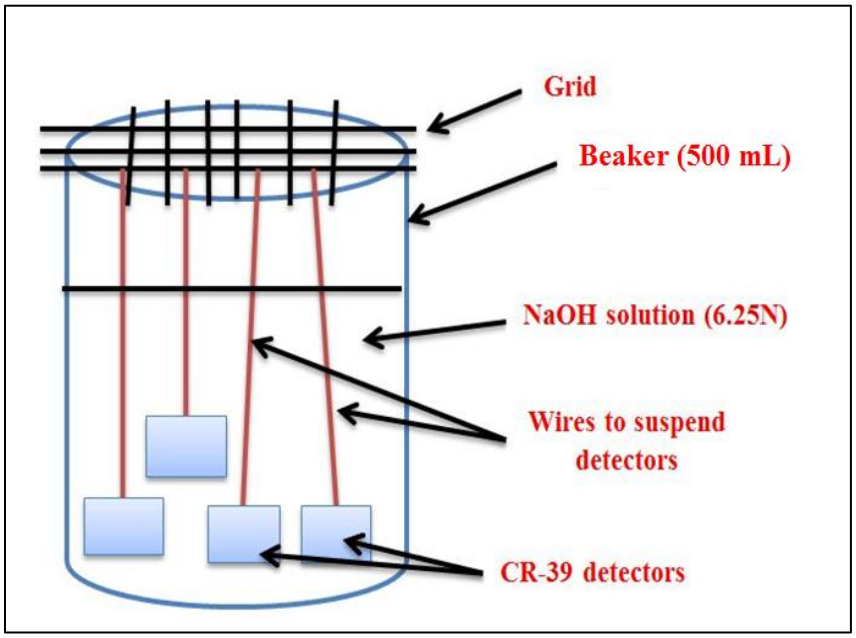


**Figure (3 – 10): A schematic diagram for the beaker with detectors suspended inside it which was used in the etching process.**


**Figure (3 – 11): The water bath used in the etching process.**

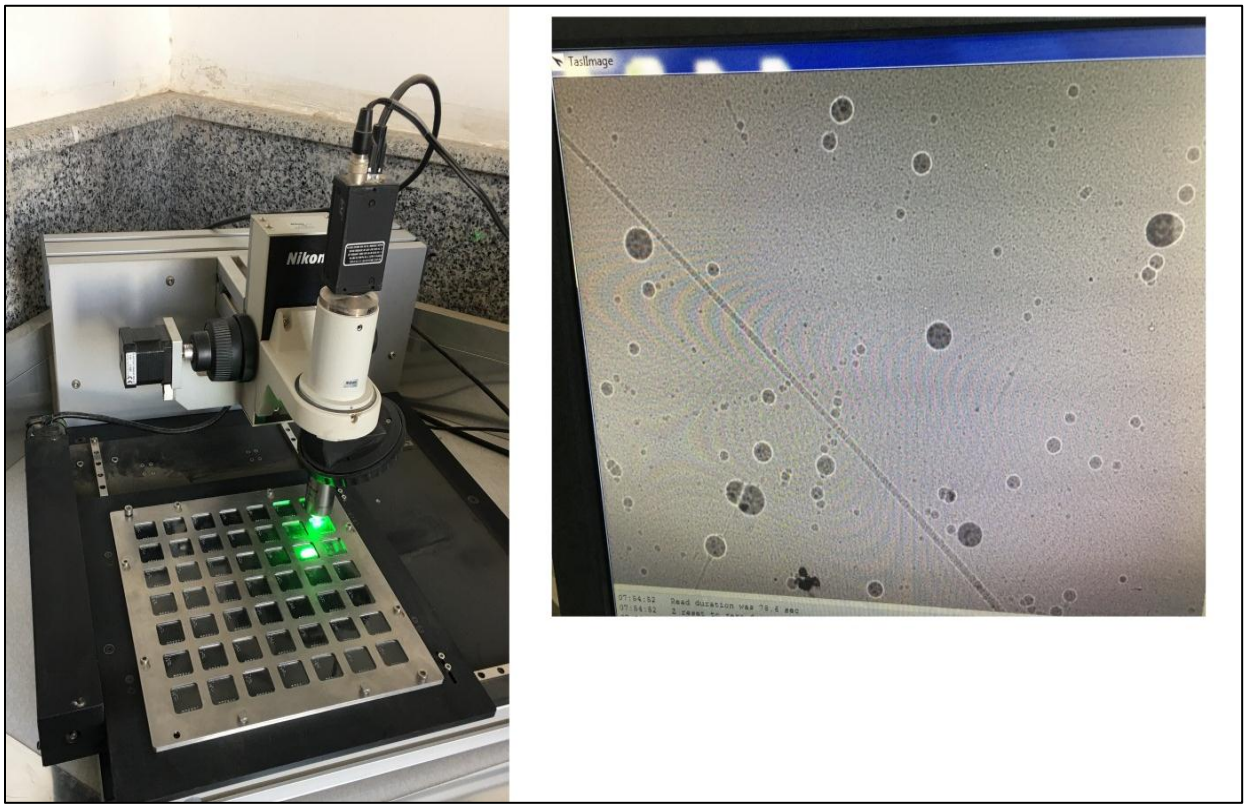


**Figure (3 – 12): (a) TASL system. (b) An image of tracks taken by TaslImage program.**

## 3.4: Passive Method Procetures

1- Sample collection and preparation: fifty samples of soil were collected from selected positions inside Al-Najaf refinery during the period (22/11/2021 – 6/12/2021) with a depth of 20 cm from the surface, as shown in Figure (3 – 9 – a), and the coordinates of each sample was taken by using google earth application and then the map of sample positions were drawn using Arcgis program. After sample collection, the samples of soil were sieved to eliminate the impurities (such as plant pieces, plastic pieces, insects ... etc) and then dried in an oven under the following conditions (time = 3 hours, temperature = 80°C, sample surface area = (30 × 30) cm and sample thickness = 5mm).

After the drying stage, the dried samples were milled with a grinder and then the powder of the dried samples was poured into the plastic cups. A sensetive scale was used to determin the mass of the soil sample inside the soil cup (10 g).

Nine samples for different types of water were taken from Al-Najaf refinery (3 samples of well water, waste water, tap water, RO drinking water, river water and water from the boiler).

The coordinates of each sample were determined using the google earth application and the map for water samples was drawn using Arcgis program as shown in Figure (3 – 3). The volume of water samples inside the cups were determined by using beaker 100 mL. The volume of water sample inside the cup equals 65 mL.

For well water samples, the motor of the wells must be worked for 15 minutes to ensure that the water comes from the bottom of the well.

2 – Storing stage: soil samples were stored for 30 days inside well-sealed soil cups to satisfy a radiological secular equilibrium. It is important to mention that this stage did not occur for water samples.

3 – Exposure stage: the detectors were swiftly implanted at the upper cover of the soil cups and water cups and the cups were left in a steady state for 60 days, as shown in Figure (3 – 13).


**Figure (3 – 13): CR-39 sticked at the bottom of the cup's cover.**

4 – Chemical etching: the detectors were carefully removed from the cups and etched with a chemical solution of NaOH with normality of 6.25 N for 5 hours by using a water bath under 70°C, as shown in Figures (3 – 10, 3 – 11), and then, the detectors were washed and left in the open air to get dry.

The dried detectors were covered with aluminium foil to stop counting. The amount of NaOH was determined in grams according to Equation (2.32) after knowing the volume of water in mL, the molecular weigh of NaOH (40 g / mole), and the required normality of NaOH solution (6.25 N).

5 – Tracks counting: after the etching process, the tracks (pits) on the surface of the detectors were counted by using the Track Analysis System Limited (TASL) as shown in Figure (3 – 12 (a, b)) (at the nuclear laboratory, College of Science, Kufa University).

6 – Calculations: radon gas concentrations in soil samples and water samples were calculated after calculation the calibration factor for the cups. The calibration factors for the cup of soil and for the cup of water were taken from a previous

research which involved many cups with heights ranging from 5 cm to 45 cm, and from the reults, the calibration factor for the cups with heights varying between 5 cm to 25 cm equals to 0.3 track.$m^3$/Bq.$cm^2$.day, and for other heights equals to 0.2 track.$m^3$/Bq.$cm^2$.day, as a result, the calibration factor for our soil cup and water cup is considered to be equal to 0.3 track.$m^3$/Bq.$cm^2$.day [102]. The concentrations of Radon–222 gas in the soil gas and water samples were calculated due to equations (2.14 and 2.15).

Several calculations such as Radium content for the soil sample ($C_{Ra}$), an exhalation rate of Radon–222 gas per unit area from the soil samples ($E_A$), an exhalation rate of Radon–222 gas per unit mass from the soil samples ($E_M$), Uranium–238 content for the soil samples ($C_U$), and Radon–222 gas concentration near the soil ($C_{near\ the\ soil}$) were calculated due to Equations (2.14 – 2.23).

The Annual Effective Doses due to inhalation of Radon–222 gas and it's progenies near the the soil at outdoor air ($AED_{outdoor\ inhalation}$) which resulted from the soil contribution were calculated according to Equation (2.9), the Annual Effective Doses due to inhalation of Radon–222 gas and it's progenies resulted from the contribution of water at indoor air ($AED_{indoor\ inhalation}$) were calculated according to Equation (2.8).

## 3.5: Active Method Materials

RAD7 monitor with a serial number 3447, RADH2O accessory manufactured by DURRIDGE company Inc – Beillerica – United States of America (USA), power supply, infrared printer, plastic bottles, desiccant containing 98% of $CaSO_4$ and 2% of $CoCl_2$ produced by DRIERITE company – United States of America (USA), as shown in Figure (3 – 14).

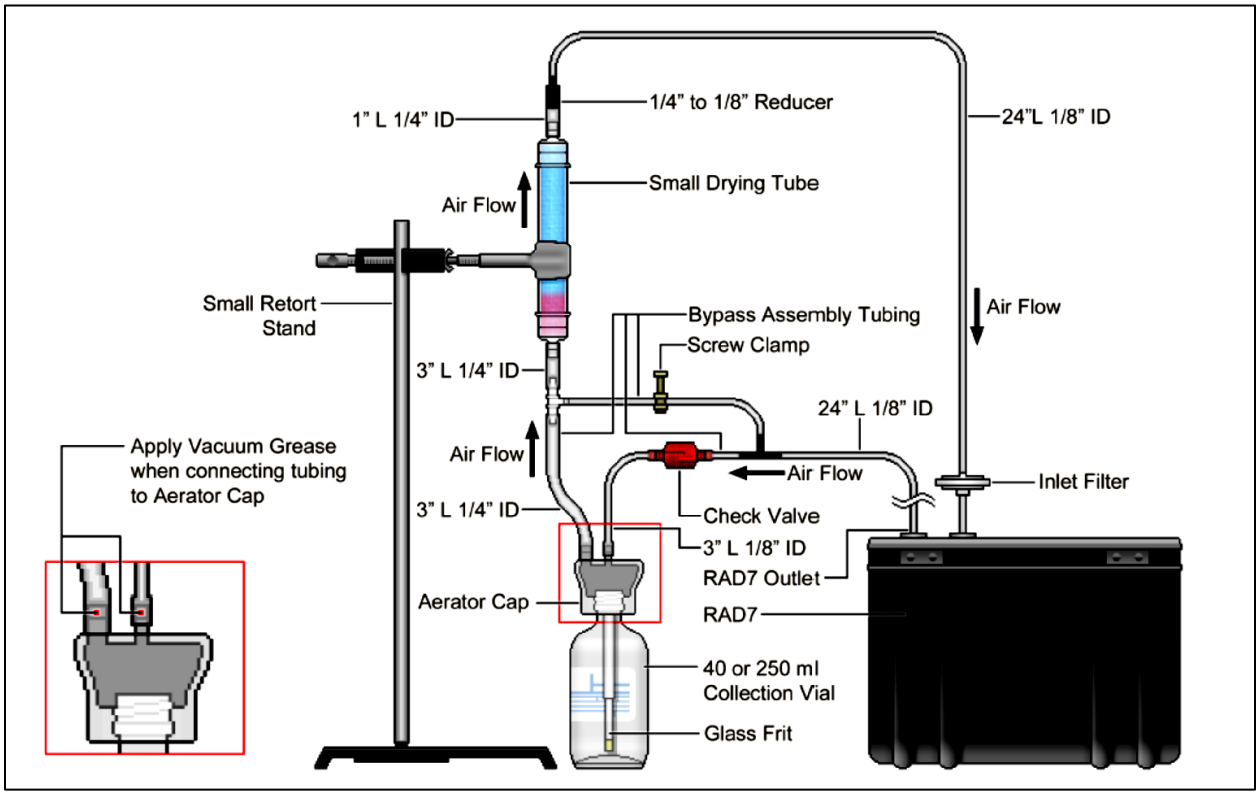


**Figure(3 – 14): The components of RADH$_2$O connected with the RAD7 monitor** [85].

## 3.6: Active Method Procedures

1 – Samples collection: water samples were collected from the wells and other sources of water inside Al-Najaf refinery during the period (22/11/2021 – 6/12/2021), Figure (3 – 3) shows the positions of water samples. For well sample, the sample was collected after 15 minutes from the operating of the motor of the well to ensure that the water is coming from the groundwater, and then all water samples (well samples and the others) were brought to the lab of advanced nuclear physics at the university of Babylon/ college of science/ physics department after 24 hours from the date of collection for testing.

2 – RAD7 monitor RADH2O assembling: the testing steps were done after assembling the components of RADH$_2$O and connecting it with the RAD7 monitor, as shown in Figure (3 – 14), and determining the suitable setting for our test

(protocol: WAT-250, cycle: 5minutes, recycle: 4, pump: Grab , tone: off, mode: water250mL, thoron: off).

3 – Purging stage: before beginning the test, the relative humidity inside the cell of RAD7 monitor should be reduced to less than 10%.

4 – Testing stage: after the purging step, the test was started by choosing a test start from the screen of RAD7 monitor, where the settings of the test were previously determined as the following: (protocol: WAT-250, cycle: 5minutes, recycle: 4, pump: Grab , tone: off, mode: Water250mL, thoron: off).

5 – Printing results: after the end of test, the result was printed by an infrared printer settled on the RAD7 monitor, as shown in Figure (3 – 15 – a).

**Figure (3 – 15): (a) RAD7, RADH2O, and an infra–red printer.**

**(b) The process of aeration [85].**

Figure (3 – 15 - b) shows the aeration process inside a vial to agitate Radon–222 gas dissolved in water and transfer it to the air, after agitation Radon–222 is grabbed by RAD7 monitor for measuring.

After knowing the concentration of Radon–222 gas in the samples of water, the Annual Effective Doses due to inhalation of Radon–222 gas and it's progenies resulted from the contribution of water at indoor air ($AED_{indoor\ inhalation}$) were calculated according to Equation (2.8).

Lung Cancer Risk (LCR) in case per million per year, exposure to Radon–222 progenies in WLM per year and Potential Alpha Energy Concentration (PAEC) in WL were also determined according to Equations (2.10 – 2.12).

# Chapter Four

# Results and Discussion

## 4.1: Introduction

In this chapter, the results of Radon–222 gas concentrations for the soil samples and water measured in a passive method and active method, the Annual Effective Doses (AED) resulted from soil and water contributions, Lung Cancer Risk (LCR), Potential Alpha Energy Concentration (PAEC), and an exposure per year ($E_P$) have been presented with figures illustrate the values of each one.

## 4.2: The Results of Soil Samples

Radon–222 gas concentrations in the soil gas of the soil samples (C) in Table (4 – 1) and Figure (4 – 1) were calculated by using Equations (2.14 and 2.15), after knowing: the calibration factor (k= 0.3 track.m$^3$/Bq.cm$^2$.day), Radon–222 decay constant ($\lambda_{Rn} = 0.18\, day^{-1}$). The exposure time (T= 60 day), the distance between the surface of the sample and the detector (h = 6.5 cm), and the thickness of the soil sample (0.5 cm). The results in Table (4 – 2) and Figures ((4 – 2) – (4 – 5)) were about the annual effective dose due to inhalation of Radon–222 in the outdoor air which were calculated according to Equation (2.9) after knowing the concentratration of Radon–222 gas near the soil surface which were calculated due to Equation (2.25). Where, 1760 h/y is the time spent in the outdoor air, and the equilibrium factor was considered to be equal to 0.6. ). The density of the tracks $\rho_T$ in Track/cm$^2$ which was obtained from TASL system, as shown in Figure (3 – 6). The exhalation rates per unit area and mass mentioned in Table (4 – 2) were calculated according to Equations (2.18 and 2.19), after knowing the value of Radon–222 gas concentration in the samples, Radon–222 decay constant, the volume of the soil cup (140 mL), sample weight (10 g), the surface area of the soil sample ($1.96\times10^{-3}$ m$^2$), and the time of exposure (60 day). Radium content ($C_{Ra}$) and Uranium concentration ($C_U$) mentioned in Table (4 – 2) were calculated according to the Equations (2.16 – 2.24).

**Table (4 – 1 ): The coordinates of soil samples and the concentration of Radon gas in the soil gas for each sample (C).**

| Sample Code | Coordinates | | detector number | $\rho_t$ in (track/cm$^2$) | C in (Bq/m$^3$) |
|---|---|---|---|---|---|
| | Longitude | Latitude | | | |
| S1 | 32°13'47.20"N | 44°15'33.81"E | 2839 | 23 | 180 ∓ 166 |
| S2 | 32°13'44.14"N | 44°15'31.06"E | 2840 | 100 | 784 ∓ 80 |
| S3 | 32°13'46.99"N | 44°15'30.55"E | 2841 | 97 | 761 ∓ 83 |
| S4 | 32°13'50.11"N | 44°15'31.05"E | 2842 | 715 | 5608 ∓ 609 |
| S5 | 32°13'49.59"N | 44°15'27.08"E | 2843 | 36 | 282 ∓ 151 |
| S6 | 32°13'52.47"N | 44°15'26.18"E | 2844 | 156 | 1224 ∓ 17 |
| S7 | 32°13'43.85"N | 44°15'21.55"E | 2845 | 232 | 1820 ∓ 68 |
| S8 | 32°13'46.50"N | 44°15'20.01"E | 2846 | 222 | 1741 ∓ 57 |
| S9 | 32°13'49.39"N | 44°15'20.86"E | 2847 | 467 | 3663 ∓ 332 |
| S10 | 32°13'51.52"N | 44°15'20.19"E | 2848 | 16 | 125 ∓ 174 |
| S11 | 32°14'5.12"N | 44°15'29.11"E | 2849 | 183 | 1435 ∓ 13 |
| S12 | 32°13'59.02"N | 44°15'25.79"E | 2850 | 262 | 2055 ∓ 102 |
| S13 | 32°14'1.73"N | 44°15'23.59"E | 2851 | 18 | 141 ∓ 172 |
| S14 | 32°14'3.01"N | 44°15'23.23"E | 2852 | 294 | 2306 ∓ 138 |
| S15 | 32°14'3.76"N | 44°15'22.85"E | 2853 | 360 | 2824 ∓ 212 |
| S16 | 32°14'1.32"N | 44°15'21.27"E | 2854 | 99 | 776 ∓ 81 |
| S17 | 32°13'54.65"N | 44°15'20.98"E | 2855 | 251 | 1969 ∓ 90 |
| S18 | 32°14'1.07"N | 44°15'18.10"E | 2856 | 117 | 918 ∓ 61 |
| S19 | 32°14'2.78"N | 44°15'17.81"E | 2857 | 129 | 1012 ∓ 47 |
| S20 | 32°13'41.05"N | 44°15'14.21"E | 2858 | 936 | 7341 ∓ 857 |
| S21 | 32°13'45.05"N | 44°15'15.73"E | 2859 | 95 | 745 ∓ 85 |

Next ⟶

| Sample Code | Coordinates | | detector number | $\rho_t$ in (track/cm$^2$) | C in (Bq/m$^3$) |
|---|---|---|---|---|---|
| | Longitude | Latitude | | | |
| S22 | 32°13'50.57"N | 44°15'14.64"E | 2860 | 84 | 659 ∓ 98 |
| S23 | 32°13'38.78"N | 44°15'10.75"E | 2861 | 13 | 102 ∓ 177 |
| S24 | 32°13'41.25"N | 44°15'10.82"E | 2862 | 210 | 1647 ∓ 44 |
| S25 | 32°13'39.19"N | 44°15'7.84"E | 2863 | 292 | 2290 ∓ 135 |
| S26 | 32°13'44.02"N | 44°15'7.30"E | 2864 | 130 | 1020 ∓ 46 |
| S27 | 32°13'48.15"N | 44°15'8.20"E | 2865 | 62 | 486 ∓ 122 |
| S28 | 32°13'49.79"N | 44°15'4.69"E | 2866 | 73 | 573 ∓ 110 |
| S29 | 32°13'36.37"N | 44°15'1.44"E | 2867 | 315 | 2471 ∓ 161 |
| S30 | 32°13'43.11"N | 44°15'0.19"E | 2868 | 5 | 39 ∓ 186 |
| S31 | 32°13'48.90"N | 44°14'59.40"E | 2869 | 55 | 431 ∓ 130 |
| S32 | 32°13'58.87"N | 44°15'14.47"E | 2870 | 175 | 1373 ∓ 4 |
| S33 | 32°13'52.74"N | 44°15'7.05"E | 2871 | 86 | 675 ∓ 95 |
| S34 | 32°13'54.88"N | 44°15'6.74"E | 2872 | 96 | 753 ∓ 84 |
| S35 | 32°14'1.30"N | 44°15'8.19"E | 2873 | 330 | 2588 ∓ 178 |
| S36 | 32°13'54.14"N | 44°15'4.08"E | 2874 | 135 | 1059 ∓ 40 |
| S37 | 32°14'0.92"N | 44°15'2.97"E | 2875 | 63 | 494 ∓ 121 |
| S38 | 32°13'59.59"N | 44°15'5.40"E | 2876 | 71 | 557 ∓ 112 |
| S39 | 32°14'1.38"N | 44°15'5.25"E | 2877 | 100 | 784 ∓ 80 |
| S40 | 32°13'53.58"N | 44°15'0.64"E | 2878 | 42 | 329 ∓ 145 |
| S41 | 32°13'56.04"N | 44°14'58.63"E | 2879 | 39 | 306 ∓ 148 |
| S42 | 32°13'58.96"N | 44°15'0.21"E | 2880 | 169 | 1326 ∓ 2 |
| S43 | 32°14'0.91"N | 44°15'0.47"E | 2881 | 291 | 2282 ∓ 134 |

Next ⟶

| Sample Code | Coordinates | | detector number | $\rho_t$ in (track/cm$^2$) | C in (Bq/m3) |
|---|---|---|---|---|---|
| | Longitude | Longitude | | | |
| S44 | 32°13'51.61"N | 44°14'58.73"E | 2882 | 86 | 675 ∓ 95 |
| S45 | 32°13'53.38"N | 44°14'57.49"E | 2883 | 159 | 1247 ∓ 14 |
| S46 | 32°13'57.50"N | 44°14'58.22"E | 2884 | 122 | 957 ∓ 55 |
| S47 | 32°13'59.36"N | 44°14'57.39"E | 2885 | 258 | 2024 ∓ 97 |
| S48 | 32°13'51.37"N | 44°14'56.03"E | 2886 | 99 | 776 ∓ 81 |
| S49 | 32°13'52.94"N | 44°14'55.70"E | 2887 | 71 | 557 ∓ 112 |
| S50 | 32°13'59.43"N | 44°15'3.31"E | 2888 | 119 | 933 ∓ 58 |
| **UNSCEAR (2000)** | | | | | **4000** |
| **Maximum value** | | | | | **7341 ∓ 857** |
| **Minimum value** | | | | | **39** ∓ 186 |
| **The average** | | | | | **1342 ∓ 123** |

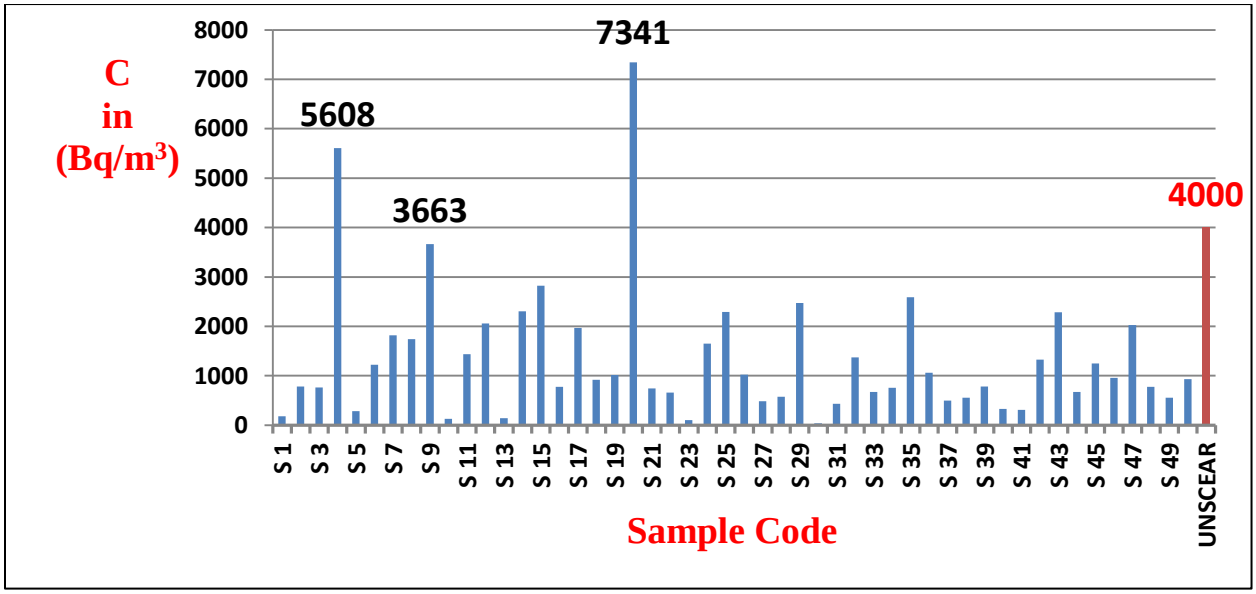


**Figure (4 – 1): Radon gas concentrations in the soil gas (C) in (Bq/m$^3$).**

**Table (4 – 2): Theoretical calculations for concentration of Radium ($C_{Ra}$), concentration of Uranium ($C_U$), area exhalation rate ($E_A$), mass exhalation rate and annual effective dose due to inhalation in the outdoors.**

| Sample code | $C_{Ra}$ (Bq/kg) | $C_u$ in (ppm) or (mg/kg) | $E_A$ (Bq/m$^2$.day) | $E_M$ (Bq/kg.day) | $C_{radon\ near\ the\ soil}$ (Bq/m$^3$) | $(AED)_{outdoorinhalation}$ (mSv/y) |
|---|---|---|---|---|---|---|
| **S1** | 0.018 | 0.200 | 0.043 | 0.008 | 0.180 | 0.002 ∓ 0.0014 |
| **S2** | 0.078 | 0.871 | 0.186 | 0.037 | 0.784 | 0.007∓ 0.0007 |
| **S3** | 0.076 | 0.845 | 0.181 | 0.035 | 0.761 | 0.007 ∓ 0.0007 |
| **S4** | 0.558 | 6.230 | 1.332 | 0.261 | 5.608 | 0.053 ∓ 0.0059 |
| **S5** | 0.028 | 0.314 | 0.067 | 0.013 | 0.282 | 0.003 ∓ 0.0013 |
| **S6** | 0.122 | 1.359 | 0.291 | 0.057 | 1.224 | 0.012 ∓ 0 |
| **S7** | 0.181 | 2.022 | 0.432 | 0.085 | 1.820 | 0.017 ∓ 0.0007 |
| **S8** | 0.173 | 1.934 | 0.414 | 0.081 | 1.741 | 0.017 ∓ 0.0007 |
| **S9** | 0.364 | 4.069 | 0.870 | 0.170 | 3.663 | 0.035 ∓ 0.0033 |
| **S10** | 0.012 | 0.139 | 0.030 | 0.006 | 0.125 | 0.001 ∓ 0.0016 |
| **S11** | 0.143 | 1.595 | 0.341 | 0.067 | 1.435 | 0.014 ∓ 0.0003 |
| **S12** | 0.204 | 2.283 | 0.488 | 0.096 | 2.055 | 0.020 ∓ 0.0011 |
| **S13** | 0.014 | 0.157 | 0.034 | 0.007 | 0.141 | 0.001 ∓ 0.0016 |
| **S14** | 0.229 | 2.562 | 0.548 | 0.107 | 2.306 | 0.022 ∓ 0.0014 |
| **S15** | 0.281 | 3.137 | 0.671 | 0.131 | 2.824 | 0.027 ∓ 0.0021 |
| **S16** | 0.077 | 0.863 | 0.184 | 0.036 | 0.776 | 0.007 ∓ 0.0007 |
| **S17** | 0.196 | 2.187 | 0.468 | 0.092 | 1.969 | 0.019 ∓ 0.0010 |
| **S18** | 0.091 | 1.020 | 0.218 | 0.043 | 0.918 | 0.009 ∓ 0.0004 |
| **S19** | 0.101 | 1.124 | 0.240 | 0.047 | 1.012 | 0.010 ∓ 0.0003 |
| **S20** | 0.730 | 8.157 | 1.743 | 0.342 | 7.341 | 0.070 ∓ 0.0083 |
| **S21** | 0.074 | 0.828 | 0.177 | 0.035 | 0.745 | 0.007 ∓ 0.0007 |
| **S22** | 0.066 | 0.732 | 0.156 | 0.031 | 0.659 | 0.006 ∓ 0.0009 |
| **S23** | 0.010 | 0.113 | 0.024 | 0.005 | 0.102 | 0.001 ∓ 0.0016 |
| **S24** | 0.164 | 1.830 | 0.391 | 0.077 | 1.647 | 0.016 ∓ 0.0006 |
| **S25** | 0.228 | 2.544 | 0.544 | 0.107 | 2.290 | 0.022 ∓ 0.0014 |
| **S26** | 0.101 | 1.133 | 0.242 | 0.047 | 1.020 | 0.010 ∓ 0.0003 |
| **S27** | 0.048 | 0.540 | 0.115 | 0.023 | 0.486 | 0.005 ∓ 0.0010 |

Next ⟶

| Sample code | $C_{Ra}$ (Bq/kg) | $C_u$ in (ppm) or (mg/kg) | $E_A$ (Bq/m$^2$.day) | $E_M$ (Bq/kg.day) | $C_{radon\ near\ the\ soil}$ (Bq/m$^3$) | $(AED)_{outdoor\ inhalation}$ (mSv/y) |
|---|---|---|---|---|---|---|
| **S28** | 0.057 | 0.636 | 0.136 | 0.027 | 0.573 | 0.005 ∓ 0.001 |
| **S29** | 0.246 | 2.745 | 0.587 | 0.115 | 2.471 | 0.023 ∓ 0.0016 |
| **S30** | 0.004 | 0.044 | 0.009 | 0.002 | 0.039 | 0.0004∓0.0017 |
| **S31** | 0.043 | 0.479 | 0.102 | 0.020 | 0.431 | 0.004∓ 0.0011 |
| **S32** | 0.137 | 1.525 | 0.326 | 0.064 | 1.373 | 0.013∓ 0.0001 |
| **S33** | 0.067 | 0.749 | 0.160 | 0.031 | 0.675 | 0.006 ∓0.0009 |
| **S34** | 0.075 | 0.837 | 0.179 | 0.035 | 0.753 | 0.007 ∓ 0.0007 |
| **S35** | 0.257 | 2.876 | 0.615 | 0.120 | 2.588 | 0.025 ∓ 0.0019 |
| **S36** | 0.105 | 1.176 | 0.251 | 0.049 | 1.059 | 0.010 ∓ 0.0003 |
| **S37** | 0.049 | 0.549 | 0.117 | 0.023 | 0.494 | 0.005 ∓ 0.001 |
| **S38** | 0.055 | 0.619 | 0.132 | 0.026 | 0.557 | 0.005 ∓ 0.001 |
| **S39** | 0.078 | 0.871 | 0.186 | 0.037 | 0.784 | 0.007 ∓ 0.0007 |
| **S40** | 0.033 | 0.366 | 0.078 | 0.015 | 0.329 | 0.003 ∓ 0.0013 |
| **S41** | 0.030 | 0.340 | 0.073 | 0.014 | 0.306 | 0.003 ∓ 0.0013 |
| **S42** | 0.132 | 1.473 | 0.315 | 0.062 | 1.326 | 0.013 ∓ 0.0001 |
| **S43** | 0.227 | 2.536 | 0.542 | 0.106 | 2.282 | 0.022 ∓ 0.0014 |
| **S44** | 0.067 | 0.749 | 0.160 | 0.031 | 0.675 | 0.006 ∓ 0.0009 |
| **S45** | 0.124 | 1.385 | 0.296 | 0.058 | 1.247 | 0.012 ∓ 0 |
| **S46** | 0.095 | 1.063 | 0.227 | 0.045 | 0.957 | 0.009 ∓ 0.0004 |
| **S47** | 0.201 | 2.248 | 0.481 | 0.094 | 2.024 | 0.019 ∓ 0.001 |
| **S48** | 0.077 | 0.863 | 0.184 | 0.036 | 0.776 | 0.007 ∓ 0.0007 |
| **S49** | 0.055 | 0.619 | 0.132 | 0.026 | 0.557 | 0.005 ∓ 0.001 |
| **S50** | 0.093 | 1.037 | 0.222 | 0.043 | 0.933 | 0.009 ∓ 0.0004 |
| **ICRP** [37] | --- | --- | --- | --- | --- | **1** |
| **WHO** [37] | --- | --- | --- | --- | --- | **0.1** |
| **Maximum value** | **0.730** | **8.16** | **1.743** | **0.3417** | **7.341** | **0.070 ∓ 0.0083** |
| **Minimum value** | **0.004** | **0.04** | **0.009** | **0.002** | **0.039** | **0.0004 ∓ 0.001** |
| **The average** | **0.134** | **1.49** | **0.319** | **0.0625** | **1.342** | **0.013 ∓ 0.001** |

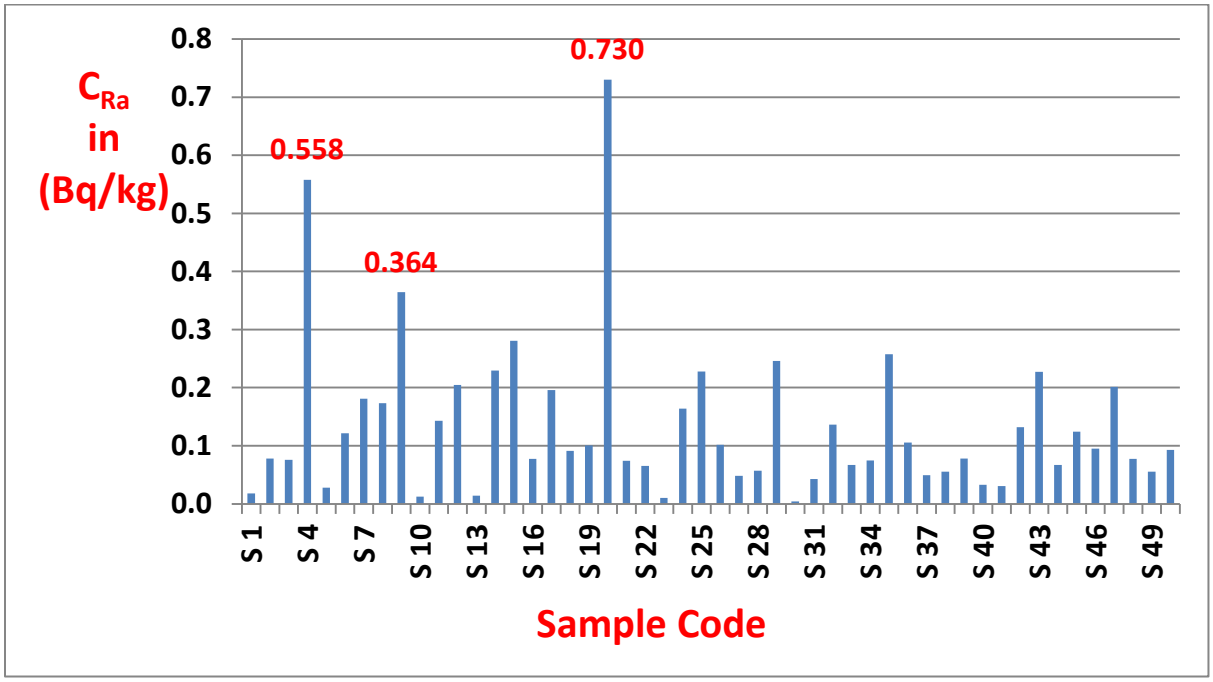


**Figure (4 – 2): Radium concentration for the soil samples.**

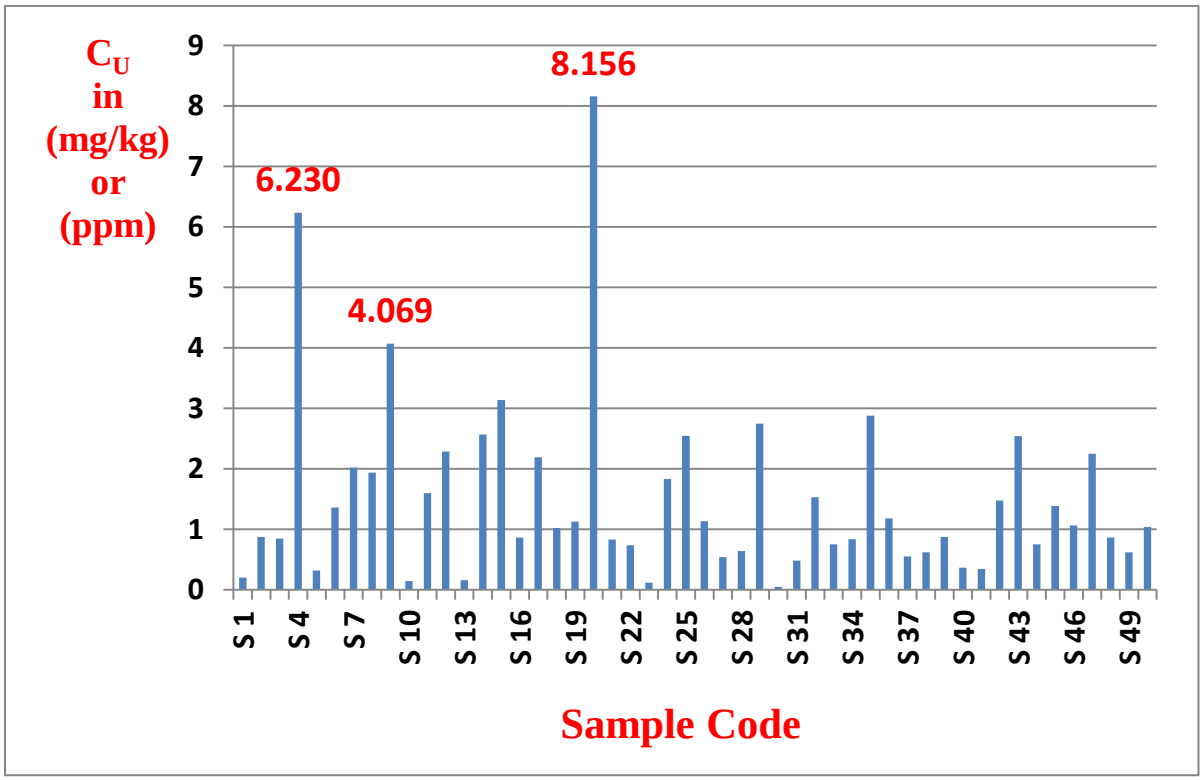


**Figure (4 – 3): Uranium-238 concentrations ($C_U$) for the soil samples.**

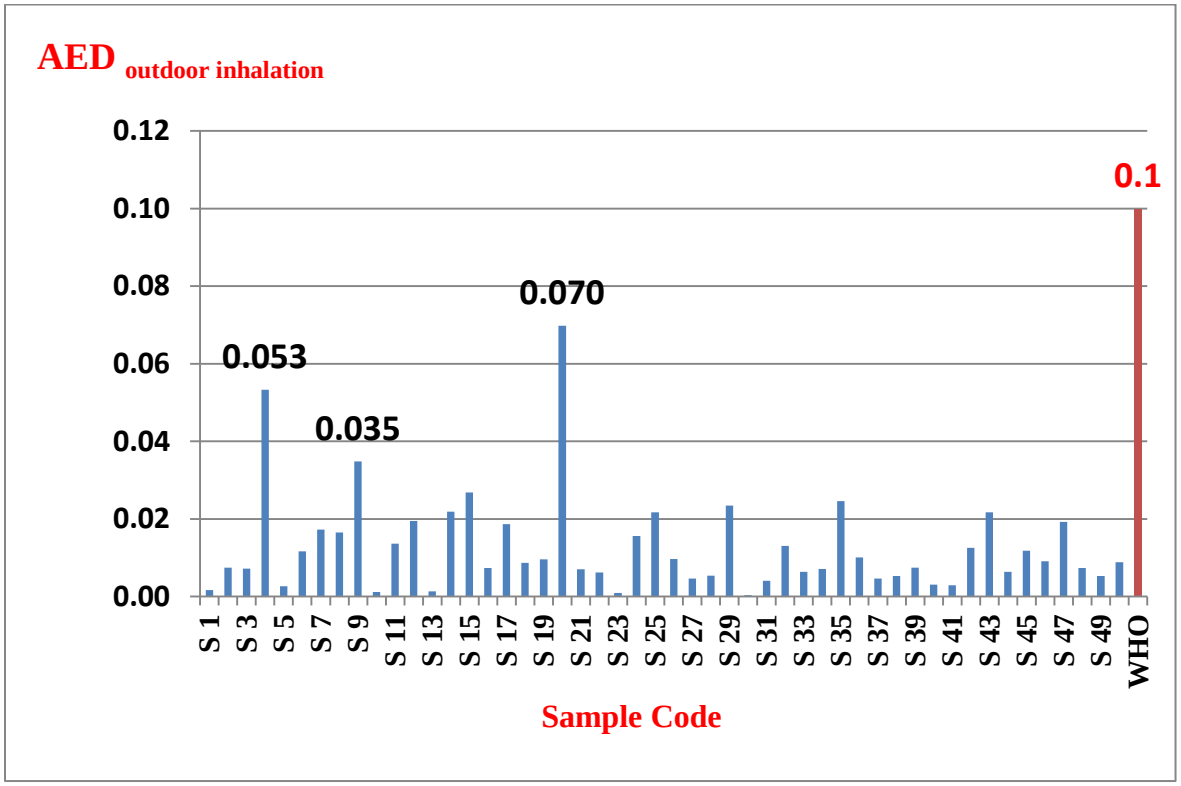


**Figure (4 – 4): The Annual Effective Dose $AED_{outdoor\ inhalation}$ due to Radon–222 gas inhalation in the outdoor air in (mSv/y).**

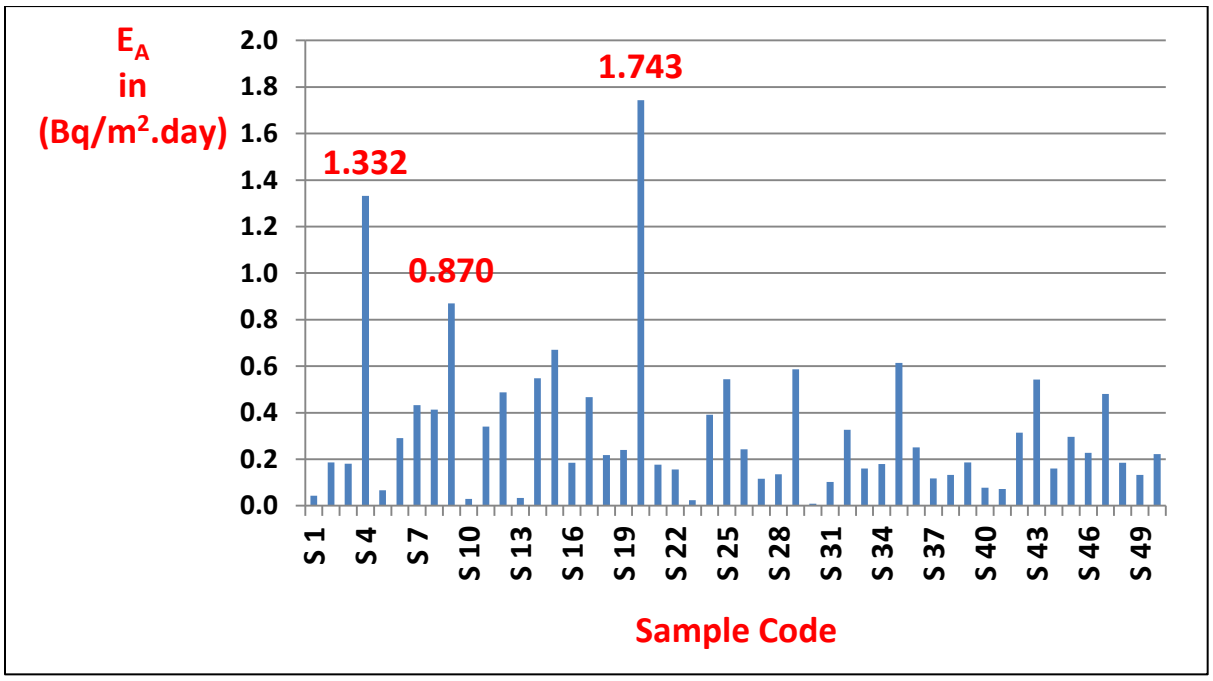


**Figure (4 – 5): The exhalation rates for the soil samples per unit area.**

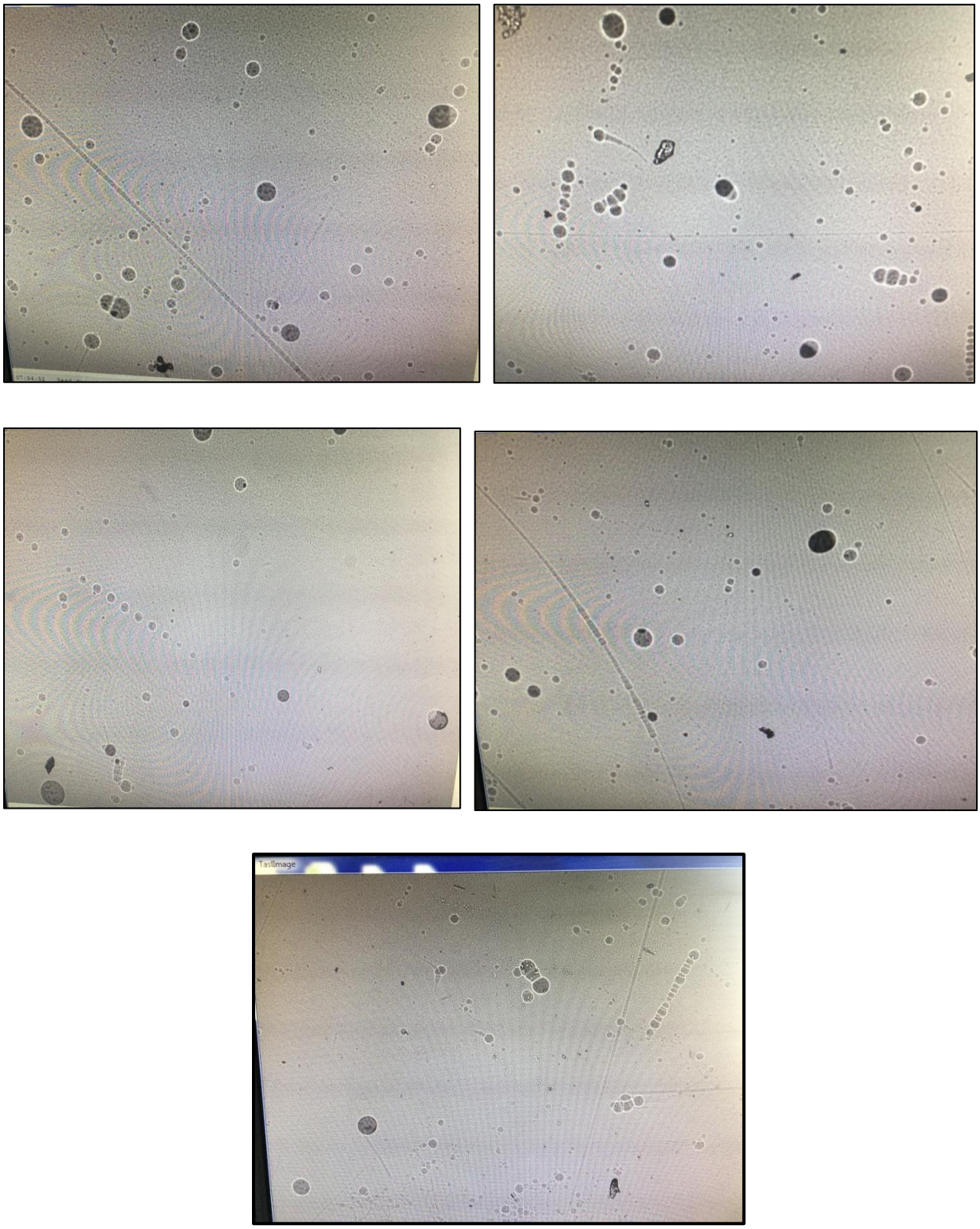


**Figure (4 – 6): Images for the tracks taken by TASL system.**

## 4.3: The Results of Water Samples

The results in Table (4 – 3) are calculated according to Equations (2.14 and 2.15) after knowing the distance between the surface of the water sample (h = 8 cm), the thickness of the sample (2 cm), the track density, the time of exposure (60 day), the calibration factor (K= 0.3 track.m$^3$/Bq.cm$^2$.day) and ($\lambda_{Rn} = 0.18$ day$^{-1}$).

**Table (4 – 3):The concentration of Radon gas for different types of water was measured by using CR-39 detector (passive method).**

| Sample code | Coordinates | | Position description | Water type | Detector number | $\rho_T$ (Track/cm$^2$) | C (Bq/m$^3$) |
|---|---|---|---|---|---|---|---|
| | Longitude | Latitude | | | | | |
| **W1** | 32°14'5.38"N | 44°15'31.21"E | At the RO unit inside the efinary | Well | 2899 | 123 | 297 ∓ 53 |
| **W2** | 32°13'43.17"N | 44°15'33.31"E | Behind the service center | Well | 2947 | 26 | 63 ∓ 30 |
| **W3** | 32°13'53.22"N | 44°14'54.74"E | At the end of the refinery | Well | 2944 | 50 | 121 ∓ 10 |
| **W4** | 32°13'40.81"N | 44°15'18.24"E | Behind refining units | Waste | 2948 | 105 | 253 ∓ 37 |
| **W5** | 32°13'52.51"N | 44°15'29.40"E | At high studies unit | Tap | 2943 | 30 | 72 ∓ 27 |
| **W6** | 32°14'4.20"N | 44°15'30.06"E | At the RO unit inside the refinary | RO | 2945 | 96 | 232 ∓ 30 |
| **W7** | 32°14'5.24"N | 44°15'27.17"E | At the RO unit inside the refinery | River water at refinery | 2946 | 89 | 215 ∓ 24 |
| **W8** | 32°13'46.03"N | 44°15'21.43"E | At the refining units | Boiler water | 2941 | 5 | 12 ∓ 48 |
| **W9** | 32°13'36.39"N | 44°15'8.28"E | Near the flare | Well | 2915 | 29 | 70 ∓ 28 |
| **WHO (2008) [42]** | --- | --- | --- | --- | --- | --- | **400** |
| **EPA [7]** | --- | --- | --- | --- | --- | --- | **11000** |
| **Max.** | | | | | | 123 | 297 ∓ 53 |
| **Min.** | | | | | | 5 | 12 ∓ 48 |
| **Ave.** | | | | | | 61.4 | 148 ∓ 32 |

Table (4 – 4) shows the results obtained from RAD7 monitor, where the results were immediately printed after the end of the test, and the result for each sample were an average value for four cycles of measuring. The spectra of alpha particles were shown in Figure (4 – 7).

**Table (4 – 4):The average of Radon gas concentration for different types of water was measured by using RAD7 monitor (active method).**

| Sample code | $\overline{C_w}$ in (Bq/m$^3$) | Standard deviation in (Bq/m$^3$) | $\overline{C_w}$ in (pCi/L) | Standard deviation in (pCi/L) | $\overline{C_w}$ in (kBq/m$^3$) | Standard deviation in (kBq/m$^3$) |
|---|---|---|---|---|---|---|
| **W1** | 471 | 218 | 17427 | 8066 | 0.471 | 0.218 |
| **W2** | 72.4 | 145 | 2678.8 | 5365 | 0.072 | 0.145 |
| **W3** | 109 | 72.4 | 4033 | 2678.8 | 0.109 | 0.0724 |
| **W4** | 72.4 | 83.6 | 2678.8 | 3093.2 | 0.0724 | 0.0836 |
| **W5** | 109 | 72.4 | 4033 | 2678.8 | 0.109 | 0.0724 |
| **W6** | 36.2 | 72.4 | 1339.4 | 2678.8 | 0.0362 | 0.0724 |
| **W7** | 36.2 | 72.4 | 1339.4 | 2678.8 | 0.0362 | 0.0724 |
| **W8** | 0 | 0 | 0 | 0 | 0 | 0 |
| **W9** | 72 | 83.2 | 2664 | 3078.4 | 0.072 | 0.0832 |
| **WHO (2008)** [42] | **400** | **---** | **14800** | **---** | **0.400** | **---** |
| **EPA** [7] | **11000** | **---** | **407000** | **---** | **11** | **---** |
| Average | **108.69** | **91.04** | **4021.50** | **3368.64** | **0.11** | **0.09** |
| Maximum value | **471** | **218** | **17427** | **8066** | **0.471** | **0.218** |
| Minimum value | **0** | **0** | **0** | **0** | **0** | **0** |

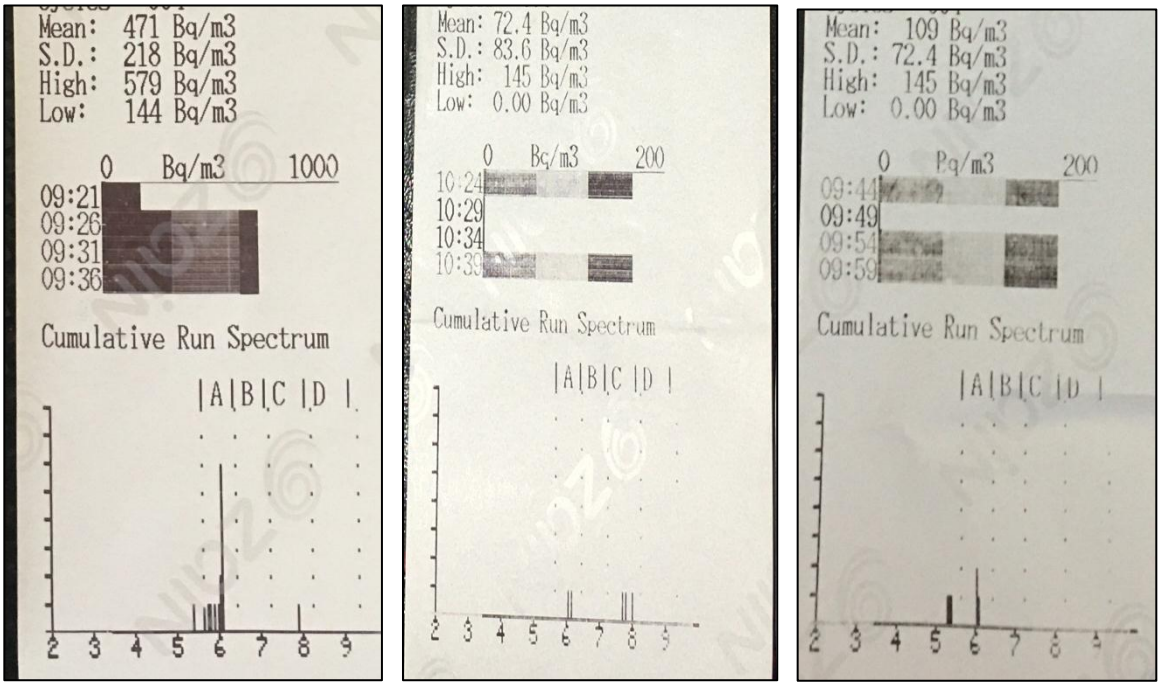


W1 W2 W3

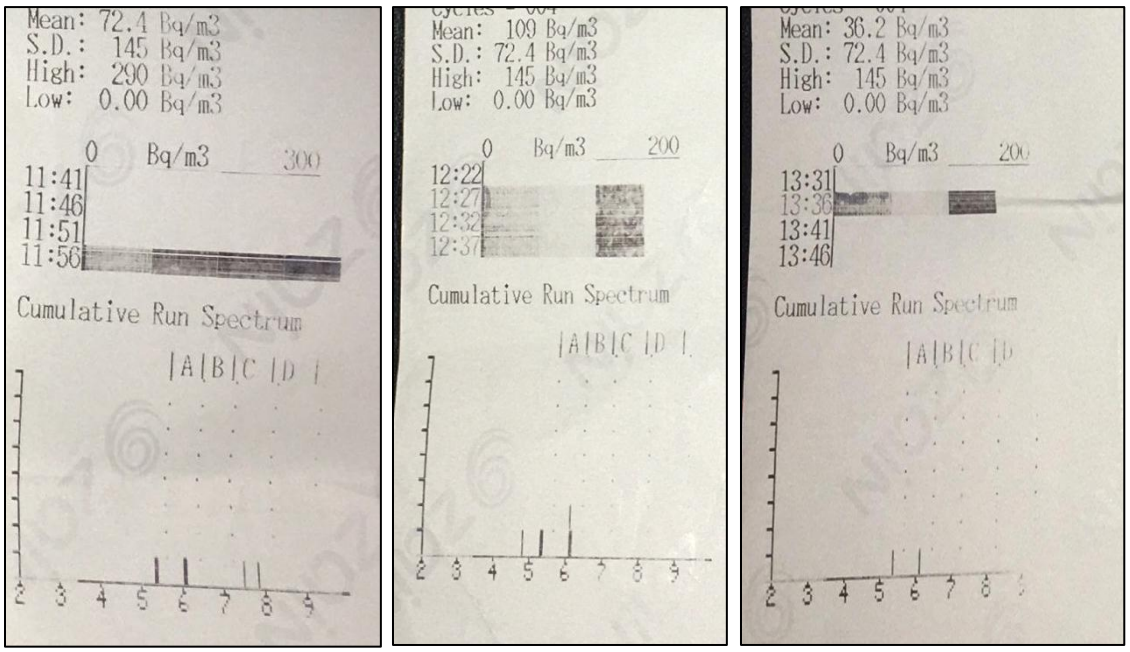


**W4** **W5** **W6**

**Figure(4 – 7): The spectra of alpha particles energy and the highest and lowest values of Radon gas concentration for the samples W1, W2, W3, W4, W5 and W6 in the refinery.**

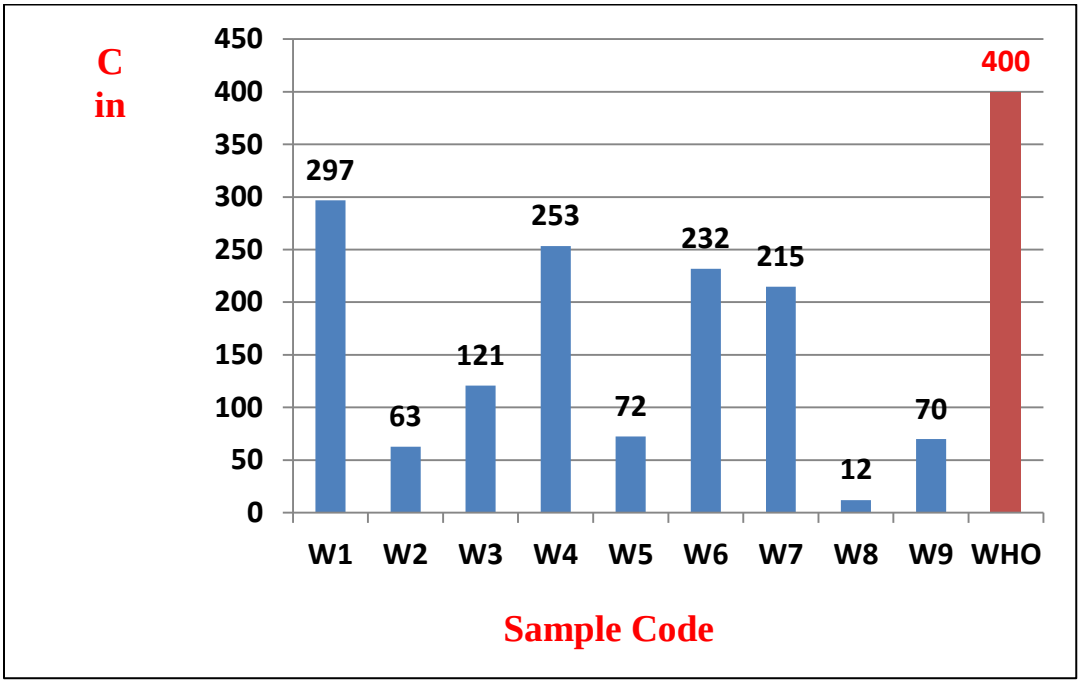


**Figure (4 – 8): The concentrations of Radon gas for different types of water measured by CR-39 detectors.**

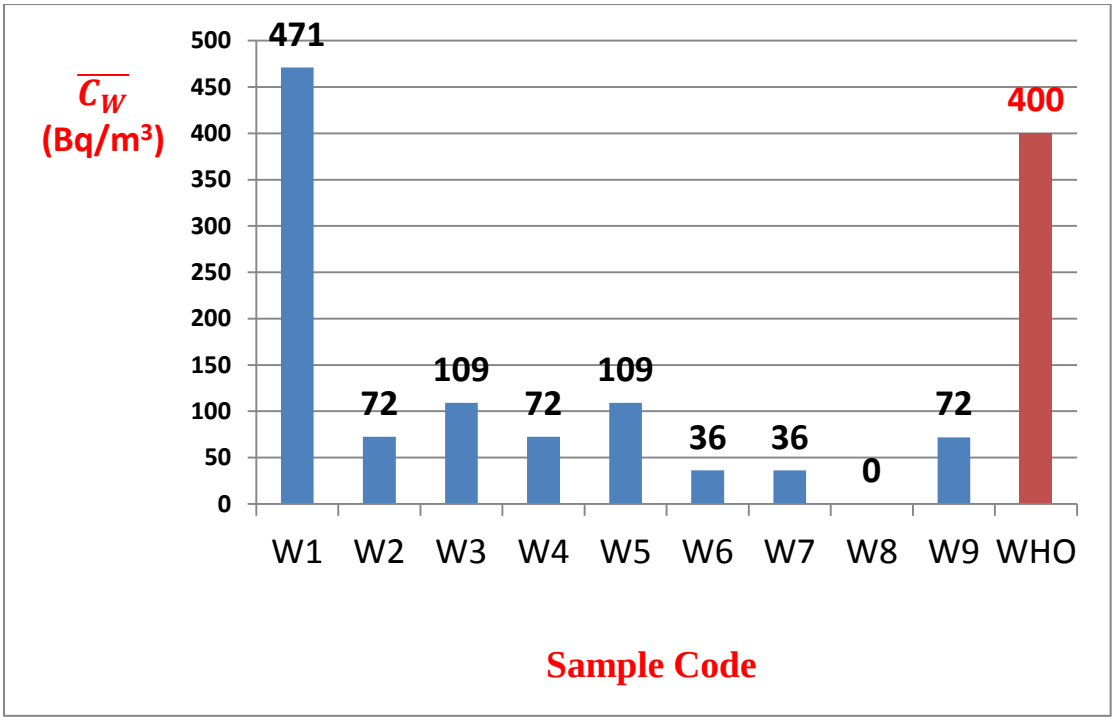


**Figure (4 – 9): The concentrations of Radon gas for different types of water measured by RAD7 monitor.**

From the results of soil samples, and as shown in Figure (4 – 1), it is clear that some samples were with high concentrations of Radon–222 gas in the soil gas, this may be due to industrial operations conducted in the study area (AL-Najaf refinery) which may cause an increase of the Radium content, as oily wastes (sludge and scale) have a complex and variable composition.

Geological reasons may be behind the high levels of Radon–222 in the soil gas such as a fracture in the bed rock under the soil of the area, the porosity of the soil, and the composition of the rocks from which the soil is derived.

From the results of water, and as shown in Figures (4 – 8 and 4 – 9), it is clear that the average Radon–222 gas concentration of well water at the RO unit is the highest because the water of the well (ground water) is in contact with rocks at the bottom of the well which contains an amount of Radium–226 that is come from a naturally occurring radioactive element Uranium-238, and this affects the levels of radon in drinking water as the drinking water in the refinery before treating is a mixture of river water and well water, the water in the boiler is Radon – free water, as the radon decayed into its progenies in the reservoirs before entering the refining units, or as it is transmitted into the air as the water boils.

Radon–222 gas concentration in the tap water is lower than in well water, as it is a mixture of well water and river water.

Radon concentration in wastewater comes from oily wastes (sludge resulting from refining operations) while the water before entering the process of refining (in the boiler) is radon-free water.

Radon–222 gas concentration in tap water comes mainly from the water of the well as tap water in the refinery is a mixture of well water and river water. River water has Radon–222 gas concentration less than well water because the water of the river is in motion through open air.

## 4.4: Estimations related to Radon–222 Gas in Water

In Table (4 – 5), the concentration of Radon–222 gas in air from water contribution was estimated due to Equation (2.2) after substituting the value of the transfer factor ($10^{-4}$), and the values of Radon–222 gas in water (passive method and active method). The Annual Effective Doses due to inhalation of Radon–222 gas at indoor air which was resulted from water contribution are calculated according to Equation (2.8), after knowing the time of existence at indoor air per year (7000 h/y), dose conversion factor (9 $nSvy^{-1}(Bq/m^3)$, Radon–222 gas concentration in water, the transfer factor ($10^{-4}$), and the equilibrium factor (0.4).

**Table(4 – 5): The estimation of the average of Radon gas concentration in the air and AED due to inhalation the indoor air.**

| Sample code | $\overline{C_a}$ in (Bq/m3) Passive method | $\overline{C_a}$ in (Bq/m3) Active method | $AED_{indoor\ inhalation}$ $\times 10^{-7}$ (mSv/y) Passive method | $AED_{indoor\ inhalation}$ $\times 10^{-6}$ (mSv/y) Active method |
|---|---|---|---|---|
| A1 | 0.030 | 0.0471 | $7.48 \mp 1.33$ | $1.19 \mp 0.324$ |
| A 2 | 0.006 | 0.00724 | $1.58 \mp 0.76$ | $0.18 \mp 0.033$ |
| A 3 | 0.012 | 0.0109 | $3.04 \mp 0.24$ | $0.27 \mp 0.001$ |
| A 4 | 0.025 | 0.00724 | $6.39 \mp 0.94$ | $0.18 \mp 0.033$ |
| A 5 | 0.007 | 0.0109 | $1.82 \mp 0.68$ | $0.27 \mp 0.001$ |
| A 6 | 0.023 | 0.00362 | $5.84 \mp 0.75$ | $0.09 \mp 0.064$ |
| A 7 | 0.021 | 0.00362 | $5.41 \mp 0.59$ | $0.09 \mp 0.064$ |
| A 8 | 0.001 | 0 | $0.30 \mp 1.21$ | $0.00 \mp 0.096$ |
| A9 | 0.007 | 0.0072 | $1.76 \mp 0.70$ | $0.18 \mp 0.033$ |
| WHO [37] | --- | --- | 1000000 | 100000 |
| ICRP [37] | --- | --- | 10000000 | 1000000 |
| Average | | 0.01 | $3.735 \mp 0.799$ | $0.272 \mp 0.072$ |
| Maximum value | | 0.0471 | $7.48 \mp 1.33$ | $1.19 \mp 0.324$ |
| Minimum value | | 0 | $0.30 \mp 1.21$ | $0.00 \mp 0.096$ |

In Table (4 – 6), theoretical estimations for the number of cases of lung cancer during the year per million (LCR) are estimated according to Equation (2.10) after knowing the Annual Effective Dose (AED) due to inhalation. The exposure rate due to inhalation Radon–222 gas and it's progenies are calculated according to Equation (2.11) after substituting the number of hours in the year (8760 h/y), the number of working hours in the month (170), the concentration of radon–222 gas in the air.

The concentrations of the energy of alpha particles in air (PAEC) are calculated due to Equation (2.12), after substituting the concentration of Radon–222 gas in the air and the equilibrium factor (F= 0.6).

**Table (4 – 6): LCR, PAEC and $E_P$ as a result of inhalation of Radon gas and its' progenies which come from different types of water inside the refinery.**

| Sample code | LCR $\times 10^{-6}$ (case/year. Million) | PAEC (WL) $\times 10^{-6}$ | $E_P$ (WLM/y) $\times 10^{-6}$ |
|---|---|---|---|
| A1 | 2.136 | 5.092 | 209.906 |
| A2 | 0.328 | 0.783 | 32.266 |
| A3 | 0.494 | 1.178 | 48.577 |
| A4 | 0.328 | 0.783 | 32.266 |
| A5 | 0.494 | 1.178 | 48.577 |
| A6 | 0.164 | 0.391 | 16.133 |
| A7 | 0.164 | 0.391 | 16.133 |
| A8 | 0.000 | 0.000 | 0 |
| A9 | 0.327 | 0.778 | 32.088 |
| Average | 0.493 | 1.175 | 48.438 |
| Max. Value | 2.136 | 5.092 | 209.906 |
| Min. Value | 0 | 0 | 0 |

## 4.5: Comparison The Results with Local and International Studies

The results of the soil samples of Al – Najaf refinery were near the results obtained from previous studies conducted in Al – Najaf governorate in 2011, 2012, 2015, and 2017, except the results of samples with codes (S4, S9, and S20). In copmarison the results of soil samples with the results of some studies mentioned in Table (4 – 7), the results are higher than those mentioned in this table.

The results of RO water and well water are near the results of the previous studies conducted in Al-Najaf governorate in 2013, 2015, and 2020. In comparison the results of well water inside Al – Najaf refinery with the results mentioned in Table (4 – 7), the results of the well water are much less than those mentioned in this table.

**Table (4 – 7): Radon gas concentrations from international previous studies and local studies.**

| Country, Region and year | Sample type | Results in (Bq/m3) | Technique | Refrence |
|---|---|---|---|---|
| Saudi Arabia, Qassim, 2019 | Well water | 1200 – 15430 | RAD7 monitor | [103] |
| Palestine, Bethlehem, 2018 | Soil | 19 – 572 | CR-39 | [104] |
| India, Northern Rajasthan, 2016 | Soil | 941 – 1050 | RAD7 monitor | [69] |
| India, Northern Rajasthan, 2016 | Well water | 500 – 22000 | RAD7 monitor | [69] |
| India, Gopalpur and Rushikulya beach, Orissa | Sand | 389 – 997 | LR-115 typeII | [105] |

**Next** ⟶

| Country, Region and year | Sample type | Results in (Bq/m3) | Technique | Refrence |
|---|---|---|---|---|
| Italy, Neapolitan catacombs, 2014 | Soil | 440 – 1299 | LR-115 typeII | [106] |
| Iraq, Al–Najaf governorate, 2011 | Soil | 9290 – 9 | RAD7 monitor | [28] |
| Iraq, Al–Najaf governorate, 2012 | Soil | 56 – 758 | CR-39 | [29] |
| Iraq, Al–Najaf governorate, 2013 | Water | 2.4 – 225 | RAD7 monitor | [31] |
| Iraq, Al–Najaf governorate, 2015 | Water | 1270 – 66 | RAD7 monitor | [33] |
| Iraq, Al–Najaf governorate, 2017 | Soil | 506 – 1194 | CR-39, CN-85 | [35] |
| Iraq, Al–Najaf governorate, 2020 | Water | 174 – 2000 | RAD7 monitor, CR-39 | [39] |
| Iraq, Al–Najaf governorate, Al–Najaf refinery, 2022 | Soil | 7341 – 39 | CR-39 | **Present study** |
| Iraq, Al–Najaf governorate, Al–Najaf refinery, 2022 | Water | 471 – 0 | RAD7 monitor | **Present study** |
| Iraq, Al–Najaf governorate, Al–Najaf refinery, 2022 | Water | 297 – 12 | CR-39 | **Present study** |

# 4.6: Statistical Results:

## 1- For The Soil Samples

**Table (4 – 8 ): Pearson correlation coefficients for the results of the soil samples calculated using SPSS program.**

| | | C | AED | $E_A$ | $E_M$ | $C_U$ | $C_{Ra}$ |
|---|---|---|---|---|---|---|---|
| **C** | Pearson Correlation | 1 | 1** | 1** | 1** | 1** | 1** |
| | Sig. (2-tailed) | | 0.000 | 0.000 | 0.000 | 0.000 | 0.000 |
| **AED** | Pearson Correlation | 1** | 1 | 1** | 1** | 1** | 1** |
| | Sig. (2-tailed) | 0.000 | | 0.000 | 0.000 | 0.000 | 0.000 |
| **$E_A$** | Pearson Correlation | 1** | 1** | 1 | 1** | 1** | 1** |
| | Sig. (2-tailed) | 0.000 | 0.000 | | 0.000 | 0.000 | 0.000 |
| **$E_M$** | Pearson Correlation | 1** | 1** | 1** | 1 | 1** | 1** |
| | Sig. (2-tailed) | 0.000 | 0.000 | 0.000 | | 0.000 | 0.000 |
| **$C_U$** | Pearson Correlation | 1** | 1** | 1** | 1** | 1 | 1** |
| | Sig. (2-tailed) | 0.000 | 0.000 | 0.000 | 0.000 | | 0.000 |
| **$C_{Ra}$** | Pearson Correlation | 1** | 1** | 1** | 1** | 1** | 1 |
| | Sig. (2-tailed) | 0.000 | 0.000 | 0.000 | 0.000 | 0.000 | |
| **. Correlation is significant at the 0.01 level (2-tailed). | | | | | | | |

## 2- For Water Samples

**Table (4 – 9 ): Pearson correlation coefficients for the results of the water samples calculated using SPSS program.**

| | | $C_{Rn}$ with CR-39 | $C_{Rn}$ with RAD7 | AED (CR-39) | AED (RAD7) |
|---|---|---|---|---|---|
| **$C_{Rn}$ with CR-39** | Pearson Correlation | 1 | 0.524 | 1** | 0.524 |
| | Sig. (2-tailed) | | 0.148 | 0.000 | 0.148 |
| **$C_{Rn}$ with RAD7** | Pearson Correlation | 0.524 | 1 | 0.524 | 1** |
| | Sig. (2-tailed) | 0.148 | | 0.148 | 0.000 |
| **AED (CR-39)** | Pearson Correlation | 1** | 0.524 | 1 | 0.524 |
| | Sig. (2-tailed) | 0.000 | 0.148 | | 0.148 |
| **AED (RAD7)** | Pearson Correlation | 0.524 | 1** | 0.524 | 1 |
| | Sig. (2-tailed) | 0.148 | 0.000 | 0.148 | |
| **. Correlation is significant at the 0.01 level (2-tailed). | | | | | |

From Table (4 – 8), the correlation was obvious (Pearson coefficient equals 1) between the concentration of Radon gas in the soil samples (C) and the quantities: Annual Effective Dose (AED), area exhalation rate ($E_A$), mass exhalation rate ($E_M$), Uranium concentration ($C_U$) and Radium content as their relations with (C) were linear relations.

From Table (4 – 9), the correlation was obvious (Pearson coefficient equals 1) between the concentration of radon gas in the water samples ($C_{Rn}$) and Annual Effective Dose (AED) was a linear relation.

The correlation was weak (Pearson coefficient equals 0.5) between the concentration of Radon gas measured by RAD7 monitor ($C_{Rn}$) and the concentration of Radon gas measured by CR-39 detectors ($C_{Rn}$), the weak correlation between both techniques may happens according to the difference in the time of measurements using both techniques, where RAD7 monitor requires 30 minutes at least to complete the test, this depends on the humidity and CR-39 detectors require 60 day of exposure.

# Chapter Five

# Conclusions

# And

# Future Work

## 5.1: Conclusions

1 – Radon–222 gas concentrations in the soil gas of the soil samples are higher than in water samples.

2 – The concentrations of Radon–222 gas in the soil gas for the soil samples with codes (S4 and S20) excede the action level recommended by UNSCEAR (2000).

3 – Radon – 222 gas concentration in the soil gas is changing from location to another, this happens due to the geological composition of the locations of soil samples.

4 – The Annual Effective Doses due to Radon–222 gas inhalation in the outdoor air which is resulted from the soil contributions are all less than the value recommended by WHO, and there is no any radiological risk resulted from radon gas inhalation to the health of the workers of the refinery if they existed in the positions of soil samples for a long period (long – term exposure).

5 – For water samples, the conentrations of Radon–222 gas measured by CR-39 detectors (passive method) are near the concentrations obtained by RAD7 monitor (active method).

6 – The concentrations of Radon – 222 gas in the samples: well water (W1), waste water (W4), RO water (W6), and river water (W7) measured by CR-39 detectors (passive method) are lower than the value recommended by WHO.

7 – Radon–222 gas concentration of the sample collected from the well water (W1), which is measured by RAD7 monitor (active method) is slightly higher than the value recommended by WHO.

8 – The Annual Effective Doses due to Radon–222 gas inhalation in the indoor air which is resulted from water are lower than the value recommended by WHO and ICRP.

9 – The maximum theoretical values for risk parameters such as the rate of exposure, Lung Cancer Risk (LCR), and Potential Alpha Energy Concentration (PAEC) in the air which contains an amount of Radon–222 and it's progenies resulted from water contribution are too low, this means that the health risk due to radon gas inhalation is also low in the places where the water is used.

## 5.2: Recommendations

1 – Avoid existing for a long time in the places where the concentrations of Radon gas are high.

2 – If the workers exist in the places where Radon gas concentrations are high, a protective procedures should be taken such as ventilation, sealing the cracks in the basement of ground and using special systems.

3 – Measure Radon gas concentrations in the soil and water from time to time to ensure that the levels in water are safe.

4 – If Radon levels in water are high, the water should be treated by using special systems to get a free – Radon water.

## 5.3: Future Work

1 – Measuring Radon gas concentrations in the soil gas using other techniques such as RAD7 monitor, and with other depths.

2 – Measuring Radon gas concentrations resulted from the oily products and wastes.

3 – Measuring Radon–222 gas concentrations for different types of water in other seasons.

4 – Measuring Radon–222 gas concentrations in the indoor air of poorly ventilated places or a place in which well water is used alot by using RAD7 monito or other equipements.

5 – Measuring transfer coefficients from water to air at selected sites in which the water is used alot, and estimate the vlaues of Radon–222 gas concentration related to the quantity of water used.

6 – Measuring transfer coefficients for Radon – 222 from the oily wastes to the waste water and air.

# References

## References

[1] G. F. Knoll, *Radiation Detection and Measurement*, fourth edition, USA: Wiley, 2010.

[2] M. I. Ojovan and W. E. Lee, *An Introduction to Nuclear Waste Immobilisation*, First edit. Amsterdam: Elsevier, 2005.

[3] L. Weinstein, *Nuclear Physics Explained*, first edition, USA, Virginia: The Great Courses, 2018.

[4] F. Martin and J. Taylor, *Production of The Raionuclides in the Earth and Their Hydrogeologic Significance, with Emphasis on Chlorine–36 and Iodine–129*, first edition, USA: U.M.I, 1988.

[5] A. H. Ismail and M. S. Jaafar, "Interaction of Low-Intensity Nuclear Radiation Dose With the Human Blood: Using the New Technique of CR-39NTDs for an in Vitro Study," *Appl. Radiat. Isot.*, vol. 69, no. 3, pp. 559–566, 2011.

[6] M. F. L'Annunziata, *Handbook of Radioactivity Analysis*, third edition, USA: Academic Press, 2012.

[7] National Research Council (US) Committee on Risk Assessment of Exposure to Radon in Drinking Water., "Risk Assessment of Radon in Drinking Water," National Academies Press (USA), Washington, 1999.

[8] I. Hore-Lacy, *Nuclear electricity*, sixth edition, Australia: Uranium Information Center, Mineral council of Australia, 2000.

[9] J. M. Samet, "Radiation and Cancer Risk: A Continuing Challenge for Epidemiologists," *Environ. Heal. A Glob. Access Sci. Source*, vol. 10, no. 1, pp. 1–9, 2011.

[10] BL. Cohen, "Cancer Risk from Low-level Radiation," *AJR Am J Roentgenol*, vol. 179, no. 5, pp. 1137–1143, 2002.

[11] R. Antoni and L. Bourgois, *Applied Physics of External Radiation Exposure*, first edition, Arpajon, France: Springer, 2017.

[12] R. Teoule, "Radiation-Induced DNA Damage and its Repair," *Int. J. Radiat. Biol. Relat. Stud. Physics, Chem. Med.*, vol. 51, no. 4, pp. 573–589, 1987.

[13] F. Hutchinson, "Chemical Changes Induced in DNA by Ionizing Radiation," *Prog. Nucleic Acid Res. Mol. Biol.*, vol. 32, no. 1, pp. 115–154, 1985.

[14] J. B. Little, "Radiation Carcinogenesis," *Carcinogenesis*, vol. 21, no. 3, pp. 221–242, 2000.

[15] JM. Samet, *Radon. In Comprehensive Toxicology*, second edition, New York: Elsevier;McQueen CA, 2010.

[16] J. Pouget and S. Mather, "General aspect of the cellular response to low and high-LET radiation," *J. Nucl. Med.*, vol. 28, no. 1, pp. 541–561, 2001.

[17] International Atomic Energy Agency - IAEA, *Extent of Environmental Contamination by Naturally Occurring Radioactive Material (NORM) and Technological Options for Mitigation*, TRS-419. Vienna: IAEA, 2003.

[18] International Atomic Energy Agency - IAEA, *Technologies for the Treatment of Effluents from Uranium Mines, Mills and Tailings*, TECDOC 129. Vienna: IAEA, 2002.

[19] E. M. Pontedeiro, P. F. L. Heilbron and R. M. Cotta, "Assessment of the Mineral Industry NORM/TENORM Disposal in Hazardous Landfills," *J. Hazard. Mater.*, vol. 139, no. 3, pp. 563–568, 2007.

[20] E. M. El Afifi, M. A. Hilal, S. M. Khalifa and H. F. Aly, "Evaluation of U, Th, K and Emanated Radon in Some NORM and TENORM samples," *Radiat. Meas.*, vol. 41, no. 5, pp. 627–633, 2006.

[21] J. J. Bevelacqua, *Basic Health Physics: Problems and Solutions*, first edition, Hoboken, New Jersey, USA: John Wiley & Sons, 2010.

[22] H. A. Khan and N. A. Khan, "Solid State Nuclear Track Detection (

SSNTD): A Useful Scientific Tool for Basic and Applied Research," *J. Islam. Acad. Sci.*, vol. 4, no. 1, pp. 303–312, 1989.

[23] A. M. Bhagwat, *Solid State Nuclear Track Detection: Theory and Applications*, Second Edi. Kalpakkam, Tamil Nadu: Indian Society for Radiation Physics, 1993.

[24] L. Cerrito, *Radiation and Detectors, Introduction to the Physics of Radiation and Detection Devices*, first edition, London: Springer, 2017.

[25] ICRP, "Publication 60. Recommendations of the ICW," *Ann. ICRP*, vol. 21, no. 1, pp. 1–2, 1991.

[26] J. Pouget and S. Mather, "General Aspect of the Cellular Response to Low and High-LET Radiation," *Eur. J. Nucl. Med.*, vol. 28, no. 1, pp. 541–561, 2001.

[27] J. Pouget and S. Mather, "Calculations of Stopping Power, and Range of Ions Radiation (Alpha Particles) Interaction with Different Materials and Human Body Parts," *Int. J. Phys.*, vol. 5, no. 3, pp. 92–98, 2017.

[28] A. K. Hasan, A. R. H. Subber and A. R. Shaltakh, "Measurement of Radon Concentration in Soil Gas using RAD7 in the environs of Al-Najaf Al-Ashraf City-Iraq," *Adv. Appl. Sci. Res.*, vol. 2, no. 5, pp. 273–278, 2011.

[29] I. K. Ahmed, "Measurement of Radon-222 Concentration in Soil Samples of some Regions in AL-Ansar Historical District in The Southern of AL- najf city Using Nuclear Track Detector CR-39," *Al- Mustansiriyah J. Sci*, vol. 23, no. 8, pp. 125–132, 2012.

[30] Z. A. Hussein, M. S. Jaafar and A. H. Ismail, "Measurement of Radium Content and Radon Exhalation Rates in Building Material Samples Using Passive and Active Detecting Techniques," *Int. J. Sci. Eng. Res.*, vol. 4, no. 9, pp. 1827–1831, 2013.

[31] A. A. AboJassim and A. R. Shitake, "Estimated the Mean of Annual

Effective Dose of Radon Gases for Drinking Water in Some Locations at Al-Najaf city," *J. Kufa-physics*, vol. 5, no. 2, pp. 1–20, 2013.

[32] A. A. Ridha, M. S. Karim, N. Farhan Kadhim and N. F. Kadhim, "Measurement of Radon Gas Concentration in Soil and Water Samples in Salahaddin Governorate-Iraq Using Nuclear Track Detector (CR-39)," *Civ. Environ. Res.*, vol. 6, no. 1, pp. 24–30, 2014.

[33] A. A. Abojassim, H. H. Al-Gasaly, F. A. Al-Temimie and M. A. Al-Aarajy, "Study of Time Measured Factor on Measuring Radon Concentrations in Groundwater," *Int. Sci. J. Theor. Appl. Sci.*, vol. 21, no. 01, pp. 16–21, 2015.

[34] K. H. Hatif, M. K. Muttaleb and A. H. Abass, "Measurement of Radioactive Radon Gas Concentrations of Water in The Schools for Kifel," *Wold Sci. News*, vol. 54, no. 1, pp. 191–201, 2016.

[35] A. A. Abojassim, "Alpha Particles Concentrations from Some Soil Samples of Al-Najaf (Iraq)," *Polish J. Soil Sci.*, vol. 50, no. 2, pp. 249–263, 2017.

[36] I. T. Al-Alawy and A. A. Hasan, "Radon Concentration and Dose Assessment in Well Water Samples from Karbala Governorate of Iraq," *J. Phys. Conf. Ser.*, vol. 1003, no. 12117, pp. 0–9, 2018.

[37] A. A. Sharrad and A. K. Farhood, "Radon Concentration Measurements in Soil Gas of Sawa Lake, Samawa City-South of Iraq," *Int. J. Adv. Res.*, vol. 7, no. 6, pp. 170–177, 2019.

[38] A. K. Hashim and S. S. Nayif, "Assessment of Internal Exposure to Radon in Schools in Karbala, Iraq," *J. Radiat. Nucl. Appl.*, vol. 4, no. 1, pp. 25–34, 2019.

[39] A. A. Abojassim, "Comparative Study Between Active and Passive Techniques for Measuring Radon Concentrations in Groundwater of Al-Najaf city, Iraq," *Groundw. Sustain. Dev.*, vol. 11, no. pp. 100–476, 2020.

[40] A. K. Hashim, A. N. Hmood, N. I. Ashoor and M. N. Hammood, "Radiation

Hazards due to Radon in The Air of Buildings Surrounding Imam Hussain Holy Shrine in Karbala, Iraq," *IOP Conf. Ser. Mater. Sci. Eng.*, vol. 928, no. 7, pp. 1–12, 2020.

[41] A. K. Hashim, L. A. Najam and F. M. A. Aljomaily, "Contribution of Soil in The Annual Effective Dose due to Radon in The Air of Some Dwellings in The City of Karbala, Iraq," *Polish J. Med. Phys. Eng.*, vol. 27, no. 3, pp. 233–239, 2021.

[42] A. A. Marzaali, M. A. Al-Shareefi and A. A. Abojassim, "Practical Study to Assess Radioactive Radon Gas in Groundwater Samples of Dhi-Qar Governorate," *IOP Conf. Ser. Earth Environ. Sci.*, vol. 722, no. 1, pp. 1–11, 2021.

[43] M. Baskaran, *Radon: A Tracer For Geological, Geophysical and Geochemical Studies*, first edition, Detroit, USA: Springer, 2016.

[44] National Research Council, *Evaluation of Guidelines for Exposures to Technologically Enhanced Naturally Occurring Radioactive Materials*, first edition, Washington: The National Academies, 1999.

[45] O. Catelinois, A. Rogel, D Laurier, S. Billon, D. Hemon, P. Verger and M. Tirmarche "Lung Cancer Attributable to Indoor Radon Exposure in France: Impact of the Risk models and Uncertainty Analysis," *Environ. Health Perspect.*, vol. 114, no. 9, pp. 1361–1366, 2006.

[46] N. E. Bolus, "NCRP Report 160 and What It Means for Medical Imaging and Nuclear Medicine," Journal of Nuclear Medicine, vol. 41, no. 4 , 2013.

[47] P. Krailadsiri and J. Seqhatchian, "Residual Red Cell and Platelet Content in WBCreduced Plasma Measured by a Novel Flow Cytometric Method," *Transfus. Apher. Sci.*, vol. 24, no. 3, pp. 279–289, 2001.

[48] ICRU, "Measurement and Reporting of Radon Exposure," *J. ICRU*, vol. 12, no. 2, pp. 1–208, 2012.

[49] A. S. Hussein, "Radon in the Environment : Friend or Foe ?," *Environ. Phys. Conf.*, vol. 23, no. 3, pp. 43–52, 2008.

[50] N. S. Eash, T. J. Sauer, D. O'Dell and E. Odoi, *Soil Science Simplified*, sixth edition, Hoboken, New Jersey: John Wiley & Sons, 2016.

[51] P. Anderson, B. Clavensjo, and G. Akerblom, "The Effect of The Ground on the Concentration of Radon and Gamma Radiation Indoors," *Swedish Counc. Build. Res. Rep.*, vol. 9, pp. 1–442, 1983.

[52] SK. Sahoo, "Measurement of Uranium and It's Isotopes at Trace Levels in Environmental Samples Using Mass Spectrometry," *Indian J. Phys.*, vol. 83, no. 6, pp. 787–797, 2009.

[53] W. Dyck, "Application of Hydro Geochemistry to the Search of Uranium," *Econ. Geol. Re-ports*, vol. 31, no. 1, pp. 489–510, 1979.

[54] A. Al-Hamidawi, "Assessment of Radiation Hazard Indices and Excess Life Time Cancer Risk Due to Dust Storm for Al-Najaf, Iraq," *WSEAS Trans. Environ. Dev*, vol. 10, no. 1, pp. 312–319, 2014.

[55] H. N. Majeed, A. K. Hasan and H. J. Hamad, "Measurement Natural Radioactivity in Soil Samples from Important historical locals in Alnajaf Alashraf city, Iraq," *J. J. Adv. Chem.*, vol. 8, no. 1, 2014.

[56] V. M. Choubey, PK. Mukherjee and BS. Bajawa, "Geological and Tectonic Influence of Water-Soil-Radon Relationship in Mandi-Manali area, Himachal Himalaya," Environ Geol., vol. 52, no. 6, pp. 1163–1171, 2007.

[57] A. K. Hashim and L. A. Najam, "Measurement of Uranium Concentrations, Radium Content and Radon Exhalation Rate in Iraqian Building Materials Samples," *Int. J. Phys.*, vol. 3, no. 4, pp. 159–164, 2015.

[58] A. R. H. Subber, M. A. Ali and W. H. ALmosawy, "Gamma-Ray Measurements of Naturally Occurring Radioactive Materials in Sludge, Scale and Well Cores of The Oil Industry in Southern Iraq," *Walailak J. Sci.*

*Technol.*, vol. 11, no. 9, pp. 739–750, 2014.

[59] UNSCEAR 2000 Report to the General Assembly, "Sources and Effects of Ionizing Radiation," *J. Radiol. Prot.*, vol. 21, no. 1, pp. 1–79, 2000.

[60] L. Pawlik-Sobecka, J. Górka-Dynysiewicz and J. Kuciel-Lewandowska, "Balneotherapy with The Use of Radon-Sulphide Water: The Mechanisms of Therapeutic Effect," *Appl. Sci.*, vol. 11, no. 6, pp. 1–7, 2021.

[61] H. M. Prichard, "The Transfer of Radon from Domestic Water to Indoor Air," *Am. Water Work. Assoc.*, vol. 79, no. 4, pp. 159–161, 1987.

[62] J. M. Godoy and R. P. da Cruz, "$^{226}$Ra and $^{228}$Ra in Scale and Sludge Samples and Their Correlation with The Chemical Composition," *J. Environ. Radioact.*, vol. 70, no. 3, pp. 199–206, 2003.

[63] F. S. Al-Saleh and G. A. Al-Harshan, "Measurements of Radiation Level in Petroleum Products and Wastes in Riyadh City Refinery," *J. Environ. Radioact.*, vol. 99, no. 7, pp. 1026–1031, 2008.

[64] A. M. S. Qasim, H. H. Hussain and A. A. Abojassim, "Radon Concentrations and Annual Effective Dose in Cigarette Samples (Domestic and Importer) At the Iraqi Markets," *J. Radiat. Nucl. Appl.*, vol. 3, no. 2, pp. 83–88, 2018.

[65] A. A. Abojassim, A. S. Jassim, H. M. Ahmed and H. H. Hussian, "Assessment of Radon, Radium and Uranium Concentrations in Decorative Materials (Used to walls) Samples in Iraqi Markets," *WSEAS Trans. Environ. Dev.*, vol. 17, no. 1, pp. 1210–1218, 2021.

[66] German Commision on Radiological Protection, *Radon Dose Doefficients*, first edition, no. 290. Postfach, 2017.

[67] M. Baskaran, *Radon: A Tracer for Geological, Geophysical and Geochemical Studies*, first edition, AG Switzerland: Springer Nature, 2016.

[68] IAEA, *Radiation Protection and The Management of Radioactive Waste in The Oil and Gas Industry, Training Course Series*, fortieth edition, Vienna:

IAEA, 2010.

[69] S. Mittal, A. Rani and R. Mehra, "Estimation of Radon Concentration in Soil and Groundwater Samples of Northern Rajasthan, India," *J. Radiat. Res. Appl. Sci.*, vol. 9, no. 2, pp. 125–130, 2016.

[70] R. L. Grasty and J. R. LaMarre, "The Annual Effective Dose From Natural Sources Of Ionizing Radiation In Canada," Radiation Protection Dosimetry., vol. 108, no. 3, pp. 215–226, 2004.

[71] L. Sajo-Bohus, J. Gomez, T. Capote, E. D. Greaves, O. Herrera, V. Salazar and A. Smith, "Gross Alpha Radioactivity of Drinking Water in Venezuela," *J. Environ. Radioact.*, vol. 35, no. 3, pp. 305–312, 1997.

[72] D. A. Salim and S. A. Ebrahiem, "Measurement of Radon concentration in College of Education, Ibn Al-Haitham buildings Using RAD-7 and CR-39 detector," *Energy Procedia*, vol. 157, no. 1, pp. 918–925, 2019.

[73] M. H. Kheder, H. N. Azeez, M. Y. Slewa and T. A. Zaker, "Determination of Uranium Contents in Soil Samples in AL-Hamdaniya Region Using Solid State Nuclear Track Detector CR-39," *Al-Mustansiriyah J. Sci.*, vol. 30, no. 1, pp. 199–204, 2019.

[74] V. Zareena Hamza and M. N. Mohankumar, "Cytogentic Damage in Human Blood Lymphocytes Exposed in Vitro to Radon" Mutation Research," *Mutat. Res.*, vol. 661, no. 1, pp. 1–9, 2009.

[75] G. S. Hafez, I. Hunyadi and M. Tóth-Szilágyi, "Measurement of Exhalation and Diffusion Pa-rameters of Radon in Solids by Plastic Track De-tectors," *Nucl. Track Radit. Meas*, vol. 12, no. 1, pp. 701–704, 1986.

[76] J. C. Bryan, *Introduction to Nuclear Science*, second edition, New York: CRC Press, 2013.

[77] V. E. Guiseppe, "Radon In Ground Water: A Study of The Measurement

and Release of Waterborne Radon and Modeling of Radon Variation in Bedrock Wells, ” University of Maine, 2006.

[78] W. Hofmann, R. Winkler‐Heil, H. Lettner, A. Hubmer and M. Gaisberger, “Radon Transfer from Thermal Water to Human Organs in Radon Therapy: Exhalation Measurements and Model Simulations,” *Radiat. Environ. Biophys.*, vol. 58, no. 4, pp. 513–529, 2019.

[79] D. Ghose, D. Paul and R. C. Sastri, “Radon as A Tracer for Helium Exploration in Geothermal Areas,” *Radiat. Meas.*, vol. 36, no. 1, pp. 375–377, 2003.

[80] A. Rodriguez, T. Yalile, C. Leyner and M. Fernando, “Soil Gas Radon Measurements as A Tool to Identify Permeable Zones at Las Pailas Geothermal Area, Costa Rica,” *United Nations Univ.*, vol. 20, no. 9, pp. 1–7, 2008.

[81] S. A. Durrani and R. K. Bull, *Soid State Nuclear Track Detection. Principles, Methods and Applications*, first edition, Oxford: Pergamon Press, 1987.

[82] K. H. Obayes, K. H. Mahdi and R. M. Nasif, “Measurement of Radon Concentration in Dust for Most Areas of Diwaniyah - Qadisiyah Governorate,” *Solid State Technol.*, vol. 63, no. 1, pp. 2544–2550, 2020.

[83] M. El Ghazaly and N. M. Hassan, “Characterization of Saturation of CR-39 Detector at High Alpha-Particle Fluence,” *Nucl. Eng. Technol.*, vol. 50, no. 3, pp. 432–438, 2018.

[84] K. M. Opondo and K. Sims, *Electronic Radon Detector User Manual*, first edition, Billerica, USA: Durridge Company, Radon Capture and Analytics, 2021.

[85] Durridge Company Inc., *RAD H2O User Maual*, no. 978. Billerica: 2020 Durridge Company Inc, 2020.

[86] B. G. Gilfedder, H. Hofmann and I. Cartwright., "Novel Instruments for in Situ Continuous Rn-222 Measurement in Groundwater and The Application to River Bank Infiltration," *Environ. Sci. Technol.*, vol. 47, no. 2, pp. 993–1000, 2013.

[87] G. W. Phillips, J. E. Spann, J. S. Bogard, T. VoDinh, D. Emfietzoglou, R. T. Devine and Moscovitch, "Neutron Spectrometry Using CR-39 Track Etch Detectors," *Radiat. Prot. Dosimetry*, vol. 120, no. 1, pp. 457–460, 2006.

[88] A. Stabilini, K. Meier and Yukihara, "High Dose Fast Neutron Dosimetry Using PADC Plastic Nuclear Track Detectors and Grey Level Analysis," *Radiat. Prot. Dosimetry*, vol. 180, no. 1, pp. 220–224, 2018.

[89] B. Tate and S. Long, *Acceptance Testing of The TASL Radon Dosimetry System*, first Edition, Yallambie: Australian Government, Australian Radiation Protection and Nuclear Safety Agency (ARPANSA), 2016.

[90] C. Liu, H. Ma, Z. Zeng, J. Cheng, J. Li and H. Zhang, "Measurements of Radon Concentrations Using CR-39 Detectors in China," *JinPing Undergr. Lab.*, vol. 1806, no. 1, 2018.

[91] M. H. M. Rinos and M. I. M. Kaleel, *Geographic Information System*, first edition, vol. 2017. South Eastern University of Sri Lanka: Department of Geography, South Eastern University of Sri Lanka, 2012.

[92] S. Khan, P. L. Scala and K. Mohiuddin, "Evaluating the Parameters of ArcGIS and QGIS for GIS Applications Related papers New Front iers for WebGIS Plat forms Generat Ion Evaluating the parameters of ArcGIS and QGIS for GIS Applications," *ACADEMIA*, vol. 7, no. 3, pp. 582–594, 2018.

[93] P. Alaei, "Introduction to Health Physics," *Med. Phys.*, vol. 35, no. 12, pp. 1–5959, 2008.

[94] NCRP, "Control of Radon in Houses," *Natl. Counc. Radiat. Prot. Meas.*, vol. 122, no. 3, pp. 1–341, 1889.

[95] M. Jiránek, "Sub-slab Depressurisation Systems Used in the Czech Republic and Verification of Their Efficiency," *Radiat. Prot. Dosim.*, vol. 162, no. 1, pp. 64–67, 2014.

[96] M. Fuente, D. Rábago, J. Goggins, I. Fuente, C. Sainz and M. Foley, "Radon Mitigation by Soil Depressurisation Case Study: Radon Concentration and Pressure Field Extension Monitoring in a Pilot House in Spain," *Sci. Total Environ.*, vol. 695, no. 1, pp. 1–11, 2019.

[97] S. Long, D. Fenton, M. Cremin and A. Morgan, "The Effectiveness of Radon Preventive and Remedial Measures in Irish Homes," *J. Radiol. Prot.*, vol. 33, no. 1, pp. 141–149, 2013.

[98] EPA, "Building Radon Out. A Step-by-Step Guide On How To Build Radon-Resistant Homes.," Office of Air and Radiation, USA, 2001.

[99] M. F. A. L. Ruwashdi and E. T. A. L. Khakani, "Spatiotemporal Monitoring of Urban Expansion Utilizing Remote Sensing Data : The Case Study of An Najaf Governorate," *J. Xidian Univ.*, vol. 15, no. 8, pp. 33–41, 2021.

[100] K. N. Kadhim and G. A. J. Al-Baaj, "The Geotechnical Maps for Gypsum by using GIS for Najaf city (Najaf - Iraq)," *Int. J. Civ. Eng. Technol.*, vol. 7, no. 4, pp. 329–338, 2016.

[101] M. K. J. Al-Khafaji, "Cartography Representation of The Geographical Characteristics of AL- Najaf Governorate," University of Kufa, 2012.

[102] J. H. Jebur, R. H. Subber Abdul and W. Tuama Saadon, "Calibration of CR-39 for Different Heights of Radon Dosimeters and Application of Radon Concentration in Mahajran River Sediment in Basra Governorate, Iraq," *J. Phys. Conf. Ser.*, vol. 1294, no. 2, pp. 1–9, 2019.

[103] A. El-taher, A. A. Abojassim, L. A. Najam, H. Abid and A. Bakir, "Assessment of Annual Effective Dose for Different Age Groups Based on Radon Concentrations in the Groundwater of Qassim , Saudi Arabia," *Iran. J.*

*Med. Phys.*, vol. 17, no. 1, pp. 15–20, 2020.

[104] K. M. Thabayneh, "Determination of Radon Exhalation Rates in Soil Samples Using Sealed Can Technique and CR-39 Detectors," *J. Environ. Heal. Sci. Eng.*, vol. 20, no. 16, pp. 121–128, 2018.

[105] A. K. Mahur, A. Sharma, R. G. Sonkawade, D. Sengupta, A. C. Sharma and R. Prasad, "Measurement of Radon Exhalation Rate in Sand Samples from Gopalpur and Rushikulya Beach Orissa, Eastern India," *Phys. Procedia*, vol. 80, no. 1, pp. 140–143, 2015.

[106] M. Quarto, M. Pugliese, F. Loffredo, C. Zambella and V. Roca, "Radon Measurements and Effective Dose from Radon Inhalation Estimation in The Neapolitan Catacombs," *Radiat. Prot. Dosimetry*, vol. 158, no. 4, pp. 442–446, 2014.

# Measurement of Radon Gas Concentrations for different Types of Water in AL-Najaf Refinery by Using RAD7 Monitor

**Mokhalad A. Mohammed[1*], Rawaa M. Obaid[2]**

## Abstract

In this study, the average radon gas concentration for different types of water was measured in AL-Najaf refinery by using RAD7 monitor manufactured by DURRIDGE company, USA, there are two sources of water inside the refinery, river water, and well water, at RO unit inside the refinary, they use 50% of well water (W1) and 50% of river water (W7), as drinking water after mixing and processing them, the mixed water also used as tap water (W5), or as water for oil refining process, in the refining units, the water boils before it is used in the refining process and it does not contain any concentration of radon gas as in sample (W8), and after refining process, the water becomes wastewater (W4), the other wells inside the refinery, (W3), (W9), (W4) and (W2) are used to irrigate the plants located at the borders of the refinery, the results showed that the maximum value was 471 Bq/m$^3$ in the well water (W1), and the minimum value was 0 Bq/m$^3$ in the water of the boiler at the refining units (W8), and the average of readings obtained from all water samples was of 108.6888889 Bq/m$^3$, also the estimation for the average of radon gas concentration in the refinery air was made with the help of EPA estimations and the annual effective dose for inhalation ($E_{inhalation}$), Lung Cancer Risk (LCR), exposure to radon and it's progenies ($E_P$) and Potential Alpha Energy Concentration (PAEC) were determined for the workers inside the refinary. All the results were within the accepted limits recommended by EPA and WHO.

## الخلاصة

في هذا العمل، قيسَ تركيز غاز الرادون لعينات بيئية (تربة وماء) مجموعة من مواقع مختارة في مصفى النجف. أُستخدم كاشف الآثر النووي CR-39 (الطريقة التراكمية) في قياسات التربة والماء، وكذلك استخدم جهاز RAD7 المصنع من قبل شركة DURRIDGE الامريكية في قياسات الماء. حيث قسّمَ موقع الدراسة الى اربعة قطاعات وكل قطاع تم تقسيمه الى مربعات وذلك من اجل تحقيق دراسة شاملة لموقع الدراسة.

جُمعت خمسون عينة تربة وبعمق 20 cm من السطح وتسع عينات مختلفة من الماء من المواقع التالية: وحدة RO (ماء الشرب)، ماء الحنفية، ماء الغلاية في الوحدات التكريرية، ماء البئر والماء الملوث بالمخلفات النفطية.

النتائج بينت بان تركيز غاز الرادون في غاز التربة يتراوح بين $Bq/m^3$ 857 ∓ 7341 لعينة تربة قريبة من شعلة الحرق في المصفي و$Bq/m^3$ 186 ∓ 39 لعينة تربة تقع في نهاية المصفي وبمعدل يساوي $Bq/m^3$ 123 ∓ 1342.

نتائج عينات الماء المقاس باستخدام جهاز RAD7، بينت بان تركيز غاز الرادون تقع بين 471 $Bq/m^3$ لعينة ماء البئر و$Bq/m^3$ 0 لعينة ماء الغلاية في الوحدات التكريرية، وبمعدل قراءات يساوي 108 $Bq/m^3$، ولكن بالنسبة لعينات الماء المقاسة باستخدام كاشف الآثر النووي CR−39 (الطريقة التراكمية)، النتائج بينت بان تركيز غاز الرادون يتراوح بين $Bq/m^3$ 53 ∓ 297 (0.053 Bq/L ∓0.297) لعينة ماء البئر في وحدة تصفية المياه و$Bq/m^3$ 48 ∓ 12 (0.048 Bq/L ∓ 0.012) لعينة ماء الغلاية في الوحدات التكريرية، وبمعدل $Bq/m^3$ 32 ∓ 148 (0.32 Bq/L ∓0.184).

خُمن تركيز الرادون في هواء المصفي والناتج من مساهمة الماء وفق تخمينات وكالة حماية البيئة الامريكية (EPA) وكذلك تم تخمين تركيز الرادون في الهواء القريب من التربة والناتج من مساهمة التربة. كما أُحتسبت الجرع الفعالة السنوية والناتجة من استنشاق غاز الرادون (٢٢٢) ووليداته في الهواء الداخلي والخارجي وفق العلاقات المقترحة من قبل لجنة الامم المتحدة العلمية المعنية بآثار الاشعاع الذري (UNSCEAR).

جميع الجرع الفعالة السنوية الناتجة من مساهمة عينات التربة لم تتجاوز الحد الموصى به من قبل منظمة الصحة العالمية (WHO) والذي يساوي 0.1 mSv/y. الجرع الفعالة السنوية الناتجة من مساهمة عينات الماء لم تتجاوز الحدود الموصى بها من قبل منظمة الصحة العالمية (WHO) والهيئة الدولية للوقاية من الاشعاع (ICRP) والتي تساوي0.1 mSv/y و1 mSv/y، على التوالي.

**جمهورية العراق**
**وزارة التعليم العالي والبحث العلمي**
**جامعة بابل**
**كلية العلوم**
**قسم الفيزياء**

# قياس تركيز غاز الرادون وتأثيره الصحي على العاملين في مصفاة محافظة النجف / العراق

رسالة ماجستير

مقدمة إلى قسم الفيزياء، كلية العلوم، جامعة بابل وهي جزء من متطلبات نيل درجة الماجستير

في علوم الفيزياء

من قبل

**مخلد عباس محمد عزيز**

**بكالوريوس فيزياء (٢٠٠٩)**

إشراف

**أ. م. د. رواء مزهر عبيد عاشور**

٢٠٢٢م ١٤٤٤هـ